The use of radon and complementary hydrochemistry tracers for the identification of groundwater – surface water interaction in New Zealand

Heather Martindale

A thesis presented in partial fulfilment of the requirements for the degree of

Master of Environmental Management

At
the Institute of Agriculture and Environment

Palmerston North, New Zealand

Heather Martindale

2015

Abstract

Understanding how surface waters and groundwaters interact is an integral component of managing the influence of nutrient inputs to water quality. Knowledge of the potential nutrient loads from discharging groundwater is essential for meeting the bottom line nutrient concentrations in surface waters. Radon-222 is an emerging tracer for measuring groundwater-surface water interaction which has been underexploited in New Zealand. The aim of this research was to establish the potential of using radon for measuring groundwater and river water interaction in the New Zealand environment.

Low and high resolution radon surveys were carried out in two gravel-bed rivers, the Hutt and Mangatainoka Rivers, in lower North Island of New Zealand. To provide accurate measurements of radon concentrations in surface waters containing very little radon, the development of a cost and time effective, simple and reproducible high sensitivity radon measurement method was investigated. Furthermore, the study aimed to assess the potential of using radon measurements in combination with concurrent stream flow gauging and other hydrochemistry data for providing more detailed information on groundwater and river water interaction processes.

Radon measurements were found very helpful to identify groundwater discharge and recharge locations in both the Hutt and Mangatainoka Rivers. Furthermore, a high sensitivity radon analysis method was developed with a lower limit of detection of 0.006 BqL^{-1}, a vast improvement on the direct count method, and offering practical advancements over previously published methods. This high sensitivity method was used to establish radon concentration thresholds to identify locations of groundwater discharge, potential groundwater recharge and hyporheic exchange in NZ gravel-bed rivers.

In both studied rivers the groundwater discharge and potential recharge patterns identified by radon were not always matched by the concurrent flow gauging surveys, highlighting the ambiguity surrounding the use of concurrent flow gauging in gravel-bed rivers for mapping river gains and losses. In some sections of the studied rivers the concurrent flow gauging data indicated areas of groundwater recharge or discharge where the radon data showed the opposite process to be occurring. This has led to the conclusion that underflow beneath the gravels and other parafluvial exchange processes can cause the interpretation of concurrent flow gauging results to be misleading. Flow gauging combined with radon sampling gives a more conclusive picture of the groundwater and river water interaction processes in the gravel-bed rivers.

Acknowledgements

I would like to express my thanks to my supervisor, colleague and manager, Dr. Uwe Morgenstern for having faith in, and providing me with, the opportunity to undertake my Masters study while working full time. Dr. Morgenstern not only introduced me to the topic for my thesis, but also proactively found funding to support my study. His knowledge and guidance have been invaluable and I am grateful.

I also wish to express my sincere gratitude to my supervisor Dr. Ranvir Singh. His experience, guidance and feedback have been essential for the completion of this thesis.

Thank you also to Dr. Bob Stewart for your guidance during this thesis. Your practical advice in managing workflow, workload and field work planning around health and safety issues is greatly appreciated.

I would also like to thank my fellow work colleagues, Kurt McBeth, Vanessa Trompetter and Rob van der Raaij, in the Water Dating Lab at GNS Science. Thank you for providing moral support throughout this process, for carrying the extra work load when I was on leave and to Rob, for answering all of my questions about working with dissolved gasses.

I would like to thank Abby Matthews and Horizons Regional Council for providing the funding for this study. Thank you also to the Horizons field team, particularly Darren Bentley-Hewitt, for familiarising me with the local area and providing invaluable local knowledge.

For his (hopefully) superb editing skills, I would like to thank my Father. I will be forever grateful for both his and my Mother's support, encouragement and advice throughout all of my studies.

Lastly, I would like to thank Mitchell Davis for his unrelenting support and encouragement. Unwittingly, Mitchell also found himself partaking in a Masters, spending many of his weekends trudging through rivers, providing expert kayaking support and being a sounding board for all of my ideas. Thank you.

Table of contents

List of Figures

List of Tables

List of Equations

Chapter 1- Introduction, Aims and Objectives

1.1 Introduction

Groundwater and surface water are two of New Zealand's most valuable assets upon which we rely for economic, recreational and cultural endeavours (Ministry for the Environment, 2014). They are also vital for sustaining fresh water ecosystems. Thus it is important to manage the distribution, allocation and the use of these fresh water resources in an effective and sustainable way. Our waterways are a complex interrelated system of surface waters and groundwaters. The movement or flow paths, contamination of, or use of one body of water impacts on the other (Winter, 1999b). Thus understanding how surface waters and groundwaters interact is an integral component of managing the influence of land use impacts on water quality (Stellato et al., 2013). Historically, these two resources have generally been managed as isolated systems rather than the complicated interdependent resources which they are (Davidson & Wilson, 2011; Kalbus, Reinstorf, & Schirmer, 2006; Kaye-Blake, Schilling, Nixon, & Destremau, 2014; Sophocleous, 2002). However, regional councils, researchers and catchment managers within New Zealand have been moving toward a more integrated water management approach which considers the interaction that groundwaters may have on surface waters and vice versa, particularly in relation to streams and groundwater flow (Bekesi, 2005; Davidson & Wilson, 2011).

One facet of understanding how groundwater and surface water interact is to identify locations where groundwater and surface water are exchanging within the river systems. For example, an understanding of where nitrate rich groundwater is being discharged into a river may shed light on the source of the nitrate, and on biological processes occurring downstream, such as an increase in algae at certain sites within a river. Understanding where aquifers are being recharged can aid in the groundwater management. Furthermore, identifying the locations of where surface water – groundwater interactions are occurring may aid in tracking nutrient flow pathways between the groundwater and surface water systems.

Numerous different measurement techniques have been deployed to study how groundwater and surface water in rivers interact. Differential flow gauging is frequently used to capture net stream gain or loss. However, this is time consuming and does not capture the flow gains and losses occurring between measurement points (Kalbus et al., 2006). A recent methodology which does capture exchange processes at a higher resolution is distributed temperature sensing (DTS). DTS captures temperature data at pre-set spatial intervals along a fibre optic cable (Selker et al., 2006). However, this method is expensive and the fibre optic cable is delicate, especially when it needs to be deployed for large-scale surveys. Furthermore, this method is only applicable where there is a significant temperature gradient between groundwater and surface water, which can be strongly affected by environmental conditions such as wind, turbidity and landscape features such as shadows cast by bush (Johnson, 2003).

A potential cost effective and more practical approach for measuring locations of groundwater and surface water interaction is the analysis of radon-222 concentrations in river water. Radon is a soluble, colourless, gaseous, unstable isotope (Cecil & Green, 2000). It is generated as part of the uranium decay series. Uranium is ubiquitous in almost all rocks and soils, resulting in the release of radon from uranium bearing minerals into groundwater (Stellato et al., 2013). Radon is abundant in groundwaters but has almost negligible concentrations in surface waters due to a short half-life of

3.8 days (Cecil & Green, 2000) and rapid radon loss to the atmosphere through degassing (Garcia-Vindas & Monnin, 2005; Kies, Hofmann, Tosheva, Hoffmann, & Pfister, 2005). This contrast in radon concentrations between groundwaters and surface waters enables radon to be an ideal tracer to measure groundwater-surface water interaction. Surface waters which have elevated concentrations of radon indicate a location where groundwater is discharging into the surface water. Numerous studies have been reported in the international literature that have taken advantage of this radon methodology for identifying groundwater-surface water interaction (Burnett, Kim, & Lane-Smith, 2001; Burnett, Peterson, Chanyotha, Wattayakorn, & Ryan, 2013; Burnett, Peterson, Santos, & Hicks, 2010; Close, 2014; Cook, Favreau, Dighton, & Tickell, 2003; Dimova, Burnett, Chanton, & Corbett, 2013; Dulaiova, Camilli, Henderson, & Charette, 2010; Hammond, Simpson, & Mathieu, 1977; Hoehn & Von Gunten, 1989; Kies et al., 2005; Rajashekara, Narayana, & Siddappa, 2007; Santos & Eyre, 2011; Stellato et al., 2013). However, little research has been undertaken using radon in New Zealand fluvial systems.

1.2 Aim

The use of radon-222 as a tool for measuring the interaction between groundwater and surface water has so far been underexploited in New Zealand. Two known studies using radon-222 in the New Zealand environment investigate surface water recharge to groundwater systems in Canterbury and Marlborough (Close, 2014; Close, Matthews, Burbery, Abraham, & Scott, 2014). However, little has been done to use radon-222 for investigating groundwater-surface water interaction in the North Island of New Zealand, particularly for investigating groundwater discharge into surface waters. The aim of this Master's thesis is to research the potential of radon for measuring groundwater and river water interactions, with a particular focus on groundwater discharge into gravel bed rivers, in the New Zealand environment. Two rivers in the Lower North Island were chosen for this study: the Hutt River, in the Greater Wellington Region, and the Mangatainoka River, in the Horizons Region.

The Hutt River drains through a mixture of urban and peri-urban agriculture area and is often subject to toxic algal blooms during the summer, low flow months. This is undesirable for recreational use and understanding groundwater discharges and dynamics may enable the nutrient flow pathways and cause of algal blooms to be identified.

The Mangatainoka River, in the Horizons Region, is surrounded by agricultural activity. There is limited data on the groundwater hydrology and thus nutrient flow paths of the area (Brougham, 1987). Thus, investigating the locations of groundwater and surface water interaction will not only aid in providing further insight when setting water take limits but will also create a better understanding of the fate and transport of nutrients from historical and current land use to help mitigate any potential impacts on river water quality.

1.3 Objectives

To fulfil the aim of using radon to identify locations of groundwater and surface water interaction the following objectives will be met:

- Review the existing radon measurement methods for identifying groundwater – surface water interactions and quantification of groundwater discharge or recharge.

- Develop a cost and time effective high sensitivity radon measurement technique for the detection of low radon concentrations with sufficient accuracy to enable distinguishing hyporheic exchange from small groundwater discharges and losing sections of the river.

- Apply and evaluate the high sensitivity radon measurements in conjunction with high resolution spatial radon studies to capture the groundwater-surface water dynamics in two selected New Zealand gravel bed rivers.

- Develop radon concentration thresholds to determine what measured radon concentrations in surface waters represent groundwater discharge in New Zealand gravel-bed river environments.

- Assess the potential of using radon measurements together with other complementary methods such as concurrent stream flow gauging and hydrochemistry analysis to enhance the understanding of the dynamics of groundwater – river water interactions.

Chapter 2 - Review of Literature

2.1 Introduction

This chapter first gives a brief and general description of groundwater-surface water interaction. It then reviews various methods used to measure these interactions, with particular attention given to the use of radon-222. The requirements and usefulness of radon-222 are compared to other techniques, and the radon-222 method is discussed in respect to radon generation, sampling, and analytical techniques. Case studies where radon-222 has been used are reviewed and their main findings and limitations are discussed to inform the methodology development for this study.

2.1.1 Groundwater–surface water interaction

Groundwater is the subsurface water that occurs beneath the water table (Anderson, 2003; Freeze & Cherry, 1979). It is the saturated zone beneath the water table where the pore spaces of rock and soil are completely filled with water and pore water pressure is greater than atmospheric pressure (Smerdon & Redding, 2007; Winter, 1999a). The water table is defined as the boundary between the unsaturated and saturated zones where pore water pressure is equal to the atmospheric pressure (Woessner & Anderson, 2002). Above the water table, in the unsaturated or vadose zone, the pore spaces are partially filled with water and air. The differing subsurface zones are illustrated more clearly in Figure 2.1. Precipitation infiltrated on the ground surface increases the soil moisture. When the soil water holding capacity is exceeded, the water percolates downward and recharges the groundwater.

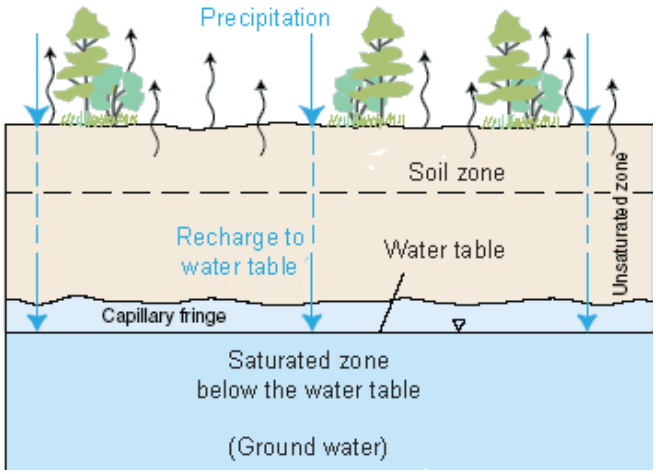

Figure 2.1: Subsurface water zones. Image adapted and retrieved from USGS, as cited in (Bureau of Reclamation, 2012)

Groundwater storage and movement in the saturated zone is mainly determined by the porosity, hydraulic conductivity, and the hydraulic head. The hydraulic head, or potential energy is the sum of elevation and pore fluid pressure divided by the density of water (Winter, 1999a). The flux of groundwater movement is governed by the principle of Darcy's law, whereby groundwater flow rate is determined by the subsurface material's hydraulic conductivity and hydraulic gradient, i.e. change in hydraulic head per unit length of the flow path (Smerdon & Redding, 2007; Winter, 1999a).

The principles of hydraulic head and Darcy's law are fundamental concepts which are important in the interaction of groundwater and surface water. They tell us that where the rock/sediment is permeable and water table elevation is higher than the elevation of water in a draining stream or river, then groundwater will discharge into the stream or river. Conversely for recharge of a stream or river water into the groundwater zone the water table must have a lower elevation than the elevation of water in the stream or river and the rock/sediment underneath must be permeable (Winter, 1999a). Thus groundwater and surface water interaction is affected by geology and geomorphology. It is also affected by anthropogenic land and water use and management, and climate conditions (Scanlon, Healy, & Cook, 2002).

Before discussing groundwater and surface water interactions any further, it is important to define two relevant terms which will be used frequently throughout this literature review. The groundwater terms, "Recharge" and "Discharge", define the direction of groundwater movement between the surface water and the groundwater. In this review the same conventions that were defined by Scanlon et al. (2001) will be used. Groundwater recharge refers to the movement of surface water into the subsurface. Groundwater discharge refers to the movement of groundwater from the subsurface to the surface (Scanlon et al., 2002).

Two other important terms to define are gaining and losing river reaches. A "Gaining" reach of the river refers to a section of the river wherein groundwater is being discharged (Fig. 2.2A). A "Losing" reach of the river refers to a section of the river where river water is being recharged into the groundwater system (Fig. 2.2B). Gaining and losing reaches of rivers have varying degrees of connectivity to the groundwater system (Scanlon et al., 2002). A river or stream which is directly connected with the groundwater zone has a continuous saturated zone between the river and the groundwater zone (Fig. 2.2A-2.2B) (Alley et al., 1999). Conversely, where there is an unsaturated zone between the river and the groundwater zone the river is considered to be disconnected from the groundwater zone (Fig. 2.2C) (Alley et al., 1999).

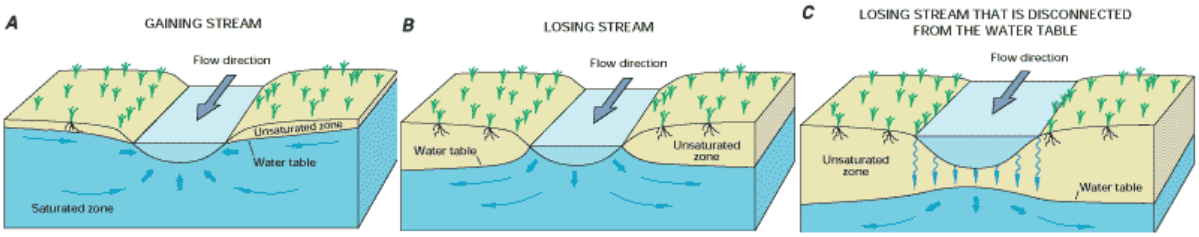

Figure 2.2: Gaining and losing streams with connectivity from the stream to the groundwater system. (A) depicts a gaining stream. (B) depicts a losing stream which is directly connected to the groundwater zone. (C) depicts a losing stream which is not directly connected with the groundwater zone. Image retrieved from (Alley, Reilly, & Franke, 1999).

The zone beneath and alongside of a river or stream bed, where surface water and groundwater are exchanged, mixed and flow, is called the hyporheic zone. This is a spatially fluctuating zone where stream water readily exchanges through the sediment and porous space in the adjacent river bed and banks (Fig. 2.3) (Boulton, Findlay, Marmonier, Stanley, & Valett, 1998; Sophocleous, 2002; Winter, 1999a). The hyporheic exchange is important to consider when looking at interactions between groundwater and surface water because it has an effect on the chemical and biological

signature of the water. Stream water can interchange between the hyporheic zone and the stream without any significant interaction with the groundwater zone. When the surface water enters the subsurface, for whatever length of time, it may capture some signatures or tracers associated with the groundwater. However, the hyporheic zone is spatially variable so the biological and chemical character of water within, and discharging from, the hyporheic zone can vary significantly throughout the course of a stream (Winter, 1999a). The scale of the hyporheic zone can range from being non-existent where impermeable rock is present, to hyporheic zones tens of metres deep which extend hundreds of meters laterally (Scarsbrook & Halliday, 1996; White, 1993). The varying location, size and water exchange of the hyporheic zone is greatly affected by streambed topography (Woessner, 2000). Exchange of water in the hyporheic zone is often associated with pools and riffles, caused by changes in streambed slope, and meanders in streams (Sophocleous, 2002; Winter, 1999a; Woessner, 2000).

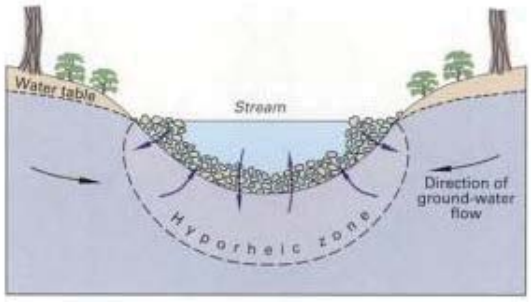

Figure 2.3: Depiction of the hyporheic zone relative to the groundwater and surface water zones. Image retrieved from (Winter, 1999a).

2.2 Methods for measuring groundwater-surface water interaction

The mechanisms which determine groundwater and surface water interaction described above barely begin to scratch the surface of the multifaceted and complicated processes of surface and groundwater movement. The interactions between groundwater and surface water are highly variable and complex and the measurement of such interactions is difficult. However, a number of techniques have been investigated and developed to gain insight into groundwater-surface water interactions. Several of these common measurement methods are reveiwed below.

Seepage meters

Seepage meters are a useful tool in measuring groundwater and surface water interaction. It is the only technique available which directly measures groundwater surface water exchange (Rosenberry, 2008). A simple form of a seepage meter was developed by Lee (1977) in which water is collected as water flows from the groundwater to the surface water. The seepage meter consists of a bottomless cylinder with a deflated plastic bag (Figure 2.4). The unit is inserted into the sediment at the sediment water interface (Lee, 1977). The flux can be calculated directly from the volume collected in the bag, the collection period and the area of the cylinder (Kalbus et al., 2006). Similarly, for losing streams, the bag can be filled prior to installation and the amount of water lost can be correlated to the flux of water recharging into the groundwater (Santos, Eyre, & Huettel, 2012). However, the bag

of the seepage meter, which is so fundamental to its design, can cause many uncertainties with measurements in the field (Anibas, Buis, Verhoeven, Meire, & Batelaan, 2011; Hatch, Fisher, Revenaugh, Constantz, & Ruehl, 2006; Kalbus et al., 2006; Murdoch & Kelly, 2003; Santos et al., 2012). The bag of the meter can fold or be distorted by flowing currents. Such distortion can effectively render the meter an obstacle in the water and disrupt the flow, giving inaccurate or misleading results. Another disadvantage of the seepage meter is that it gives no temporal data (Mwashote et al., 2010). The flux collected from the seepage meter is merely an average for the collection time period. Furthermore, a seepage meter cannot distinguish between hyporheic exchange and aquifer/surface water interaction (Kalbus et al., 2006). To overcome these problems automated seepage meters have been designed which use temperature gradients to measure flux (Mwashote et al., 2010). However, these are difficult to install in larger streams and, even the automated seepage meters do not overcome the problem that they only cover a very small area and thus are limited in the spatial data they can produce (Santos et al., 2012).

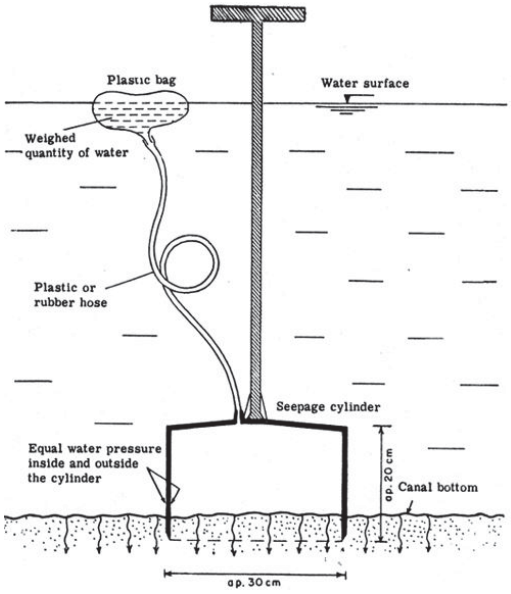

Figure 2.4: Schematic of a simple seepage meter. Image retrieved from (IAL, 2004).

Temperature sensing

Another tool for measuring groundwater-surface water interaction is the temperature sensing method. This is based on the principle that groundwater temperatures remain relatively stable whilst stream/river water temperatures vary, thus temperature differentials can be used to indicate where groundwater is discharging to a stream or vice versa (Anderson, 2005; Constantz, 1998; Kalbus et al., 2006). Temperature measurements are relatively cheap and easy to take. They can be applied both across or along a stream channel and can provide both spatial and temporal seepage information (Hatch et al., 2006). The use of heat as a tracer for groundwater-surface water interactions is advantageous for locating gaining or losing stretches of a river. However, temperature differential measurements cannot be directly used to quantify groundwater flux (Becker, Georgian, Ambrose, Siniscalchi, & Fredrick, 2004; Lowry, Walker, Hunt, & Anderson, 2007). Moreover,

temperature sensing cannot distinguish discharge that is from a groundwater aquifer or water which is discharging from the exchange of the hyporheic zone (Hatch et al., 2006). Often temperature measurements are dampened or misinterpreted due to the effects of discharge from the hyporheic zone (Johnson, 2003). Furthermore a measurable temperature gradient needs to exist. This method is not appropriate where groundwater and surface water temperatures are similar. There are several more complexities to consider when using this tool, for instance stream bed temperatures are also affected by wind speed, relative humidity, air temperature and subsurface saturation. These variables are highly changeable over short distances and are responsive to landscape features and riparian distribution (Johnson, 2003), therefore introducing more uncertainty to the measured temperature gradient.

Differential flow gauging

Differential flow gauging is a well established technique for measuring the net gain or loss of flow between two points in a river (Kalbus et al., 2006). It can be used to cover distances ranging from metres to kilometres and is easy to quantify with simple water balance equations (Hatch et al., 2006). However, while stream flow gauging is a good tool for measuring the net exchange between groundwater and surface water it does not capture the exact locations or sources of the discharges. Flow gauging also cannot be used alone to quantify the flux of discharge and recharge in a river reach as it gives only the net gain or loss rather than the total quantities of exchange processes occuring (Kalbus et al., 2006). Furthermore, higher resolution interactions such as hyporheic flow cannot be identified using this technique alone (McCallum, Cook, Berhane, Rumpf, & McMahon, 2012). Moreover, the groundwater discharges over short distances are often accompanied by high uncertainties because the differences in flow over a short distance are often smaller than the uncertainty of the measurement (Cey, Rudolph, Parkin, & Aravena, 1998). Therefore, differential flow gauging is a useful tool only where the difference in flow is found to be significantly greater than the uncertainty of the measurement (McCallum et al., 2012).

Tracer injection

Despite the draw-backs of differential flow gauging it is a good tool to use in combination with other tracer or gauging tools. One such complementary, investigative tool is tracer injection tests (Moore, 2004). Tracer injection tests, such as salt or dye injection, have been exploited since the late nineteenth centry (Flury & Wai, 2003). The injected tracers can be used to determine the flow rate between gauging points, to identify preferential flow paths, for dispersion experiments, flow connections or recharge rate estimates by injecting the dye into the soil layer and sampling at a range of depths over time (Flury & Wai, 2003; Scanlon et al., 2002; Smart & Laidlaw, 1977). The resultant concentration of the tracer after mixing allows the discharge and recharge of groundwater to be determined by differences in measured concentrations of the tracer (Angermann, Tacklenburg, & Blume, 2013; Kalbus et al., 2006). Seepage flow rates can also be measured using dyes as the flow rate is proportional to the dilution rate of the dye by the inflow of water (Kalbus et al., 2006). The advantages of using tracer injection tests for measuring groundwater-surface water interaction are numerous. Dyes and salts are relatively cheap (Davis, Thompson, Bentley, & Stiles, 1980). At higher concentrations, as low as parts per trillion, dyes can be identified visually (Davis et al., 1980; Flury & Wai, 2003). If the concentration of the dye is lower, e.g. parts per billion, the dye can be identified

easily by chemical analysis (Davis et al., 1980; Flury & Wai, 2003). However, the use of injected tracers has several disadvantages. The end measured tracer concentration can lead to misleading results as the concentration of the injected tracer can be affected by environmental conditions. Saline environments can inhibit the performance of some fluorescent dyes (Smart & Laidlaw, 1977), as can changes in temperature, pH and light conditions (Davis et al., 1980). Tracer concentrations can also be affected by adsorption between measurement sites, rendering tracer injection experiments over large distances unreliable (Davis et al., 1980; Hatch et al., 2006). A further disadvantage of tracer injection tests is that the end measured tracer concentration is only representative of the river flow rate if we assume that the point measured is homogeneous across the width and depth of the river (Hatch et al., 2006). Lastly, the injection of a foreign tracer into an environment is often not desirable, particularly as the larger the flow rate the more tracer needed to note any changes.

Hydrochemical tracers

Hydrochemical tracers are another well known tool used in investigating groundwater-surface water interaction. A hydrochemical tracer is a chemical signal which is picked up and carried in the water and gives information concerning the water body of interest. This chemical signal can be naturally occuring, such as dissolved minerals from rocks, occur through contamination from an anthropogenic source or be deliberately introduced into the water body of interest (Davis et al., 1980). Many different hydrochemical tracers exist, including radon-222. To discuss or compare all such tracers would be a monumental task. Instead, a few examples of main environmental tracers are briefly reviewed.

A number of hydro-geochemical tracers can be used to measure interactions between groundwater and surface water. These are non-conservative tracers which collect their signatures through water-rock interaction (Herczeg & Edmunds, 2000). Chemical parameters which fall under this umbrella include, but are not limited to, sodium, , silica, electrical conductivity, magnesium and other trace elements such as strontium (Kalbus et al., 2006). Comparisons are made between the groundwater concentrations of the tracer and the surface water concentrations (Baskaran, Ransley, Brodie, & Baker, 2009; Dimova et al., 2013; Kalbus et al., 2006; Shaw, White, & Gammons, 2013). Using mixing models or mixing ratios the percentage of groundwater inflow can be calculated (Katz, Coplen, Bullen, & Davis, 1997; Stellato et al., 2013). Of course this can only be done when the tracer in the groundwater is significantly different to that of the surface water. Furthermore, to refine mixing models, more than one tracer is often needed. A collection of different parameters and the costs associated with their analysis can render this technique to be expensive (Kalbus et al., 2006). As previously mentioned, radon-222 is also a hydrochemical tracer. Thus radon-222 measurements also have a cost associated with analysing samples, either by the purchase of a radon meter or the cost of individual sample analysis. While radon also has a cost associated with measurement, it is a single tracer which can be used in isolation to identify locations of groundwater-surface water interaction unlike other hydrochemical tracer approaches which often require multiple tracers to be measured to identify similar information. The need to only measure one hydrochemical tracer can render radon-222 to be a cheaper and simpler tracer to use. Further advantages, as well as disadvantages, of using the hydrochemical tracer radon-222 are discussed in Chapter 2, section 2.3.4.

Two useful environmental hydrochemcial tracers are the stable isotopes of ^{2}H and ^{18}O. Physical processes create an isoscape of spatially variable amounts of ^{2}H and ^{18}O isotopes. This is because the ^{2}H and ^{18}O isotopes are heavier than the more abundent ^{1}H and ^{16}O isotopes. ^{1}H and ^{16}O are therefore preferentially evaporated before ^{2}H and ^{18}O. However, the heavier isotopes condense to form rain preferentially over the lighter isotopes. The position of the ocean relative to the sample location, orographic uplift and previous storm events can also alter the fractionation of the isotopes (Bruckner, n.d; West, February, & Bowen, 2014). This fractionation can allow pre- and post-event waters to be distinguished (Kies et al., 2005; McDonnell, Stewart, & Owens, 1991) because the pre event stable isotope signature will be different to that of the storm water. The stable isotopes can help identify areas of water loss due to evaporation (Morgenstern et al., 2014; Morgenstern et al., 2015; Shaw et al., 2013). Groundwater flow patterns can also be detected using these stable isotopes as different water sources will have a different isotopic signature. Groundwater is also likely to have a different signature to the surface water of a river. However, the stable isotopes are not well suited in determining the locations of groundwater discharge. Due to the stability of the isotopes, mixing of the groundwater signature will occur with the surface water and it would be difficult to determine how far upstream the groundwater was discharging if isotopic change was measured.

Age dating tracers can also be used to infer knowledge on groundwater-surface water interaction. Two such age tracers are sulfurhexafluoride (SF_6) and chlorofluorocarbons (CFCs) (Busenberg & Plummer, 1992; Gooddy, Darling, Abesser, & Lapworth, 2006; Plummer & Busenberg, 2000). The concentrations of SF_6 and CFCs in the atmosphere have been recorded over time. SF_6 and CFCs can become dissolved in surface water and therefore a time signature for groundwater is provided by comparing the concentration of the dissolved gases in the groundwater to the known concentrations in the atmoshpere. Thus CFCs and SF_6 can be used to identify locations where groundwater is entering a river/stream as the concentration of the dissolved gases in the surface water will decrease with groundwater inflow. For these tracers to be useful there needs to be a noticable difference in their concentrations in the groundwater and the surface water. Furthermore, the measurement of these dissolved gases requires expensive and specialised analytical setups. If using CFCs alone, for this concentration differential to occur the groundwater needs to be at least twenty five years old (Cook et al., 2003). However, SF_6 is more useful at dating younger waters and the two dissolved gases provide more accurate age data when used together (Gooddy et al., 2006).

2.3 Radon – a tool for groundwater-surface water interaction measurement

An emerging tool for measuring groundwater and surface water interaction is radon-222 (herein referred to as ^{222}Rn or radon). Radon is a naturally occurring hydro-chemical tracer. It has been used for measuring groundwater and surface water interaction in numerous studies (Burnett et al., 2001; Burnett et al., 2013; Burnett et al., 2010; Cook et al., 2003; Dimova et al., 2013; Dulaiova et al., 2010; Hammond et al., 1977; Hoehn & Von Gunten, 1989; Kies et al., 2005; Rajashekara et al., 2007; Santos & Eyre, 2011; Stellato et al., 2013).

This thesis is primarily focused on using radon to measure groundwater discharge in gravel bed rivers in the New Zealand Environment. Thus the rest of this chapter will review and describe radon in more detail. Information reviewed will include, the origins and properties of radon, the advantageous properties radon has over other known methods for measuring groundwater and surface water interaction, how radon is sampled and measured, and how previous studies have analysed and interpreted radon surveys carried out in both riverine and non-riverine environments.

2.3.1 Origins of radon

^{222}Rn is generated from Radium-226 which is part of the decay series of Uranium-238 (Cecil & Green, 2000). Uranium is ubiquitous in sedimentary rocks and granites (Stellato et al., 2013) and is thus present in almost all types of rocks and soils (Lefebvre, Barbecot, Ghaleb, Larocque, & Gagné, 2013; Rajashekara et al., 2007). Groundwaters can become concentrated with ^{222}Rn due to radon emanation, the escape of a ^{222}Rn atom from a grain containing ^{226}Ra, from rocks and subsurface materials. Cecil et al. (2000) and Gesell and Lowder (1978) described four processes for the emanation of ^{222}Rn: solid phase diffusion, direct and indirect recoil, and the "knock out" effect (Cecil & Green, 2000; Gesell & Lowder, 1978). Solid phase diffusion contributes very little to the emanation process due to a low diffusion coefficient of radon in the solid grain. Thus the emanation process is dominated by alpha-recoil (Sakoda, Ishimori, & Yamaoka, 2011; Stellato et al., 2013). Alpha recoil occurs from an energy gain when the parent ^{226}Ra, decays to give ^{222}Rn and an alpha particle (Cecil & Green, 2000). Whether emanation occurs due to direct recoil, where ^{226}Ra decay causes the ^{222}Rn to directly diffuse out of the grain, or indirect recoil, a first particle directly recoils into a second particle causing the diffusion of the second particle out of the grain, only a small fraction of the ^{222}Rn produced actually escapes the rock in which it is housed (Hammond et al., 1977; Sakoda et al., 2011). Furthermore, ^{222}Rn is not the only isotope produced by ^{226}Ra. However, it has the longest half-life, 3.8 days, of its two other counterparts ^{219}Rn and ^{220}Rn (Lefebvre et al., 2013). The decay series of ^{222}Rn is depicted in Figure 2.5 below. Despite the limiting factors of radon production due to the long decay series of the parent nuclides ^{238}U and ^{226}Ra and typical emanation fractions of only 0.2 (Nazaroff, 1992), it is still prominent enough within groundwaters to be used as a natural tracer in environmental studies.

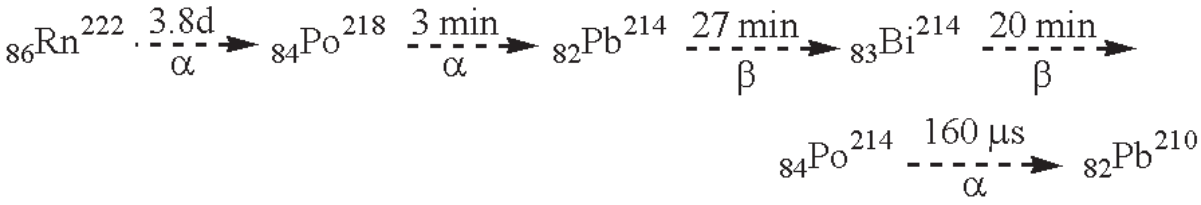

Figure 2.5: The decay series of ^{222}Rn. Image retrieved from (Kronenberg, Brucker, & Horne, 2002).

2.3.2 Properties of radon

The ^{222}Rn which escapes the rock material with its parent nuclide into the surrounding groundwater is a valuable tracer for measuring groundwater-surface water interactions. Groundwater radon concentrations vary from approximately 1 to over 1000 BqL^{-1} with typical values of 10-70 BqL^{-1} in gravels (Cecil & Green, 2000). When radon enters a surface water body, due to the low solubility of

radon (Kies et al., 2005), degassing of radon occurs very quickly. In laboratory experiments it has been shown that all of the radon in a 3 litre water sample will have degassed after seven minutes when air is pumped through it at a constant rate of 0.5 L min^{-1} (Garcia-Vindas & Monnin, 2005). This quick degassing, coupled with the relatively short half-life of radon, of 3.8 days, causes a rapid decrease of radon concentrations in surface water (Burnett & Tai, 1992; Cook et al., 2003). Due to the contrast between radon concentrations in discharging groundwater and the low concentrations of radon in surface water recharging into the groundwater, ^{222}Rn can be used as a tracer to identify locations of groundwater discharge to surface water as well as the recharge of surface water to groundwater.

2.3.3 Factors affecting radon concentrations in groundwaters

While radon is prominent in groundwaters, the release of this hydro-chemical tracer into water is highly variable (Asikainen, 1981). Even where groundwater is essentially coming from the same aquifer, with the same bedrock material, radon concentrations have been shown to vary greatly by factors of up to seven (Folger, Poeter, Wanty, Frishman, & Day, 1996). The factors affecting radon concentration relate to the physical and chemical characteristics of the aquifer as well as the uranium content of the bedrock/aquifer material (Asikainen, 1981; Ellins, Roman-Mas, & Lee, 1990). Obviously, rock materials higher in uranium, such as granites, have the potential to produce groundwaters with relatively higher concentrations of radon compared to lower uranium bearing rocks such as sands or clays (Cecil & Green, 2000). However, a strong disequilibrium occurs between radon and its parents radium-226 and uranium-238 (Asikainen, 1981; Cecil & Green, 2000) meaning a rock/sediment formation high in uranium will not always result in groundwaters high in radon concentration. The radon concentration in the groundwater is dependent on where the uranium and the decay product radium-226 are housed within the rock/sediment material. Radium which is positioned on rock fracture surfaces produces groundwaters higher in radon concentrations because the radon is able to emanate out of the rock material and into the groundwater. Thus the concentration of radon in groundwaters is dependent on the concentrations of radium-226 and uranium-238 housed on the fracture surface of subsurface materials.

Therefore, aquifer conditions which increase the movement of radium-226 and uranium-238 to fractures within the subsurface materials will likely increase the radon concentrations in groundwaters. Both the chemical conditions of the aquifer and the locations of fractures within the subsurface materials impact on the mobility of radium-226 and uranium-238 (Asikainen, 1981; Folger et al., 1996). Uranium can adopt many forms depending on hydrochemistry. Uranium is present in the +4 oxidation state at low temperatures and pressures (Skeppström & Olofsson, 2007). In oxidising environments uranium adapts to the +6 oxidation state, which is mobile. The mobile U(VI) can then form strong complexes with Fe and other commonly occurring ions in the groundwater (Skeppström & Olofsson, 2007). The mobile U(VI), as well as the mobile Ra^{2+}, preferentially migrates to fracture surfaces which are close to the rock/water interface (Cecil & Green, 2000; Folger et al., 1996; Vinson, Vengosh, Hirschfeld, & Dwyer, 2009). Like Uranium, the mobile form of radium also occurs in oxic environments. When pH is low and total dissolved solids are low, radium remains mobile in the groundwater (Ellins et al., 1990). The preference for mobile radium and uranium to bind to fracture surfaces contributes greatly to the concentration of radon. Radium has a particularly strong affinity to clay minerals and iron oxides (Yanase, Payne, & Sekine,

1995). This provides higher concentrations of radon's parent materials to be closer to the fracture surface, allowing the radon to be emanated into the groundwater. Thus the characteristics of an aquifer resulting in high radon concentrations incorporate highly fractured rock, oxic and low pH conditions, where the total dissolved solids are low (Vinson et al., 2009). Additionally, differences between radium and radon concentrations are also thought to occur because of the differences in distribution of the two species. Radon is produced by the solid phase radium as well as the mobile radium in the groundwater (Yanase et al., 1995). Another factor which can alter the concentration of radon in the groundwater is the physics derived process of adsorption. Where layers of rock are porous and exhibit large surface areas, such as peat, the radon can be adsorbed. Due to the short half-life of radon, all of the isotope decays before the reverse process of desorption occurs resulting in groundwaters having a zero radon concentration. Such a phenomena was observed in the Ruataniwha basin in Hawkes Bay, New Zealand (Morgenstern, van der Raaij, & Baalousha, 2012).

2.3.4 Advantages and disadvantages of radon over existing common measurement techniques

The short half-life of radon, its low solubility and the large difference between radon concentration in groundwaters and surface waters give it many advantageous properties for groundwater – surface water interaction investigations. For example, the naturally occuring gradient between surface water radon concentrations and groundwater radon concentrations makes radon a more versatile tool than methods such as temperature sensing, as temperature gradients are not always present or large enough to be significant. Furthermore, radon concentration measurements are exclusive of water from rainfall and surface runoff as both of these inputs contain negligible concentrations of radon (Cook et al., 2008). Moreover, the relatively short half-life of radon and that it is a gas makes it an ideal tracer to measure short term temporal variations because any radon measured will not be from historical groundwater discharge as the radon will decay and quickly degas when it is discharged to the surface, with degassing being the dominant process. Thus, unlike flow gauging, tracer injection tests and some other hydrochemical parameters, the exact locations or sources of the groundwater discharge can be captured. An additional advantageous attribute of radon measurement is that radon is inert, so it cannot be chemically or biogenically altered between its emanation and measurement. Furthermore, unlike tracer methods, such as CFC gases, there is no restriction of the age of the groundwater to measure radon concentrations for groundwater-surface water interaction. With all these advantageous properties, radon can be used to identify locations of groundwater-surface water interactions, and provides information to quanitfy groundwater discharge rates without measuring porosity, hydraulic conductivity, and the hydraulic gradient (Stellato et al., 2013).

Despite all the advantages of using radon, like all tracers for measuring groundwater and surface water interaction, the use of radon as a hydrochemical tool does have weaknesses. A disadvantage of using radon as a tracer, which applies to almost all other hydrogeochemical tracers, is that rainfall or increased flow can swamp the radon signature in surface water. Paradoxically, when measuring groundwater recharge rates rainfall can cause misleading increased radon concentrations in aquifers. This occurs due to the radon free rain water becoming enriched as it interacts with soils and rocks along flow paths through to the aquifer (Stellato et al., 2008).

The short half life, as well as the low solubility of radon, enables radon in surface waters to be almost negligible in comparison to groundwaters. However, this short half life puts constraints on the time between sampling and measurement in the laboratory. With a half life of 3.8 days (Cecil & Green, 2000) samples need to be analysed as soon as possible. Any time delay, in the order of days, causes a significant decrease of the radon concentration in the water sample and increases the analytical error, with the risk that the radon decays beyond the lower detection limit of the radiation counter.

Whilst not strictly disadvantages, the solubility of radon can cause variation in surface water concentrations depending on the climatic conditions. Turbulent waters, or high wind sampling conditions, can cause radon to degass faster than in calm conditions. Furthermore, very shallow waters are not ideal for sampling as the radon in the water is likely to have degassed. Moreover, like most hydrological measurement tools, the results are reliable on correct sampling procedures being followed. If the correct procedures for radon sampling are not followed there is a risk of the radon sample degassing.

2.3.5 Radon measurement techniques

Further cementing the use of radon as a suitable environmental tracer is its ease of measurement. The measurement technique available for this study is Liquid Scintillation Counting (LSC). Thus the review of the literature will be focused on those which have used this method. However, other methods will be reviewed in brief due to the varying array of applications other such methods allow for.

Radon is predominantly measured using the following different techniques:

- Degassing and Lucas Cell counting
- Measurement of the gamma rays from the daughter products, ^{214}Pb and ^{214}Bi, of ^{222}Rn (Freyer, Treutler, Dehnert, & Nestler, 1997).
- Semiconductor detectors
- Liquid Scintillation counting (LSC). Measurement of the alpha decay from ^{222}Rn and its two daughter products, ^{218}Po and ^{214}Pb, are measured in a low level scintillation counter.

Advantages and disadvantages of different radon measurement techniques

The sensitivities of the three different radon measurement techniques vary quite considerably (Table 2.1). While LSC has the highest counting efficiency (Eappen, 2010), the sensitivities of gamma and Lucas cell methods can be increased by increasing the sample volume. The option of increasing the sample size is not possible for the direct counting LSC method but the radon can be pre-concentrated from larger amounts of water. Experimentation by Belloni et al. (1995), shows that Lucas cells have the lowest lower limit of detection, followed by LSC, with gamma counting having the highest lower limit of detection. The lower limit of detection is important to consider when selecting a radon measurement technique for measuring groundwater-surface water interaction. The lower limit of detection of gamma counting may be suitable for measuring groundwaters in

gravel bed rivers, as they typically have concentrations of greater than 10 BqL^{-1}(Cecil & Green, 2000). However, in a river study by Cook et al. (2003), radon concentrations in river waters ranged from 0.6 to 1.1 BqL^{-1}. The lower limit of detection of the gamma measurement technique would therefore render the technique unsuitable for measuring radon concentrations in such surface waters. LSC has a reduced, lower limit of detection of 0.20 BqL^{-1} (Belloni et al., 1995). Direct LSC would therefore be sufficient for groundwater measurement as well as capturing the approximate location of groundwater discharge into river water.

Table 2.1: Comparison of efficiencies and lower limits of detection of the Lucas Cell, Liquid Scintillation and Gamma counting methods for radon measurement. Image modified from (Belloni, et al., 1995).

Efficiencies, sensitivities, background and LLD of the three investigated methods

	Efficiency		Total Sensitivity (cpm/Bq/l)	BKG (cpm)	LLD (Bq/l)
	Counting (cpm/dpm)	Rn Extraction (%)			
Lucas Cell counting	0.745 ± 0.020	0.925 ± 0.025[a]	23.57 ± 0.898	1.0 ± 0.1	0.02
Liquid scintillation counting	0.912 ± 0.009		$1.64 \quad 0.16$	0.29 ± 0.07	0.20
Gamma counting	0.044 ± 0.001		5.33 ± 0.02	$105 \quad \pm 2$	1.75

LLD formula: 4.66 S.D. (background)/sensitivity.
[a]The Rn extraction efficiency is included in the counting efficiency.

Lucas Cell

To use a Lucas Cell, pictured in Figure 2.6, radon must first be extracted from a water sample through aeration of a carrier gas. The radon enriched carrier gas is then transferred into a Lucas Cell (Eappen, 2010). Therefore the accuracy of the radon measurement will be dependent on the efficiency of the degassing process and transfer of this radon gas to the Lucas Cell. This degassing and transfer process takes approximately five minutes, with only one sample able to be collected and degassed at a time (Belloni et al., 1995). The Lucas Cell is a scintillation cell which is coated with a solid scintillator such as ZnS(Ag) (Lenzen & Neugebauer, 1996). The Lucas cell is then connected to a photomultiplier where the light pulses from the alpha radiation from ^{222}Rn and its daughter products, which exit the bottom of the cell through a glass window, are measured by the light pulses being transformed into electrical pulses (Freyer et al., 1997; Lenzen & Neugebauer, 1996). An advantage of the Lucas Cell is that the equipment to collect the radon sample and transfer it to the cell is portable. Thus the Lucas Cell is suited to grab sample field measurements. However, a time delay of four hours between sample degassing and alpha radiation counting needs to occur to allow the radon and it's daughter products to equilibrate. The counting time of the Lucas Cell is also an advantageous feature as it only needs to be counted for ten minutes (Belloni et al., 1995).

Figure 2.6: Image of a Lucas Cell used for measuring radon. The large circular base of the cell comprises a glass window which will be captured by a connected photomultiplier. Image retrieved from (Lenzen & Neugebauer, 1996).

Gamma ray counting

Gamma ray counting requires the collection of a sample in a modified 1 Litre Marinelli Beaker. The beaker is modified to allow water inflow with the ability of the beaker to have an air tight seal once the sample has been collected (Belloni et al., 1995). After sample collection the beaker can then be directly counted for gamma radiation. Gamma Counting is advantageous as most radiation measurement laboratories have the necessary instrumentation, either a NaI detector or a Ge detector, to measure the gamma radiation from radon (Belloni et al., 1995). The count time for a sample is approximately 15 minutes, which is not that much longer than the count time for the Lucas Cell.

Semiconductor detectors

Semiconductor detectors generally operate with a water sample which is connected to the device as part of a closed system. Air is then circulated through the water, through a desiccant column and then into the radon counter. The continuous flow of air through the water sample enables equilibrium between the air and the water sample to be established. Once equilibrium has been established the radon concentration can be measured (Lee & Kim, 2006). The measurement is done through a semiconductor detector at ground potential which attracts radon's positively charged polonium daughters. The energy measured from the polonium daughters is then used to calculate the concentration of radon in a sample (Burnett et al., 2001; Burnett et al., 2013)

Liquid scintillation counting

In this technique, radon is extracted from a water grab sample using a scintillation cocktail solution (e.g. OPTI-FLUOR® O by Perkin Elmer). The cocktail, or a mixture of cocktail and sample water, is then transferred to a scintillation vial. The alpha decay from ^{222}Rn and its two daughter products, ^{218}Po and ^{214}Pb, is then measured in a low level scintillation counter (Belloni et al., 1995; Cecil & Green, 2000; Freyer et al., 1997). LSC is one of the fastest measurement techniques for processing large numbers of samples and samples can be left unattended whilst the counting process is being carried out (Belloni et al., 1995; Eappen, 2010). Furthermore, per volume of sample, LSC is the most sensitive radon measurement technique. The sampling procedure simply involves collecting water samples into sample bottles without the presence of air (Hahn & Pia, 1991). Unlike the other three

methods described, LSC requires the addition of a mineral scintillation cocktail to transfer the alpha particle into photons that can be detected. LSC also requires a three to four hour time delay between sample preparation, after the addition of the cocktail, and measurement to allow radon and its daughter products to equilibrate. Belloni et al. (1995) describes LSC as the preferred analysis technique when large numbers of samples are to be analysed due to efficient sampling procedure and the attribute of large numbers of samples able to be measured at one time. This conclusion drawn by Belloni et al. (1995) appears to be validated by the large number of studies that have been conducted using LSC (Cook et al., 2003; Cook et al., 2008; Dimova et al., 2013; Gómez Escobar, Vera Tomé, Lozano, & Sánchez, 1996; Hahn & Pia, 1991; Kies et al., 2005; Kiliari & Pashalidis, 2008; Leaney & Herczeg, 2006; Lefebvre et al., 2013; McCallum et al., 2012; Shaw et al., 2013; Stellato et al., 2008; Stellato et al., 2013). However, a disadvantage of the LSC method is its limited sensitivity if it is counted directly. In the direct counting LSC method only 10 mL of sample water is measured. The sensitivity of Lucas cell and gamma counting can be increased because the sample size of these methods can be increased. If a higher sensitivity measurement is required for LSC, the scintillation cocktail must be pre-concentrated in radon by a greater volume of sample water before it is measured. Attempts to overcome the limited sensitivity of LSC are described in more detail in section “Liquid scintillation counting sensitivity” below.

Continuous radon monitors

The LSC method is simple, accurate and relatively cost effective. However, the downfall of the LSC method, and any other grab sampling method, is that only a single measurement of radon is taken. While providing a snapshot, this methodology does not give continuous records to monitor changing temporal variations. To overcome this, continuous measurement sampling techniques, though not being used in my study, are being used more frequently as technological improvements have enabled the measurement sensitivity and accuracy to increase. Continuous measurement devices employ the use of the semiconductor measurement technique. Commercially sold products, such as RAD AQUA and ALPHA GUARDS used in conjunction with AQUA KITS, or similar variations thereof, have been used in a number of studies to measure groundwater inflow into surface water bodies (Burnett et al., 2013; Burnett et al., 2010; Dimova et al., 2013; Dulaiova et al., 2010; Rajashekara et al., 2007). In reference to these continuous measurement techniques, the phrase “continuous radon measurement”, or the like, appear to be used interchangeably with two different types of measurement devices, a continuous grab sample device or a device which has water continuously running and measuring water samples.

Continuous radon measurement has its advantages. However, the establishment of equilibrium and the subsequent output of the radon concentration can take a minimum of 10-15 minutes per sample with modified equipment (Burnett et al., 2013; Dulaiova et al., 2010) and can take as long as 30 minutes. For a full river survey of radon this would be hugely time consuming in contrast to LSC which requires only filling a bottle in the field. Large numbers of samples can then be measured using LSC automatically in the lab as the LSC method allows multiple samples to be measured at once. However, the sensitivity of the continuous radon meter is superior to the LSC method. The lower limit of detection is 0.2 BqL^{-1} for the LSC method, whereas the lower limit of detection is 0.037 BqL^{-1} for the RAD AQUA. The sensitivities are based on similar counting times of 20 minutes. However, the time constraints of taking radon measurements in the field as well as the feasibility of

carrying the portable meter over long stretches of river render the LSC method more suitable for studies where large numbers of samples are taken over a short time period. Furthermore, as the LSC methodology requires collecting a grab sample in the field followed by measurement later in the laboratory, multiple sample collection teams can be deployed at once. This would not be possible if only one continuous measurement device were used.

Liquid scintillation counting sensitivity

A disadvantage of the direct count LSC method is the fact that the sensitivity to which it can measure is limited by the sample size. The standard sampling technique involves the collection of 20 mL water samples, of only which 10 mL is measured. Other radon measurement techniques can alter the sensitivity of the analysis by increasing the sample size. Unfortunately for LSC, even if a greater volume of water sample was collected, only a 20 ml vial can go into the scintillation counter. Measuring radon via the LSC direct count method gives a lower detection limit of only approximately 0.2 BqL^{-1} (Leaney & Herczeg, 2006). However, there have been several attempts to increase the sensitivity of the LSC method.

One method to increase the sensitivity of the radon measurement is to concentrate the radon from a larger amount of water into the 20 mL standard volume of LSC (Noguchi, 1964; Noguchi & Wakita, 1973; Saito & Takata, 1992). Cook et al. (2003) and Kies et al. (2005) both did this by concentrating the radon from a sample bottle size of 950 ml and 250 ml, respectively. The radon in the larger bottles is absorbed into 20 mL of scintillation cocktail, and then transferred into a scintillation vial. Radon has a much higher affinity towards the mineral oil cocktail than water thus radon diffuses from the sample into the mineral oil (Hahn & Pia, 1991). The methodology of Freyer et al. (1997) also uses a 1 litre glass sample bottle with 20 mL of cocktail. In all three methods only the cocktail is removed and placed into the scintillation vial. In the direct count method the scintillation vial contains a combination of cocktail and sample water, normally in a ratio of 1:1. To remove only the added cocktail a Teflon coated separating funnel can be used (Cook et al., 2003; Saito & Takata, 1992). Saito et al. (1992) transfers the bottled sample water to a separating funnel. However, this transfer introduces the risk of significant radon degassing. Cook et al. (2003) overcomes this through directly collecting samples into the funnel. However, Cook's method is not appropriate for my study. This is because the process could not be practical or easy on a large scale as separating funnels are not easily posted/couriered to clients and may be confusing for them to sample with. In addition to this, Cook's method also involves mixing the scintillation cocktail with the sample water after sampling, before sending the sample to the laboratory. Again, such a method which requires the sampler to extract the radon themselves would be impractical on the basis of sending the equipment to untrained people. Furthermore, extracting the cocktail from the separating funnel in the field on a large survey would be difficult, if the sampling was being carried out in a boat or kayak, as well as very time consuming. Therefore there is a need to further develop an easy to carry out, cost effective and easily reproducible, high sensitivity radon analysis method for LSC.

An attempt at a cost effective and practical method which also reduces the uncertainty created in removing the cocktail from a larger volume radon sample was carried out by Leaney and Herczeg (2006). Sampling was carried out in large, 1.3 L to 2.5 L, polyethylene terephthalate (PET) bottles. Once cocktail has been added to the PET bottle the bottle is shaken and left until the cocktail has

separated out on top of the water. The sample bottle lid is then removed and replaced with a glass fitting with a thin, 1 mm, capillary tube. The PET bottle is then squeezed gently. The pressure forces liquid up through the capillary tubing and into the scintillation vial. Because the flow of cocktail out of the sample bottle is easily controlled by the pressure applied by squeezing the bottle, it is easy to remove only the cocktail and no sample water. Increasing the sample size using PET bottles resulted in the lower detection limit being reduced to 3 $mBqL^{-1}$. However, the use of PET bottles results in some loss of radon due to diffusion through the plastic. Despite this drawback, the uncertainty associated with this method is much lower than the direct counting method (the method used when only 20 mL of sample is collected) (Cook & Herczeg, 2000).

Another LSC method to increase sensitivty is a methodology very closely related to the Lucas Cell method. A sample bottle of a chosen size has air circulated through the sample and a scintillation vial, containing 20 mL of cocktail, using a peristaltic pump. The system is closed so only the air in the tubing connecting the pump, scintillation vial and sample bottle is used to extract the radon (Theodorsson & Gudjonsson, 2003). This method is inexpensive to run and gives flexibility in the volume of the sample which can be collected. It also provides a very low detection limit of approximately 5 $mBqL^{-1}$. However, it is quite a time and labour intensive procedure thus would be unsuitable when a large number of samples need processing as would be needed for my study.

Sampling techniques for radon LSC

The chosen radon measurement technique for the studies to be done in the Hutt and Mangatainoka Rivers, LSC, has a simple and efficient sampling procedure. The collection of groundwater or surface water samples is almost always carried out by the standard EPA sampling technique, the modification of this technique by Belloni (1995) or a similar variation thereof. A few of these variations are described below.

Surface water samples are collected through the use of a submersible pump and Teflon tubing. Water is pumped from a specified depth, which is dependent on the depth of the river but predominantly as close to the river bed as possible, and then pumped. The water is transferred through the tubing directly into sample bottles (Cook et al., 2003) with scintillation cocktail added to the sample bottle after the sample has been collected. The bottles are then capped and sent to a laboratory for analysis.

Shaw, White and Gammons (2013) follow an almost identical method. However, to minimise contact of radon in air, they pump the sample water into a bucket. The 250 ml sample bottle is placed into the bucket and the Teflon tubing is placed in the bottle. Once enough water has been passed through the bottle to displace the equivalent of three buckets worth of volume, the sample bottle is capped while still submerged under water (Shaw et al., 2013). The addition of scintillation cocktail and the subsequent analysis of these samples then take place in a laboratory.

To further eliminate radon contact with air Freyer et al. (1997) designed a 1 litre sample bottle with a long narrow neck. They placed 20 mL of cocktail into the sample bottle, inserted Teflon tubing and fed the water sample through this tubing underneath the cocktail in the bottle using a submersible pump (Freyer et al., 1997). The air and river water contact is therefore minimised because the sample water sits underneath the cocktail. Freyer et al. (1997) also conducted tests to see whether

the pumping rate affected the resulting measured radon concentration. Pump rates between 0.15 $m^3 h^{-1}$ and 1.92 $m^3 h^{-1}$ were tested. The measured radon concentrations were found to be unaffected by the rate of pumping (Freyer et al., 1997).

In other studies samples are syringed directly from the Teflon tubing. The syringed river water is then transferred from the syringe to the sample bottle (Belloni et al., 1995; Stellato et al., 2013).

Groundwater radon samples are collected in much the same way and follow the same principles as those outlined by in the standard national groundwater quality sampling protocols (Daughney et al., 2006). Either a pump is submerged down a well or a tube is connected to the water faucet. The tube can either be placed into a bucket, directly into a sample bottle or have water removed from it with a syringe (Belloni et al., 1995).

In summary, sampling techniques are required to minimise the sample waters contact with air. Glass or Teflon coated sample bottles are also used to prevent diffusion of the radon gas. This is especially important when LSC is used to measure the radon as there is often a time delay of several days between sample collection and analysis.

2.4 Applications of radon as a hydrogeological tool

Regardless of the technique used, sampling and measuring groundwaters or surface waters for radon is relatively simple. Perhaps this is one of the reasons why radon is increasingly being used in a number of different groundwater-surface water interaction studies (Burnett et al., 2001; Burnett et al., 2013; Burnett et al., 2010; Cook et al., 2003; Dimova et al., 2013; Dulaiova et al., 2010; Hammond et al., 1977; Hoehn & Von Gunten, 1989; Kies et al., 2005; Rajashekara et al., 2007; Santos & Eyre, 2011; Stellato et al., 2013). A few of these studies are reviewed and summmarized below. These studies demonstrate a variety of applications in which radon has been used as a hydrological investigative tool.

The groundwater discharge patterns in lakes has been investigated using radon as a tracer. In Cambodia, the Tonle Sap Lake, is cut off from the Mekong River in the dry months. Using radon as a tracer the lake could be treated as a closed system, as radon's half-life is so short. The only inputs of radon to the Lake are from groundwater inflow and radon released from sediments. The outputs of radon are due to isotopic decay and degassing. A study of radon concentrations over the lake allowed the radon flux to be calculated by finding the differences between the radon inputs and outputs. Using these fluxes and known radon concentrations in groundwater from surrounding wells, total groundwater discharge into the lake was calculated (Burnett et al., 2013). Electrical conductivity was measured in conjunction with radon in the Tonle Sap Lake. Burnett et al. (2013) found an inverse relationship between radon concentrations and electrical conductivity. Usually groundwater is associated with higher electrical conductivities than surface waters. However, in this study area the opposite relationship was found. The low electrical conductivity measurements found in conjunction with the high radon concentrations aided in confirming Burnett et al. (2014) findings of groundwater contributions to the lake. Electrical conductivity is an easy and cost effective parameter to measure. This parameter should be considered for my study in the Hutt and Mangatainoka Rivers. However, it requires a significant difference between the electrical

conductivities of the groundwaters and surface waters for any indication of groundwater discharge to be identified.

A similar study in several Florida lakes was carried out by Dimova et al. (2013). They used radon in combination with methane concentrations and electrical conductivity, to find areas of groundwater discharge into the lakes. Using these paramaters a groundwater discharge model could be built using a mass balance box model approach (Fig. 2.7). Unlike the study carried out in Cambodia by Burnett (2013), Dimova et al. (2013) included the end member radon concentration in the mass balance by measuring ^{222}Rn in the groundwater pores and the ^{222}Rn and ^{226}Ra in sediment samples from the lake. Suspended ^{226}Ra in the lake water was also measured (Dimova et al., 2013).

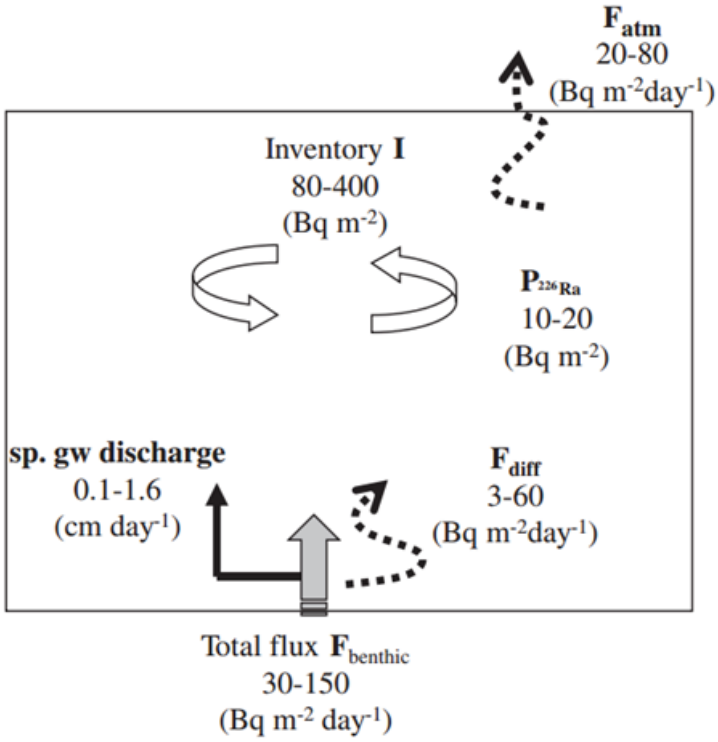

Figure 2.7: Diagram representing a box model of radon inputs and outputs used for the mass balance approach of calculating groundwater flux in Florida Lakes. Image retrieved from (Dimova et al., 2013). The inputs into the model include the radon measured in the lake water multiplied by the depth to provide the radon inventory *(I)*, radon contributions from groundwater discharging into the lake *($F_{benthic}$)* and the contribution of radon from dissolved ^{226}Ra *(F_{diff})*. Outputs of radon from the model is from atmospheric evasion *(F_{atm})*.

Finding the groundwater discharge rates and flux is important as it enables the nutrient concentrations being discharged by groundwater to be established (Burnett et al., 2013; Burnett et al., 2010; Dimova et al., 2013; Dulaiova et al., 2010; Santos & Eyre, 2011). However, an extensive study of Georgetown Lake, using radon, stable isotopes, water quality indicators and major ion chemistry, showed that groundwater discharge and recharge rates cannot be calculated without the parameters of ^{222}Rn diffusive flux from sediment and ^{222}Rn depth integrated samples (Shaw et al., 2013). However, the study did provide a useful map of radon discharge indicating where the

groundwater was entering the lake. As expected, these radon hotspots were found along the fault line edge on the lake, where groundwater discharges through fractured limestone.

Radon mapping can also be used to find areas of submarine groundwater discharge in harbours or coastal waters. The purpose of knowing where these areas are is that they can indicate sources of non-point source pollution (Dulaiova et al., 2010). In a study by Dulaiova et al. (2010) a modified, continuous radon measurement device was used in conjunction with continuous measurement of methane and dissolved inorganic nitrogen (DIN) in Boston Harbour and Waiquoit Bay, Massachusetts. Although methane is affected by biochemical and microbial processes, it could be sampled with the continuous measurement device at shorter intervals than radon. Methane is found in higher concentrations in groundwater than surface water (Dimova et al., 2013). This is because the production of methane is prevelent in anoxic groundwater systems where organic material is present. Thus areas where higher concentrations of methane are measured supports the assertion of groundwater discharge locations identified by higher measured concentrations of radon. The combination of the measured datasets thus gives a good representation of groundwater discharge as randon sampling alone produces smoothed data due to the time delay in sequential samples. The dissolved inorganic nitrogen (DIN) was found to be high at several radon hot spots concluding that radon is a good tracer to locate non point source pollution.

Hammond et al. (1977) investigated transport of radon across the sediment-water interface in the Hudson River Estuary. By estimating the rate of gas exchange in the Hudson River they could construct a mass balance for radon. Throughout the study they found temporal changes due to tidal patterns as well as significant temporal changes with no apparent explanation. Their best guess for the significant changes in radon concentrations, and thus groundwater discharge, was due to the slumping or dredging of the sediment in the river. This is significant for my chosen case study areas. The Hutt River feeds into the Wellington harbour and has a tidal influence. Also, both case study areas are gravel bed rivers. The flow path of these gravel bed rivers is often reworked after heavy rainfall/high flow which could lead to significant temporal changes in radon concentrations.

Another application of radon is to indicate when an observation well is adequately purged so groundwater samples can be taken (Freyer et al., 1997). The well can be assumed as adequately purged when radon concentration measurements are consistent. However, this application would not be applicable to the LSC method that I am using in my study, as real time measurements are required. If a continuous radon measurement device were being used then this application would be useful.

A further application of the use of radon as a tracer is for measuring hydrograph separation in storm events (Kies et al., 2005). The saturated zone will have a higher radon concentration than the unsaturated zone due to radon degassing in the soil pore space of the unsaturated zone (Kies et al., 2005). Kies et al. (2005) demonstrated that in a micro-basin in the Attert River catchment in Luxembourg radon concentrations of an ephemeral stream increased with rainfall (Fig. 2.8). This increased radon concentration with rainfall relationship occurs because the rainfall increases the hydrostatic pressure and thus raises the water table. Radon-rich water, which is housed in underground fracture zones but not normally in direct flow paths, is forced to the surface. Electrical conductivity was also meausured before, during and after rainfall events in conjunction with radon.

Electrical conductivity often decreased during rainfall events where radon concentrations increased. The phenomena is likely caused because the electrical conductivity is reduced by surface runoff. The increased radon concentrations occur after a slight time delay to the electrical conductivity decrease when the radon rich water is discharged through hydrostatic pressure changes (Kies et al., 2005). Thus Kies et. al. (2005) demonstrated that radon could be used to show hydrograph separation and pathways by which water discharges into a river before, during and after a rainfall event.

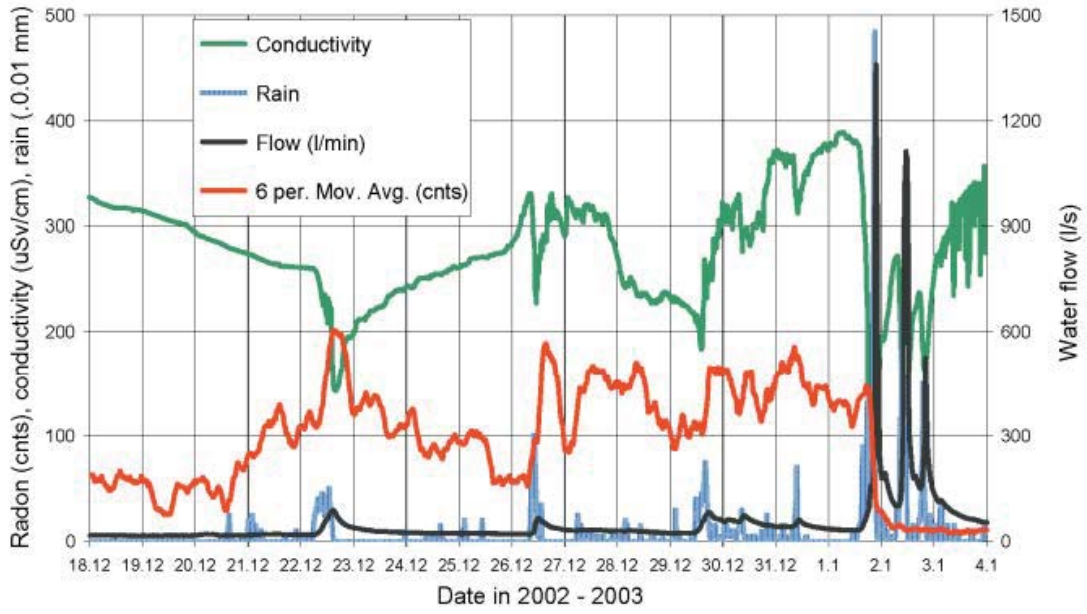

Figure 2.8: River water radon (red) and electrical conductivity (green) versus time measured at an ephemeral stream in Luxembourg at the outflow of the micro basin area. After 2 January the radon measurement device became faulty and reading beyond this date should be ignored. Image retrieved from (Kies et al., 2005).

The application of radon most important to my study is to measure and map groundwater interaction between groundwater and surface water in a river. There have been several studies undertaken to measure groundwater recharge and discharge into rivers, all of which use a number of tracers, not just radon in isolation, to draw the conclusions of their study. For example, Cook et al. (2003) used a mass balance approach using radon, CFCs, electrical conductivity, temperature and flow gauging to constrain a model to find rates of groundwater discharge to a lowland river in the Northern Territory of Australia. The parameters measured in addition to radon validated the conclusions drawn by the radon measurement. The Cook et al. (2003) study demonstrates that a multi-tracer approach should be used. However, age dependent parameters are not suitable in my study of the Hutt River as the age of the water in the Lower Hutt groundwater system is between 0.5 and 3.5 years old (Stewart & Morgenstern, 2001). This is important to consider for my studies in the Mangatainoka and Hutt Rivers, as I will need to find other suitable parameters to confirm my conclusions found through radon measurements.

Another multi-tracer investigation was undertaken by Burnett et al. (2010). Groundwater flux was calculated in man made canals in Florida using continuous radon measurements in combination with an acoustic current meter. Current meter readings were combined with cross sectional

measurements of the sites to give flow. Corrections were made to the flux with ^{226}Ra meaurements in the canal water and measuring the radon end member concentration (Burnett et al., 2010). Burnett et al. (2010) shows that the combination of radon measurements with current flow data provides good information on the discharge of groundwater. Therefore, the measurement of flow should be incorporated into my study sampling method of both the Hutt and Mangatainoka Rivers.

In Luxembourg the spatial variability of a tributary of the Colpach River was investigated using radon and salt tracers (Angermann et al., 2013). While radon provides insight into where the groundwater is flowing, the salt tracer allows for the determination of the loss/gain between sections of the tributary and travel time. The salt tracer can also account for hyporheic exchange, which can be missed by radon measurements alone. Angermann et al. (2013) found high spatial variability in discharge quantity and composition down to the scale of few metres. This short spatial variability needs to be considered when deciding upon the distance between the radon sampling points in the Hutt and Mangatainoka Rivers. If such short spatial variability also exists in my case study areas then groundwater discharge or other river characteristics could be overlooked if the distance between samples is too large.

Most literature using radon in rivers uses elevated radon concentrations in surface waters to find areas of groundwater discharge. Radon at the source of the discharge into the river in Cook et al. (2003) study was found to be between 3-10 BqL^{-1} and approximately 8.7 BqL^{-1} in Burnett et al. (2010) study. However, Stellato et al. (2013) used radon to find groundwater recharge locations and rates. Their study is based on the fact that surface water, with little or negligible radon concentration, entering the groundwater system will be enriched in radon until it reaches equilibrium with the groundwater concentration. Equilibrium is likely to be reached after approximately 3 weeks which is equivalent to 5 half-lives (Asikainen, 1981). Stellato et al. (2013) collected surface water from the river and groundwater samples from nearby wells. The study showed that recharge rates were dependent on hydraulic head fluctuations of both the river and the aquifer. Contradictory to the finding of Shaw et al. (2013), Stellato et al. (2013) were able to find the infiltration velocities of the surface water through the sampling transect without the parameters of ^{222}Rn diffusive flux from sediment and ^{222}Rn depth integrated samples. The velocities and inflow rates were calculated by also combining the radon tracer measurements with $\delta^{18}O$ and total dissolved solids measurements. Using these three tracers a mixing model was constructed to establish water recharge and velocity (Stellato et al., 2013).

A New Zealand case study of using radon to measure groundwater recharge locations and velocities has been carried out in the Wairau River in Marlborough (Close, 2014). In this study grab samples were taken from four different sites in the Wairau River and in 11 shallow wells within 5 km of the river. The grab samples were then sent to the laboratory and measured using LSC. Temperature, dissolved oxygen and pH was also measured in addition to radon. Using an ingrowth model with optimised equilibrium radon concentrations, the groundwater velocity and the travelling distance, Close (2014) was able to determine the groundwater recharge velocities for two zones of groundwater seepage, 94 m day^{-1} and < 25 m day^{-1}.

Another study worth noting using radon in rivers is a recent study by McCallum et al. (2012). Differential flow gauging was taken at numerous sites along three rivers to measure groundwater

discharge. To determine net flow and gross flow other hydrochemical parameters, including radon, chloride and electrical conductivity, were chosen to estimate a mass balance. These etimates were then used to build and constrain a flow model (McCallum et al., 2012). The gas transfer velocity rates were also measured in this study through the injection of SF_6. Not only does McCallum's study reiterate the point that the ^{226}Ra concentration does not need to be known, but it also reinforces the idea, like almost all other literature mentioned, that a multi-variable/tracer approach is best used if radon is to be used to quantify groundwater discharge rates rather than just spatially identify where the groundwater inflow points are. Additionally, the multi-tracer approach enabled the hyporheic flow to be accounted for as well.

McCallums et al. (2012) study emphasises the point addressed by many of the studies previously mentioned, that more than one type of tracer needs to be used to find useful and reliable information relating to a study site. This concept of a multi-tracer approach is one that needs to be carried through into my studies. Parameters other than just radon will need to be collected in the Hutt and Mangatainoka Rivers to enable reliable conclusions to be drawn from the collected data. This is particularly important for sampling when flow or rainfall conditions change.

Estimating groundwater flux is the ultimate end goal for taking radon measurements. Flux calculations undertaken in rivers are more complicated than those estimated in lakes, where a closed system, relative to radons half-life, can be assumed. In the literature discussed in this review where groundwater flux is calculated several assumptions need to be made when measuring radon (Dimova et al., 2013; Hoehn & Von Gunten, 1989; Stellato et al., 2013):

1) The average distribution of the radon's parent material, ^{238}U and ^{226}Ra, is homogeneous on a macroscopic level.

2) A constant ^{222}Rn input flux occurs on a short temporal scale.

3) ^{222}Rn is well mixed through the water column.

4) The losses of ^{222}Rn between the saturated zone and unsaturated zone are constant or negligible.

Groundwater flux will not be calculated in the studies of the Hutt and Mangatainoka Rivers carried out in this thesis. However, these general assumptions for radon measurements are important to consider as natural progression of the studies being carried out in the study rivers will be to use radon concentrations to estimate groundwater discharge quantities in the future.

2.5 Chapter summary

Measurement of surface water and groundwater interactions has been gaining increasing attention to understand the connectivity and dynamics of these two seemingly isolated yet highly interdependent systems. This is helping to further develop integrated management of water resources and the influence of nutrient inputs to water quality. A number of techniques such as differential flow gauging, temperature sensing, tracer injection tests, and environmental tracers have been developed and used to measure groundwater and surface water interactions. One such measurement technique is the analysis of radon-222 concentrations in surface waters and groundwaters.

Radon is a chemically and biogenically inert gaseous product of the Uranium decay series. This gaseous product is a versatile, hydrological investigative tool which has many advantages over other common measurement techniques for measuring groundwater and surface water interaction. Radon's short half-life of 3.82 days and its low solubility enable it to be useful for capturing the locations of short term spatial interactions between groundwater and surface waters, rendering radon advantageous over other measurement methods such as flow gauging and tracer injection tests. Unlike some tracers which are dependent on measurable gradients between surface water and groundwater, such as temperature sensing or some hydrochemical tracers, a gradient in radon concentrations between groundwater and surface waters almost always exists. This gradient in radon concentrations between surface waters and groundwaters occurs because radon is a soluble gas and thus is present in groundwaters. However, it quickly degasses when it comes into contact with air, causing concentration differentials between surface waters and groundwater.

While most groundwater-surface water measurement methods have desirable characteristics as an investigative tool, they also have challenges and weaknesses, with radon being no exception to this. Radon concentrations can be diluted to negligible concentrations during periods of heavy rainfall or increased flow. Moreover, due to the short half-life of radon, it is critical that a time delay of no more than several days between sample collection and measurement occurs. Furthermore, several assumptions, including the homogenous distribution of radon's parent material as well as homogeneous mixing through the water column, need to be made. Despite these limitations, radon concentration measurements can, and have, been used to locate areas and calculate flux of groundwater discharge into surface water or the reciprocal recharge into groundwater aquifers. Ideally such interactions are best measured using a multi tracer approach as radon concentrations can be influenced by rainfall patterns. To further exploit the advantageous properties of using radon as tracer, further work needs to be done to find a cost effective, reliable and reproducable high sensitivity Liquid Scintillation Counting method. Once this is established radon profiling will give more insight into areas of a river which are gaining, and/or losing and which are subject to hyporheic exchange.

Chapter 3 - Development of a high sensitivity radon measurement method

3.1 Introduction

Liquid scintillation counting (LSC) is the most efficient and sensitive measurement technique for measuring large numbers of radon samples (Belloni et al., 1995). The standard LSC method involves mixing approximately equal proportions of sample water and a scintillation cocktail in a 20 mL scintillation vial. The scintillation cocktail is made up of two components: a solvent and a solute containing fluor molecules. When sample water is mixed with the scintillation cocktail the radon from the sample water partitions preferentially to the solvent. The scintillation vial is then left to stand for three hours to allow for regrowth of the daughter products before being measured in a low level scintillation counter. The radon is measured through the alpha decay from radon and it's two daughter products (Belloni et al., 1995; Hahn & Pia, 1991; Kies et al., 2005; Leaney & Herczeg, 2006). The measurement of radon is achieved through the second component of the scintillation cocktail, the solute containing fluor molecules. When an alpha particle is released from radon or its daughters, ^{218}Po and ^{214}Pb, the kinetic energy of the alpha particle is absorbed by the solvent, which in turn can transfer this energy to the solute. This raises the solute to an excited state. To return to the ground state the solute releases a photon of UV light. The photons measured relates to the amount of dissolved radon in the solvent (University of Wisconsin - Milwaukee, n.d). Radon samples prepared in this way have a lower limit of detection of approximately 0.2 BqL^{-1} (Leaney & Herczeg, 2006). This relatively poor sensitivity of the LSC method limits its application for measuring surface water samples that are low in radon concentration close to, or below, the detection limit of the direct count LSC measurement.

3.1.1 Objectives

The main objective of this chapter is to develop a cost and time effective, reproducible method for high sensitivity radon measurement which can be applied to large scale radon surveys. This chapter first evaluates what has already been done to produce higher sensitivity radon measurements and the limitations of such methods. Variations in methodology to enrich scintillation cocktail with radon are trialled with the effects of sample size, sample bottle shape, cocktail volume, head space in the sample vessel, enriched cocktail extraction method and shake time, on the sensitivity of the radon measurement evaluated. A new high sensitivity radon method is then detailed and discussed. The high sensitivity method developed in this chapter aims to overcome major drawbacks of the already established high sensitivity radon measurement methods and further increase the sensitivity of radon measurement.

3.1.2 Established high sensitivity methods

Efforts to increase the sensitivity of the radon measurements have been undertaken by many researchers by developing methods to enrich scintillation cocktail in radon with a greater volume of sample water (Leaney & Herczeg, 2006; Noguchi, 1964; Noguchi & Wakita, 1973; Saito & Takata, 1992). In 1964 Noguchi published a method wherein 1 L of sample water is mixed with toluene. (Leaney & Herczeg, 2006). The radon enriched mineral cocktail is then separated from the sample water using a separating funnel and placed in a scintillation vial containing a scintillation solution. Other researchers have further developed this method (Horiuchi & Murakami, 1981; Noguchi & Wakita, 1973; Saito & Takata, 1992). The development by Saito et al. (1973) came in the form of

using a 500 mL separating funnel and 30 mL of toluene. They employed almost exactly the same method as Noguchi (1964) but used weight instead of volume to calculate the radon concentration of the sample and improved the Noguchi (1964) radon concentration equations by incorporating the temperature dependence of the solubility of radon in toluene.

More recently, Cook et al. (2003) used separating funnels in the field. They collected 950 mL of sample water in 1 L Teflon coated separating funnels and added 20 mL of scintillation cocktail to the funnel in the field. The funnel is shaken and then the cocktail is extracted and placed in a scintillation vial. This method produced an extraction and measurement efficiency of 49% (Cook et al., 2003). To produce a higher sensitivity radon method which provides an improvement over that developed by Cook et al. (2003), an extraction and measurement efficiency of greater than 49 %, without increasing the volume of sample water, is preferable. The in-field extraction process has the advantage of not having to carry large volumes of sample water during the survey as once the radon enriched mineral cocktail has been extracted from the separating funnel the remaining sample water can be discarded. However, there are several steps within this methodology which make it undesirable as a cost and time effective, reproducible method for high sensitivity radon measurement. Adding the scintillation cocktail and subsequently extracting the radon enriched cocktail from the separating funnel in the field would be time consuming. If large numbers of samples are to be collected in one sampling event a fast sampling method is desirable. Performing this process in the field would also be difficult if, for example, it were windy, raining or sampling was being carried out from kayaks. Furthermore, the higher sensitivity radon method needs to be simplistic enough that it can be reproduced easily and cost-effectively by sampling staff following simple instructions. For sending samples to the lab, couriering or mailing scintillation cocktail is undesirable as the conditions in which it is stored or handled are variable. It would be hazardous to mail handlers if the organic scintillation cocktail were to leak. Lastly, Teflon separating funnels are approximately thirty times more expensive than glass sample bottles.

Another method which uses separating funnels to increase the sensitivity of radon measurements was carried out by Freyer et al. (1997) which varies in how the water sample is collected and how the mineral cocktail is added. The sample is collected in a modified glass volumetric flask with an elongated neck (Fig. 3.1). First, 20 mL of cocktail is added to the flask, and then the volumetric flask is filled with sample water using a glass tube in such a way that the water fills the flask from underneath the cocktail and does not come into contact with air. The glass sample bottle is then transported to the laboratory, where it is shaken for ten minutes and then the cocktail extracted. This method advantageously produces a lower detection limit for radon of approximately 0.05 BqL^{-1}. However, it has similar draw-backs to that of the Cook et al. (2003) method. Such drawbacks include the cost of the sample bottles, the difficulty of sampling and the transportation of scintillation cocktail out of the lab and into the field.

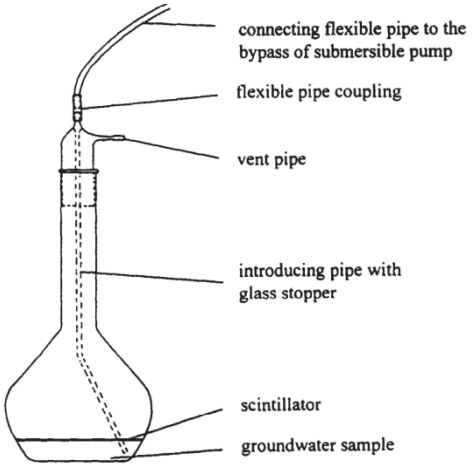

Figure 3.1: Schematic of the sample collection procedure using a modified glass volumetric flask. Image retrieved from (Freyer et al., 1997).

Leaney and Herczeg (2006) developed an enriched radon extraction method which does not use separating funnels. Their method uses 1 L polyethylene terephthalate (PET) bottles to collect a water sample. Once the sample is collected, 50 mL of sample water is removed with a syringe. Scintillation cocktail, 20 mL, is then added to the sample before it is shaken for 4 minutes. The plastic cap of the sample bottle is then removed and a glass nozzle with capillary tubing is placed on the bottle. The plastic bottle is then squeezed and the pressure forces the enriched mineral cocktail out of the PET bottle and into a scintillation vial for counting (Leaney & Herczeg, 2006). The lower limit of detection achieved using this method is 0.003 BqL^{-1}. The advantage of using PET bottles for sampling is that they are easily available and can be obtained in supermarkets. Therefore, sample bottles do not need to be sent out for radon surveys. Furthermore, the addition of the mineral cocktail can occur either in the laboratory or the field. However, the major drawback of this sampling method is that radon gas can diffuse through PET bottles. Radon lost through diffusion in the samples tested by Leaney and Hercezeg (2006) ranged from 1-10% over the first hour of storage (Leaney & Herczeg, 2006). However, the percentage of loss through diffusion is greatly dependent on the type of plastic bottle, the storage temperature and the area to volume ratio of the bottle. A correction to the measured samples would need to be made for the amount of radon lost through diffusion, which would be dependent on the type of bottles used and the storage temperature.

Despite the advancements made in improving the ability to increase the sensitivity of LSC radon measurements, there is still a need for further development. The existing methods appear to have limitations in fulfilling all of the requirements of being reproducible, robust, as well as cost and time effective, and can be applicable to large scale radon surveys in low radon concentration environments.

3.1.3 Calculating radon concentrations – general theory

To understand why enriching the scintillation cocktail in higher concentrations of radon will produce more accurate measurements, one firstly needs to know how radon is measured and calculated. In all the calculations used it is assumed that there is no chemo luminescence occurring.

Radon is calculated from the measured alpha decays from radon and it's two daughter products, ^{218}Po and ^{214}Pb, counts per minute (cpm), in a sample, relative to a calibrated standard to obtain the absolute concentration in becquerels per litre (BqL^{-1}). The Rn concentration needs to be corrected for Rn decay between the time of sampling and measurement. Radon concentration is calculated similarly to the calculation of the tritium concentration in Morgenstern & Taylor (2009), equation 1:

$$C = C_{0s}\frac{n_g - n_b}{n_s - n_b}\frac{1}{Z}e^{-\lambda t_0} \qquad \text{Equation 1}$$

where, C is the radon concentration at sample collection time t, C_{0s} is the concentration of the radon standard water, n_g, is the gross count rate for the radon sample, n_b and n_s are the count rates for the background sample and standard water, Z is the enrichment factor, λ is the radioactive decay constant of radon and t_0 is the time difference between the sampling and measurement. Direct counting samples, which follow the standard EPA procedure with 10 mL of sample water and 10 mL of mineral cocktail (Hahn & Pia, 1991), are not enriched and therefore Z is equal to 1.

The error of the radon measurement is calculated to one sigma standard error according to the equations (2) and (3) adapted from Morgenstern & Taylor (2009) as follows:

$$\frac{\sigma(C)}{C} = \sqrt{\left[\frac{\sigma(n)}{n}\right]^2 + \left[\frac{\sigma(n_s)}{n_s}\right]^2 + \left[\frac{\sigma(Z)}{Z}\right]^2 + \left[\frac{\sigma(P)}{P}\right]^2} \qquad \text{Equation 2}$$

where P is the reproducibility error of sample preparation and n is the net sample count rate. The counting error $\sigma(n)$ according to the Poisson statistics is given by equation (3)

$$\sigma(n) = \sqrt{\frac{n + n_b}{t_s} + \frac{n_b}{t_b}} \qquad \text{Equation 3}$$

where, t_s is the length of time in minutes the sample was measured, and t_b is the length of time in minutes the background was measured. Where a direct count sample is measured, the enrichment error, $\sigma(Z)$, can be ignored as there is no enrichment process.

Figures 3.2a and 3.2b below demonstrate how n, n_b, t_s and t_b affect the uncertainty of the radon measurement. The longer the counting time, t_s and t_b, the lower the uncertainty (Fig 3.2a). However, given the short half-life of radon, a counting time longer than 100 minutes would become impractical. Furthermore, the closer the net sample count rate n is to the background count rate n_b, the greater the error in the sample measurement (Fig. 3.2b). Thus for samples which have a low net count rate the water sample needs to be enriched (Z). However, enriching the sample adds an additional error, $\sigma(Z)$. Therefore, high concentration radon samples are more accurately measured without enrichment.

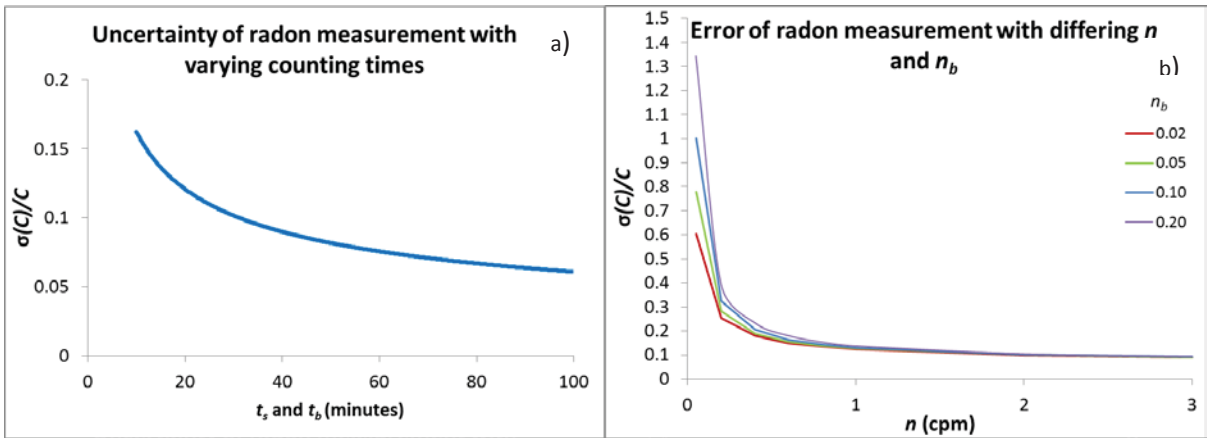

Figure 3.2: Theoretical, graphical representation of how the uncertainty calculated by equations 2 and 3 changes with counting time t_s, and t_b when t_s and t_b are equal, (a) and the net count rate of the sample, n, (b), wherein the radon sample measured has a concentration of 0.5 BqL^{-1}.

Scintillation cocktail can be enriched in radon by mixing the cocktail with a larger volume of sample water. The enriched cocktail is then extracted, placed into a scintillation vial and measured in a low level scintillation counter. The enrichment (Z) can be calculated by comparing the count rates of enriched samples with direct count samples of a known concentration (Equation 4)

$$Z = \frac{n_{enr}}{n_{dir}} \qquad \text{Equation 4}$$

where, η_{enr} is the net count rate for the enriched sample and n_{dir} is the net count rate for the direct count sample.

The enrichment factor, Z, is given by Equation 5

$$Z = \frac{n_{enr}}{n_{dir}} = \frac{V_s}{10} \times \eta_{TTE} \qquad \text{Equation 5}$$

where, V_s, is the volume of sample water used for enrichment, which is divided by the volume of the measured standard, and η_{TTE} is the total transfer efficiency of the radon from the sample water to the scintillation vial.

The total transfer efficiency, η_{TTE}, is the product of the efficiency of the radon transfer from the sample water to the scintillation cocktail, η_{TSW}, and the efficiency of the transfer of the enriched cocktail into the scintillation vial, η_{TEC} , (Equation 6).

$$\eta_{TTE} = \eta_{TSW} \times \eta_{TEC}$$ Equation 6

The efficiency of the transfer of the radon enriched cocktail into the scintillation vial, η_{TEC}, is calculated by the division of the volume of scintillation cocktail transferred from the sample bottle into the sample vial, $V_{(Scint)}$, by the volume of scintillation cocktail mixed with the sample water, $V_{Tot(Scint)}$ (Equation 7).

$$\eta_{TEC} = \frac{V_{(Sc\,\mathrm{int})}}{V_{Tot(Sc\,\mathrm{int})}}$$ Equation 7

The effect of changing the sample volume used for enrichment, V_s, as well as the total transfer efficiency, η_{TTE}, as used in equations 5, 6 and 7, is demonstrated in Figure 3.3a below. The greater the sample volume, V_s, and the higher the total transfer efficiency, η_{TTE}, the higher the enrichment factor, Z. A higher Z, will increase the net count rate, n, and thus reduce the error of the measured radon concentration (Figure 3.3b). This reduced error will lead to a lower limit of detection for LSC for high sensitivity radon measurement.

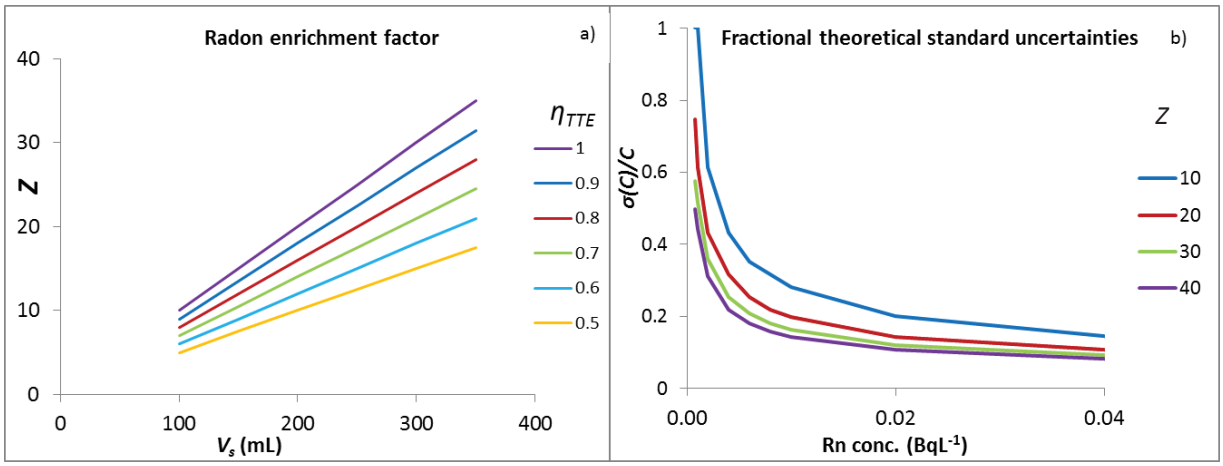

Figure 3.3: Theoretical enrichment factor, *Z*, of an enriched radon sample when differing volumes of sample water, V_s, and total transfer efficiencies, η_{TTE}, are used (a) and the fractional theoretical standard uncertainties of an enriched radon sample based on theoretical values of the enrichment factor, *Z*.

Another factor which can affect the measurement uncertainty and lower limit of detection is the counting efficiency of the QUANTULUS liquid scintillation counter, η_{QC}. From Figure 3.2b it can be seen that samples which have a higher measured cpm have a lower associated error. Thus low level scintillation counters which are optimised to give the highest counting efficiency will have a lower error, wherein the counting efficiency, η_{QC}, is given by equation 8.

$$\eta_{QC} = \frac{cpm}{dpm}$$ Equation 8

where, *cpm* is the measured counts per minute of a sample and *dpm* is the known disintegrations per minute of the same sample.

The error of the enrichment can be calculated by performing reproducibility tests, i.e. $\sigma(Z)$ is calculated by the standard deviation of repeated measurements.

When calculating the error for the concentration of the enriched samples the sample preparation error, P, can be ignored. This is because any error in the sampling procedure will be taken into account by the mean of the enriched samples and thus the calculation of $\sigma(Z)$.

3.2 Methods and materials

Theoretical consideration described (Equations 5-7) above demonstrate that to produce an optimum high sensitivity radon measurement method, the sample volume needs to be increased and the radon transfer efficiencies need to be optimised. The radon transfer efficiencies are controlled by a number of physical variables including: the volume of sample water used, the volume of scintillation cocktail used, the volume of air space in the vessel when the cocktail and sample water are shaken together and the extraction method. This section describes these different parameters and the ways in which they were tested to develop a high sensitivity radon measurement method. The high sensitivity radon measurements were tested in conjunction with the standard direct counting procedure (Hahn & Pia, 1991) to ensure a comparison and assess the improvement achieved. A high sensitivity radon measurement method is deemed to be the most successful when it provides the smallest measurement errors in comparison to the direct counting method. Furthermore, the sample preparation error of the developed high sensitivity method must be smaller than the direct count method and must also be minimal otherwise the sensitivity of the method will be reduced.

3.2.1 Water sampling procedures for all testing

The water sampling procedures for the high sensitivity measurements and the 25 mL direct count measurements are the same, with the exception of the sample bottle size and the method of flushing out any water exposed to air.

The initial sample water for high sensitivity methodology testing was tap water from the water dating lab at GNS Science, located in the Lower Hutt, North Island. Tap water in the Lower Hutt is pumped directly from the aquifer and is relatively high in radon, ranging approximately from 25 to 35 BqL^{-1}. Therefore, provided all water samples used in comparison to one another were sampled at the same time, tap water was considered suitable to be used for initial tests. Tap water samples were collected using the following methodology:

- Tubing is attached to a tap and placed inside a beaker greater in height than the sample collection bottle.
- The tap is turned on to allow the beaker to overflow with water.
- Once the beaker has over filled around three times its volume a radon sample bottle of varying size, depending on the experiment being conducted, is placed in the beaker.
- The tubing is then placed inside the sample bottle to allow any sample water which had been in contact with air to be flushed out.
- After overflowing the sample bottle approximately three times its volume the bottle is capped underwater.
- The sample must be free of air bubbles or else the sample must be discarded and the sampling procedure repeated.

Following the initial tests, samples were collected directly from the groundwater well R27/1183, the Avalon Studios in the Lower Hutt. The same sampling methodology as described above was used with the addition of the well being purged before sampling.

Reproducibility tests to establish whether the sample preparation procedure in the lab could be reproduced in the field in rivers were conducted. Field samples were collected using the following methodology:

- A sample bottle is submerged in flowing river water and the cap removed.
- To remove any sample water in the bottle that has been in contact with air a small object, such as a stick or glass rod, is pushed in and out of the bottle.
- The sample bottle is capped while still submerged under the flowing river water.
- The sample must be free of air bubbles or else the sample must be discarded and the sampling procedure repeated.

3.2.2 Standards and background preparations and testing

Analysis of all direct count and high sensitivity radon samples was conducted in a low level liquid scintillation counter, QUANTULUS Liquid Scintillation Spectrometer from Perkin Elmer. Whenever a sample was measured a background sample and a standard sample was also measured**.**

Three standards were prepared for the radon analysis using a standard radium-226 sample with a concentration of 17.82 $BqmL^{-1}$. The standards were prepared using a balance sensitive to four decimal places in grams. Standards were mixed with OPTI-FLUOR® O by Perkin Elmer and radon free water in the following quantities:

- ^{222}Rn standard 1: 1.0031 g of ^{226}Ra solution, 9.00 g radioactively dead water, 10 mL OPTI-FLUOR O
- ^{222}Rn standard 2: 1.0008 g of ^{226}Ra solution, 19 mL OPTI-FLUOR O – no dead water added
- ^{222}Rn standard 3: 1.0311 g of ^{226}Ra solution, 20 mL OPTI-FLUOR O – no dead water added

The direct count samples have 10 mL of scintillation cocktail and 10 mL of sample water in the scintillation vial. The high sensitivity radon samples are likely to comprise 20 mL of cocktail and no water. The purpose of preparing standards with varying quantities of scintillation cocktail was to determine the counting efficiency close to the anticipated cocktail volume of 20 mL without water. Standard 3 was prepared so it would contain 20 mL of scintillation cocktail only. To prepare standard 3, 1.0311 g of ^{226}Ra solution was placed into a scintillation vial. The vial was then placed in an oven at 65 °C for approximately four hours to allow the water from the ^{226}Ra solution to evaporate. Every 10-20 minutes the vial was swirled so that all of the radium remained dissolved in water. When nearly all of the water had evaporated, the sample was removed from the oven and 20 mL of cocktail was added. While nearly free of water (similar to the anticipated sample cocktails), this cocktail contains a calibrated amount of Ra for measurement of the counting efficiency of a cocktail without water.

To determine whether the differing volumes of cocktail placed in the QUANTULUS for alpha decay measurement affect the count rates or the counting efficiencies, standard 1, with 10 mL of cocktail, standard 2, with 19 mL of cocktail, and standard 3, with 20 mL of cocktail, were measured for 100 minutes eight times.

The background samples were collected six weeks before the experimentation began to ensure that any radon in the water had decayed before measurement. Whenever a background sample was used, another sample was collected to ensure the background sample supply did not run out. The background samples were collected from distilled water produced in the laboratory in 25 mL glass radon sample bottles with foil lined caps. The background samples were prepared at the same time as the experimental samples using the same sample preparatory methods as used for preparing direct count radon samples.

The sample preparation procedures undertaken during the direct count and high sensitivity sampling are detailed below.

3.2.3 Direct count radon analysis methodology

The direct count radon measurement method follows very similar methodology to that described by the standard EPA sampling and measurement technique (Hahn & Pia, 1991). The direct count method used for all high sensitivity comparison testing as well as the Hutt and Mangatainoka River direct count samples in chapters 4 and 5 is as follows:

- A water sample is collected in a 25 mL glass vial with a foil lined cap.
- In the laboratory, 10 mL of mineral cocktail is placed in a 25 mL scintillation vial.
- Approximately 1 mL of water from the top of the glass sample vial is then removed using a 10 mL syringe. The syringe is then flushed with this water and the 1 mL of water is discarded.
- The syringe needle is then placed at the bottom of the sample vial of sample water and 10 mL of water is syringed out.
- The syringe needle is then placed underneath the mineral cocktail in the scintillation vial and the 10 mL of sample water is injected underneath the cocktail.
- The bottle is then capped and shaken by hand for 30 seconds.
- The scintillation vial is then left for three hours to allow the radon daughter products to equilibrate. The vial is then placed in a low level scintillation counter for radon measurement. Each sample is measured 10 times for 10 minutes with a total measurement time of 100 minutes.

3.2.4 High sensitivity testing – parameters altered and tested

As described above, the success of a high sensitivity radon method is determined by optimising the radon measurement procedure and reducing experimental errors. A consistent and efficient method for enriching radon from sample water into the mineral scintillation cocktail and the transfer of this

cocktail into the scintillation vial needs to be established. The parameters varied to improve these two factors were the volume of sample water used, the volume of scintillation cocktail used, the volume of air space in the vessel when the cocktail and sample water are shaken together and the extraction method. The experiments designed to test these parameters were continuously developed as results from initial tests were found. The details of how these parameters were varied and tested are described below.

The principle of the high sensitivity radon method is that a greater volume of sample water is used to enrich the scintillation cocktail that gets measured in the QUANTULUS Counter. Once the cocktail has been enriched with radon from the sample water it needs to be separated out from the water and placed into a scintillation vial. Equation 7 shows that the efficiency of the transfer of enriched cocktail into the scintillation vial, η_{TEC}, is optimised when all of the scintillation cocktail added to the sample water is extracted. Furthermore, to reduce uncertainty of the measurements, equation 2 demonstrates that the error associated with the extraction of the enriched cocktail needs to be kept as low as possible.

Two methods of extracting the enriched scintillation cocktail from the sample water were investigated: first, using a syringe to extract 20 mL of cocktail from the sample bottle containing the sample and enriched radon, and second, transferring the shaken sample and enriched radon to a separating funnel to collect the mineral cocktail.

In the case of the separating funnel, after shaking the sample bottle, samples were left for 1 minute to allow the mineral cocktail and sample water to partition. The entire contents of the bottle were then transferred to the separating funnel. The sample was then left for another minute while the sample and mineral cocktail separated out into their oil and water phases. The sample water was then tapped out and discarded. The remaining scintillation cocktail was collected in a scintillation vial.

The syringe extraction method involved shaking the sample bottle, then leaving the sample for 2-4 minutes to allow for the water and oil phase to separate out. The times chosen for the separation to occur were chosen based on sight, as it is visibly clear when all of the scintillation cocktail has settled on top of the sample water. A 30 mL syringe was then inserted into the sample bottle approximately 0.5 cm above the point at which the water and cocktail phases lie to limit the exposure of air to the cocktail being measured. Using the syringe, 20 mL of cocktail is then extracted and placed in a scintillation vial. A summary of the parameters trialled for this experiment are listed in Table 3.1.

Table 3.1: Parameters used for testing the cocktail extraction method of using a separating funnel or a syringe.

Bottle vol. (mL)	Sample water (mL)	Cocktail added (mL)	Head space (mL)	Shake time	Extraction method
125	100	20	5	2	Separating funnel
125	90	30	5	2	Syringe

The shape of the sample bottle was important to consider for the extraction of the scintillation cocktail using a syringe. The shape of the bottle determined how difficult or easy it was to remove 20

mL of cocktail without introducing air to the sample or extracting sample water. The sample preparation error is reduced if the extraction procedure is easy. The optimum bottle shape will allow for the least amount of cocktail to be used, and thus have the least amount of cocktail not extracted into the scintillation vial. Three bottle shapes of differing volumes were trialled: 125 mL, 273 mL and 1000 mL.

The 125 mL sample bottles are the sample bottles used nationally for chlorofluorocarbon sampling in groundwaters (Fig. 3.4a) (Ministry of Health, 2008). The diameter of the bottle is consistent until it nears the top of the bottle, where the shoulder narrows slightly.

The 1000 mL sample bottles have a very similar shape to the 125 mL sample bottles (Fig 3.4b) and are used nationally for sulphur hexafluoride sampling in groundwaters (Ministry of Health, 2008).

The 273 mL sample bottles are custom made glass flasks with a Teflon lined cap (Fig 3.4c). The flasks have an elongated neck which can house a volume of 30 mL to facilitate separation.

The 125 mL and 1000 mL are similar in shape. One experiment was run to test how the shape of the 125 mL bottle would impact the efficiency and reproducibility of the radon enriched cocktail. The experiment details are summarised in Table 3.2.

Table 3.2: Parameters used for testing the efficiency and reproducibility of extracting radon enriched cocktail from a 125 mL bottle using a syringe.

Bottle vol. (mL)	Sample water (mL)	Cocktail added (mL)	Head space (mL)	Shake time	Extraction method
125	100	20	5	2	syringe

Figure 3.4: Photographs of the different sample bottles tested: a) 125 mL sample bottle, b) 1000 mL sample bottle, and c) 273 mL sample bottle.

Equation 5 shows that the greater the water sample volume mixed with the scintillation cocktail, the greater the enrichment, as there is more radon present for the cocktail to be enriched with. However, too large volumes makes field sampling difficult and inefficient as samples become too bulky and heavy to transport. Different bottle sizes were tested to investigate which bottle volume

provided enough sample water to enrich the added scintillation cocktail, whilst not needing large volumes of scintillation cocktail or very long mixing times for enrichment of the cocktail to occur. Three sample bottle sizes were tested; 125 mL, 273 mL and 1000 mL. Initially only the 125 mL and 1000 mL sized sample bottles were tested, as the third bottle type was still being manufactured, a summary of which is tabulated below in Table 3.3.

Table 3.3: Parameters used for testing the efficiency and reproducibility of extracting radon enriched cocktail from 125 mL and 1000 mL bottles using a syringe.

Bottle vol. (mL)	Sample water (mL)	Cocktail added (mL)	Head space (mL)	Shake time (minutes)	Extraction method
125	90	30	5	2	Syringe
1000	965	30	5	2	syringe

The total transfer efficiency of the enriched radon measurement is also dependent on the radon transfer from the sample water to the scintillation cocktail, η_{TSW}, as demonstrated in equation 6. Parameters which affect this efficiency include the volume of scintillation cocktail added, sample water used and head space in the mixing bottle. These three parameters are dependent on one another. For example if you change the volume of sample water but not the scintillation cocktail, the volume of head space is inadvertently changed.

As a consequence of poor transfer efficiencies obtained in high sensitivity method testing of the bottle size, bottle shape and extraction method, tests conducted to establish the optimum parameters for transferring the radon in the sample water to the cocktail were only conducted using the 273 mL sample bottles.

In order to mix the sample water with scintillation cocktail, sample water must be removed from the full sample bottle so that space is created for the cocktail to be added. In the experiments trialled the volume of water removed ranged from 20 mL to 50 mL. In all experiments sample water was removed using a 30 mL or 60 mL syringe, depending on the volume of water being removed. To more accurately determine the volume of water being syringed out of the full sample bottle, sample water removal was carried out on a balance. This also minimises the sample preparation uncertainty.

Once sample water was extracted from the sample bottle, a volume of mineral scintillation cocktail was added to the sample. Tests were carried out to determine the volume of cocktail needed to allow for the optimum transfer efficiency to occur. The range of volume of cocktail added was between 20 mL and 40 mL.

The head space in the sample bottle was another parameter varied throughout the high sensitivity experiments. The head space refers to the volume of air in the sample bottle after the scintillation cocktail has been added. Head space is needed to allow for the movement of the cocktail through the water sample to enable radon transfer from the water to the cocktail. The head space in the experiments trialled ranged from 5 mL to 14 mL in order to find the head space volume which provided the optimum transfer efficiency.

A summary of the different volumes of head space, sample water and scintillation cocktail trialled are tabulated below (Table 3.4).

Table 3.4: Parameters used for testing the efficiency and reproducibility of extracting radon enriched cocktail from 273 mL bottles using a syringe with a 6 minute shake time.

Sample water (mL)	Cocktail added (mL)	Head space (mL)	Sample water (mL)	Cocktail added (mL)	Head space (mL)
221.7	40	12.8	238.2	30	7.3
218.7	40	12	242.6	26	6.1
222.4	40	10.7	240.2	26	5.9
232.8	30	9.5	243.5	26	7
232.6	30	9.3	236.9	25	9.5
232.6	30	12.3	239.3	25	9.1
231.9	35	5.2	237.8	25	9.6
229.6	35	7.2	240.8	25	6.5
231.8	35	4.9	242.2	25	6.4
238.4	29.6	6.9	244.1	24	6
237.8	28.5	7.5	244	23	5.8
237.4	28	7	244	23	6.2
228.8	32	9.5	243.3	23	6.1
232.4	32	9.4	243.2	23	6
232	32	8.4	244.9	22	5.9

Once mineral scintillation cocktail has been added to the sample bottle, the sample bottle is again capped and shaken. All samples for high sensitivity method establishment were shaken by hand. The time the sample bottle was shaken for to find the smallest required shaking time for optimum radon transfer was also tested. Shaking time was varied from 15 seconds to 7 minutes. A summary of the parameters tested to find the optimum shake time is tabulated in Table 3.5 below.

Table 3.5: Parameters used for testing the efficiency of extracting radon enriched cocktail from sample water depending on the time the sample bottle containing the cocktail and sample water are shaken together.

Bottle vol. (mL)	Sample water (mL)	Cocktail added (mL)	Head space (mL)	Shake time minimum (minutes)	Shake time maximum (minutes)
125	90	30	5	0.25	7
273	232	32	9	0.25	6
273	243.5	23	6.5	3.5	7

3.2.5 Establishment of enrichment factor (Z) and experimental errors

After optimisation of the sample bottle size and shape, the extraction method, the shake time, the volume of the cocktail and sample volume used, as well as the counting parameters, samples with relatively high radon were collected for establishing the enrichment factor, by comparing the results of the direct and enriched measurement, as shown by equation 5.

To do this 20 water samples from the Avalon pumping well were collected: ten 25 mL, direct count samples, and ten high sensitivity samples. The ten direct count and ten high sensitivity samples were prepared for analysis in the laboratory following the standard direct count sample procedure and the newly optimised high sensitivity method. The samples were then measured in a QUANTULUS for 100 minutes.

3.2.6 Loss of radon through storage

There is almost always a time delay between collecting a radon sample and analysing the sample. This time delay can range from a couple of hours to a couple of days. An experiment was undertaken to ensure no radon was lost through diffusion through the sample bottle during storage while waiting for analysis. For this experiment, 10 samples, comprising, 4 samples of 25 mL and 6 samples of 273 mL, were collected from the Avalon well. Within 2 hours of collection, two samples of each volume were prepared and analysed in the lab following the direct count sample preparation methodology and the newly developed high sensitivity radon measurement method. The remaining 8 samples were stored in a chilly bin in the laboratory. Approximately 20 hours later two more of the 273 mL samples were prepared and analysed. The remaining four samples were prepared and analysed 65 hours after the samples were collected.

3.3 Results and discussion

3.3.1 Effect of measuring different volumes of scintillation cocktail

The repeated measurement of standards 1-3, with the same concentrations of ^{226}Ra standard but with varying volumes of cocktail and water, show that the counting efficiencies, as calculated using equation 8, of the sample are affected by the volume of scintillation cocktail in the vial (Fig 3.5a and 3.5b). There is a large difference between the counting efficiencies of identical concentrations of standards when 10 mL of cocktail in the scintillation vial is used in comparison to 20 mL. However, there is no statistically significant difference in the counting efficiencies between the two standards which use 19 mL and 20 mL of cocktail. Optimum counting efficiencies are achieved by either 19 mL or 20 mL of cocktail used.

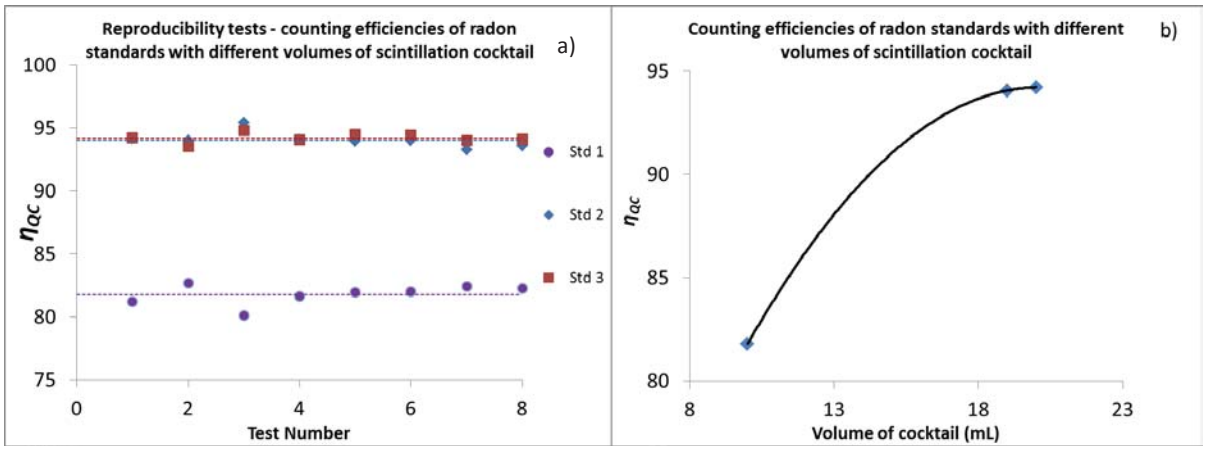

Figure 3.5: Counting efficiencies of standard 1, purple, standard 2, blue, and standard 3, red, wherein the corresponding coloured dashed line represents the mean (a) and the counting efficiencies depending on the water to cocktail volume ratio (b).

An increase in the measured cpm for the samples comprising the larger volume of scintillation cocktail is not unexpected. In LSC the radon distributes itself within the three phases, water, cocktail and air, within the scintillation counting vial (Cantaloub, Higginbotham, Istok, & Semprini, 1998). The radon distribution in the vial is described by Cantaloub et al. (1998) through the fraction in the cocktail phase (Equation 9) and the fraction in the air phase (Equation 10). As the volume of cocktail increases, the greater the fraction within the cocktail phase and the less in the air phase.

$$F_c = \frac{K}{\left[K + (V_s / V_c) + (V_v / V_c)H\right]} \qquad \text{Equation 9}$$

$$F_v = \frac{H}{\left[H + (V_s / V_v) + (V_c / V_v)K\right]} \qquad \text{Equation 10}$$

where F_c is the fraction of radon in the cocktail phase, F_v is the fraction of radon in the air phase, K is the radon partition coefficient of the sample and cocktail, H is the radon partition coefficient of the air and water, and V_s, V_c and V_v are the sample, cocktail and head space volume respectively of the sample (Cantaloub et al., 1998).

Using the values from Cantaloub et al. (1998) for K and H of 32 and 4 respectively, the fraction of radon in the cocktail and air space can be calculated for the 3 standards used in the high sensitivity experimentation. The calculate values (Table 3.6) are only slightly larger than the measured yields (Fig. 3.5), with the difference between the standards due to self-absorption of the radon in the water. Thus, a sample with the smallest volume of water and highest volume of cocktail will have the maximum counting efficiency. It should be noted however, that the differences in fractionation values between standards 2 and 3 are so small that using 19 mL or 20 mL of cocktail will not cause any significant statistical difference in counting efficiencies, as demonstrated in Figure 3.5 above.

Table 3.6: Fractional values of radon in the cocktail phase and air space phase for the three standards used in the high sensitivity experimentation.

Standard	Volume water (mL)	Volume Cocktail (mL)	F_c	F_v
1	10	10	0.8649	0.0580
2	1	19	0.9666	0.0318
3	0	20	0.9697	0.0303

Due to the different total counting efficiencies depending on the volume of water in the cocktail, the samples need to be measured against a standard with the same volume of water. If this does not occur, then the results need to be adjusted using the measured values (Fig. 3.5).

3.3.2 Optimisation of sample parameters for high sensitivity methodology

The optimisation of radon transfer efficiencies is essential for developing an improved high sensitivity radon measurement method. To calculate the radon transfer efficiencies, a direct count analysis was undertaken concurrently with every high sensitivity experiment. Using the radon concentration from the direct count sample, the enrichment factor, Z, was back calculated for the high sensitivity samples using equation 2. Once the enrichment factor was determined, the transfer efficiencies were calculated as per equations 5, 6 and 7.

To optimise the extraction procedure using a syringe, a minimal volume of scintillation cocktail is left behind in the sample bottle, while still allowing for effective enrichment of the radon from the sample water into the cocktail, as shown by Equations 6 and 7. Initial tests showed that the shape of the 125 mL and 1000 mL samples bottles are ineffective for radon enrichment using a syringe to extract the enriched radon. When 20 mL of cocktail was added to the sample bottles for enrichment and subsequent extraction, the results were inconsistent. This was due to the difficulty in extracting only the 20 mL of cocktail from the sample bottle. Inevitably, either sample water, air or both, are extracted by the syringe as the volume of cocktail in the sample bottle reduces. This introduces significant error into the preparation procedure and undermines the purpose of enriching the samples. To prevent this error a larger volume of cocktail, 30 mL, was added to the sample.

However, this resulted in a reduced efficiency of the transfer of the enriched cocktail into the scintillation vial, η_{TEC}, as 10 mL of enriched cocktail is not extracted for measurement.

Due to the inconsistent results found in the bottle shape tests, the parameters used to trial the extraction methods to collect the enriched cocktail using a syringe were slightly different to the parameters used for the separating funnel. In the syringing method 30 mL of cocktail is added to 90 mL of sample water to allow for easy extraction of only 20 mL of the enriched cocktail, leaving 10 mL of the cocktail behind. In theory, removing only cocktail using a separating funnel when only 20 mL of cocktail is initially added should be possible without inconsistencies. Therefore, 20 mL of cocktail was added to the 100 mL of water using the separating funnel method.

The separating funnel extraction method had a higher total radon transfer efficiency, η_{TTE}, than the syringing method (Fig. 3.6a). This is largely due to one third of the cocktail used in the syringing method not being measured as 10 mL of cocktail is left behind. Despite this, the radon transfer from the sample water to the scintillation cocktail, η_{TSW}, for the syringing method was higher than the separating funnel method (Fig. 3.6b). This difference is unexpectedly large, which indicates another source of radon loss which is most likely degassing during transfer from the sample bottle to the separating funnel (Leaney & Herczeg, 2006).

The processing of the samples using the separating funnel took a minimum of two minutes longer per sample than the syringing method. This is because the oil phase sits on top of the sample water. Once the oil and water have separated out then the water phase must first be removed. The sample water near the partition between the two phases must be discarded with extreme care as none of the oil phase should be discarded. This part of the process was difficult, and thus took more time, because both phases are of similar colour. The use of a separating funnel also introduces a step of transferring the sample from the sample bottle to the separating funnel which can introduce error (Leaney & Herczeg, 2006). Ultimately these factors, especially the reduced η_{TSW}, were thought to out weigh the benefits of the increased total efficiency with the separating funnel method and further experiments were only conducted with the syringing extraction method.

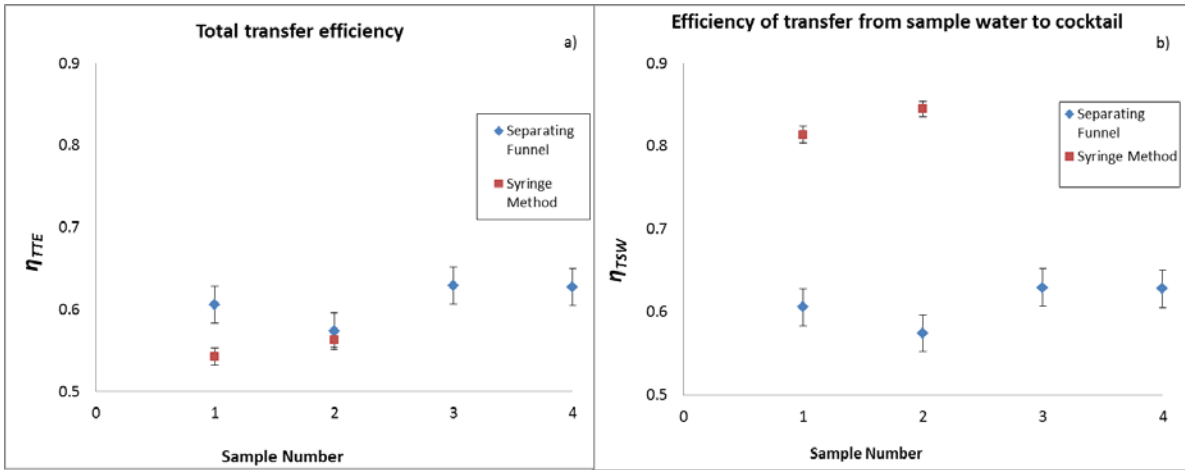

Figure 3.6: Total radon transfer efficiency, a), and radon transfer efficiency from the sample water to the scintillation cocktail, b), for the syringing and separating funnel extraction methods, wherein the sample number refers to the sample ID. Error bars are estimated based on the standard deviation of the measurements.

To aid in the development of an optimum method, customised volumetric flasks were designed. The 273 mL flasks are a standard volumetric flask with an elongated neck that has a 30 mL volume. The shape of the sample bottle allows maximum contact between the sample water and the cocktail during shaking, while still allowing for good separation between the phases for extraction without the risk of syringing out sample water or air.

The tests conducted on the 273 mL sample bottles, which investigated how the volume of cocktail effects the radon transfer efficiencies unsurprisingly showed the same trends as the 125 mL and 1000 mL sample bottles. The η_{TEC} decreases with increasing volumes of scintillation cocktail added to the sample vial (Fig 3.7a). This is explained by equation 7 as a larger portion of enriched cocktail is left behind in the sample bottle and not measured in the scintillation vial. However, η_{TEC} increases with increasing volumes of water. The more sample water available in the 273 mL flasks the greater η_{TEC} (Fig 3.7b) which results in a higher η_{TTE}.

The volume of head space in the sample bottle, in the range of 5-13 mL, did not appear to have any impact on the radon transfer efficiencies (Fig 3.7c). If the head space does have some influence on the result, the effect of the sample water volume and scintillation cocktail volume overrides any impact the head space may have with the range of volumes that were experimented with.

The results of the experimentation of varying head space, sample water volume and cocktail volume in the 273 mL sample bottles showed that the best radon transfer and total efficiencies were gained when the sample water volume was maximised and the cocktail left in the sample bottle after 20 mL is extracted for measurement is minimised (Fig. 3.7d). The smallest volume of cocktail that could be added to the 273 mL sample bottles, without any extraction difficulties of withdrawing sample water or air, was found to be 23 mL. Enough of the sample water from the full sample bottle needs to initially be extracted before the 23 mL of scintillation cocktail can be added. The volume of sample water initially removed for the optimised method was 29 mL. This provides the most amount of sample water to be mixed with the scintillation cocktail, while still providing enough head space to enable adequate mixing when shaken.

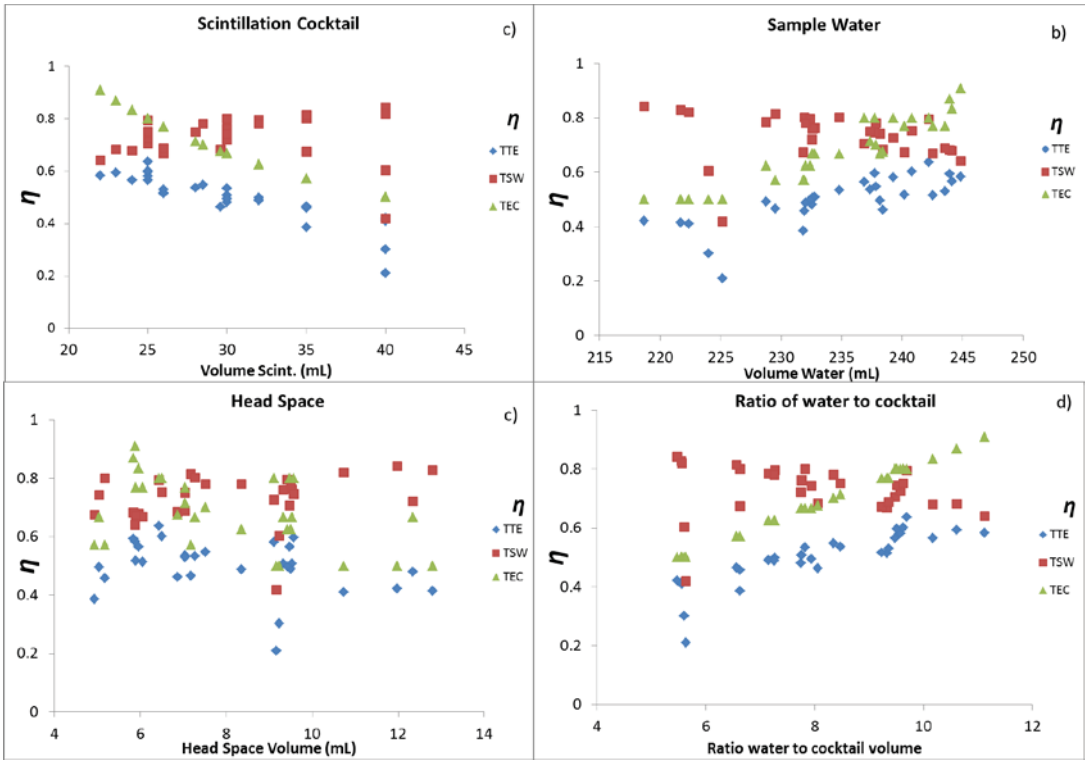

Figure 3.7: Radon transfer efficiencies for tap water samples using 273 mL sample bottles, the syringe extraction method and varying volumes of cocktail (a), sample water (b), head space (c), and the ratio of sample water to cocktail (d), wherein colours denote efficiency: total radon transfer efficiency, η_{TTE}, blue, transfer efficiency of the enriched cocktail into the scintillation vial, η_{TEC}, green and transfer efficiency of from the sample water to the scintillation cocktail, η_{TSW}, red.

All samples for high sensitivity analysis were shaken by hand to mix the scintillation cocktail with the sample water. Shaking samples by hand has the potential to introduce sample preparation errors. However, during all experimentation all shake times used were greater than what was established to be the minimum required shake time to reduce such errors. For example, the shake time required for 273 mL samples with 32 mL of scintillation cocktail added to it was between 4-6 minutes for the maximum radon transfer to the cocktail (Fig. 3.8). Therefore during all 273 mL experimentation all samples were shaken for 6 minutes to be conservative.

Once the high sensitivity method was optimised, the shake time for the methodology which adds 23 mL of cocktail to the sample bottle was investigated. A shake time of 3.5 minutes appears to be the minimum time required for optimum radon transfer (Fig. 3.8). Although the radon transfer efficiency does increase after 6 minutes of shaking (Fig. 3.8), it is within experimental error of the sample shaken for 3.5 minutes. Therefore, 3.5 minutes was the minimum time experimented with these flasks with 23 mL of cocktail as experiments undertaken using 32 mL of cocktail took greater than 3.5 minutes for optimum radon transfer to occur. Further experimentation could be undertaken to establish if shake times of less than 3.5 minutes can be used for the 273 mL flasks when 23 mL of scintillation cocktail is added. This would significantly reduce sample preparation time. Interestingly, the minimum time required for shaking for optimum radon transfer efficiency for the 125 mL flask is 15 seconds (Fig. 3.8). This is vastly shorter than the 273 mL flasks. A likely reason for this is that the shape of the 125 mL sample bottle allowed for easier movement of the cocktail within the sample

bottle when shaken. For mixing in the 273 mL sample bottle the bottle had to be inverted until the air bubble in the bottle neck moved to the opposite end of the bottle, the bottle was then inverted again. This action was repeated continuously during the shake time. Another reason for the shake time difference could be due to a higher ratio of cocktail to sample water, 0.33, in the 125 mL sample bottle, as opposed to 0.09 in the 237 mL sample bottle.

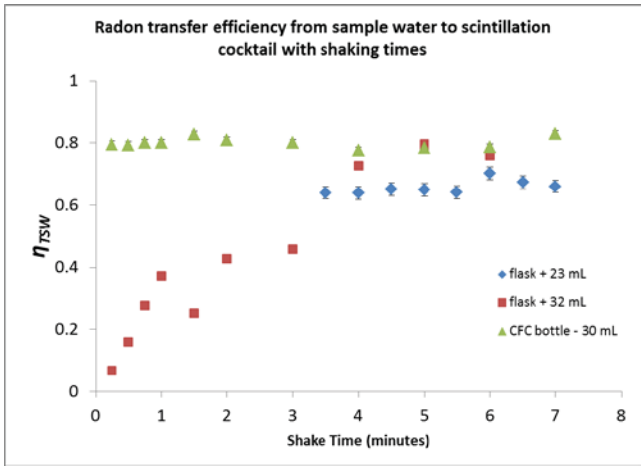

Figure 3.8: Radon transfer efficiency from sample water into the scintillation cocktail, η_{TSW}, for tap water samples using 273 mL sample bottles and 23 mL cocktail (blue), 273 mL sample bottle and 32 mL cocktail (red) and 125 mL sample bottle and 30 mL of cocktail (green). Error bars are estimated based on the standard deviation of the measurements wherein optimum η_{TSW} was reached.

3.3.3 Calculation of enrichment factor (Z) and experimental errors

Reproducibility tests of the enrichment method involving 23 mL of cocktail and approximately 244 mL of sample water were conducted to establish the enrichment factor, *Z*. Ten direct count samples were compared to ten high sensitivity samples from the same sample source (Fig. 3.9).

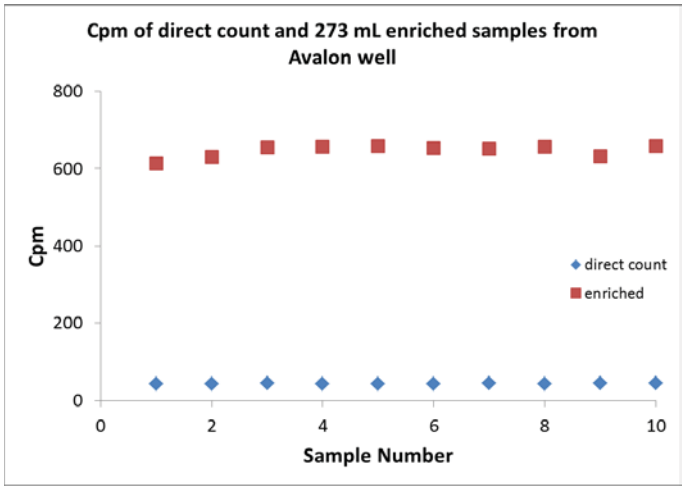

Figure 3.9: Cpm of 25 mL direct count and 273 mL enriched samples from the Avalon well for the establishment of the enrichment factor, *Z*. Error bars are estimated based on 1 standard deviation of the counting measurement and are too small be seen on the graph scale.

Using the average cpm measured for these reproducibility tests, *Z* was calculated using equation 4.

$$Z = \frac{645.9}{43.3} = 14.9$$

The *σ(Z)* is calculated by the standard deviation of the repeated measurements and was found to be 0.3.

With the enrichment factor and the associated uncertainty now known, the lower limit of detection was calculated. The lower limit of detection was calculated to be when *σ(C)/C* is 50% (Morgenstern & Taylor, 2009). Other methods of calculating the lower limit of detection have been used by other authors, such as taking the mean of the background plus the background standard deviation (Freyer et al., 1997). However, in this experiment the method of Morgenstern & Taylor (2009) was followed. By rearranging equation 1 for the count rate, *n*, and then equation 2 for the radon concentration, *C*, the lower detection limit can be found graphically (Fig. 3.10). The lower limit of detection for the high sensitivity optimised method was found to be 0.006 BqL^{-1}. A comparison between the method established in this chapter and previously published methodologies is summarised in Table 3.7. The calculated lower limit of detection of 0.006 BqL^{-1} is an eight fold improvement on the high sensitivity method proposed by Freyer et al. (1997). However, the difference can also be contributed to the different methods of calculating the lower limit of detection. Also, unlike the methods of Freyer et al. (1997) and Cook et al. (2003), the scintillation cocktail is not handled in the field. This makes the sampling process more efficient and eliminates the risks associated with couriering or mailing scintillation cocktail. The 0.006 BqL^{-1} lower limit of detection is slightly higher than the method proposed by Leaney & Herczeg, 2006. This is most likely due to Leaney & Herczeg enriching the scintillation cocktail in 1.3 L of sample water whereas the proposed high sensitivity method only uses 0.244 L. However, unlike the Leaney and Herczeg (2006) method, there is no loss of radon during storage due to diffusion through the sample bottle (Fig. 3.11). The sample bottles are also smaller in volume, and thus lighter to carry while carrying out a large radon survey. The Leaney & Herczeg (2006) method does have the advantage over the newly proposed method of the sample bottles being more durable. Their sample bottles are less likely to break if dropped or if there is a dramatic change in temperature than the glass bottles used in the proposed methodology.

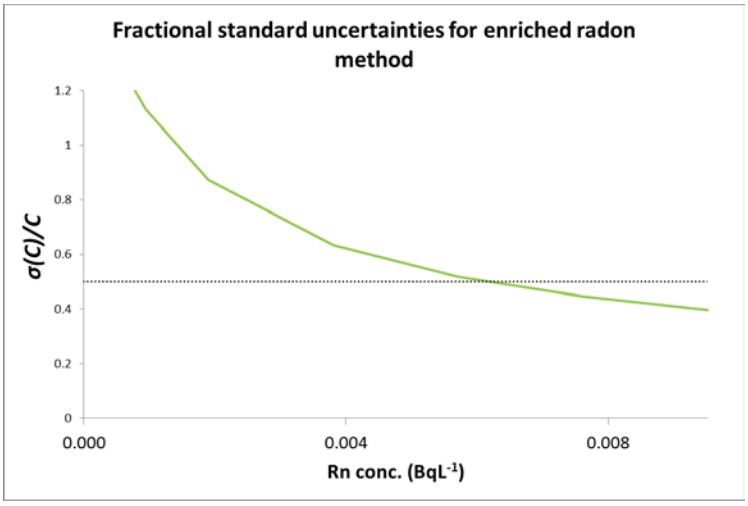

Figure 3.10: Calculated fractional standard uncertainties for the enriched radon method wherein Z is 14.9, the counting time is 100 minutes and nb is 0.01.

Table 3.7: Comparison of high sensitivity methods

Method	TTE	LLD (BqL^{-1})	Volume Sample Water (mL)
Method established in this chapter	60 % ± 2	0.006	244
Cook et al. (2003)	48 % ± 2	Not given	950
Freyer et al. (1997)	Not given	0.05	1000
Leaney and Herczeg (2006)	43 %	0.003	1300

The sample preparation error, *P*, as used in equation 2, for the direct count samples was calculated using weight measurements taken during the reproducibility tests. Generally when carrying out the direct count radon analysis the masses of the scintillation cocktail and the sample water used are not measured. The masses of both these parameters are measured based on the graduated markings on the syringe. Using the masses weighed during the reproducibility tests the sample preparation percentage error can be calculated (eq. 11).

$$P = \left(\frac{\sigma_{Sc\,\mathrm{int}}}{Mean_{Sc\,\mathrm{int}}} + \frac{\sigma_{Water}}{Mean_{Water}} \right) \times 100 \qquad \text{Equation 11}$$

$$P = \left(\frac{0.09}{8.59} + \frac{0.07}{9.98} \right) \times 100 = 2\%$$

Wherein σ_{Scint} and σ_{Water} are the standard deviations of the mass of scintillation cocktail and sample water used respectively, and $Mean_{Scint}$ and $Mean_{Water}$ are the means of the mass of scintillation cocktail and sample water used respectively.

As previously mentioned in Section 3.1.3, there is no need to calculate the sample preparation error for the enriched sample, as the sample masses are weighed during the procedure and any further errors are already accounted for by $\sigma(Z)$. This is because any error in the sampling procedure will be taken into account by the mean of the enriched samples used to calculate the enrichment factor.

3.3.4 Loss of radon through storage

The 273 mL sample bottles, for enriched radon samples, and the 25 mL sample bottles, for direct count samples, were found to be gas tight. This was apparent when over a period of 65 hours between sample collection and sample preparation, there was no radon loss other than that by radioactive decay (Fig. 3.11). This is important to establish as it means the high sensitivity radon method established is suitable for large scale radon surveys commercially wherein the samples are often not received by the laboratory for preparation until several days after the sample was collected. This is advantageous over the Leaney & Herczeg (2006) method which has diffusion of radon gas through their PET sample bottles. It should be noted that in waters low in radon concentrations the measurement errors would increase significantly as the radon decays with increasing storage time. However, this is not demonstrated in Figure 3.11, as the sample water measured in this experiment had high radon concentrations and thus high count rates.

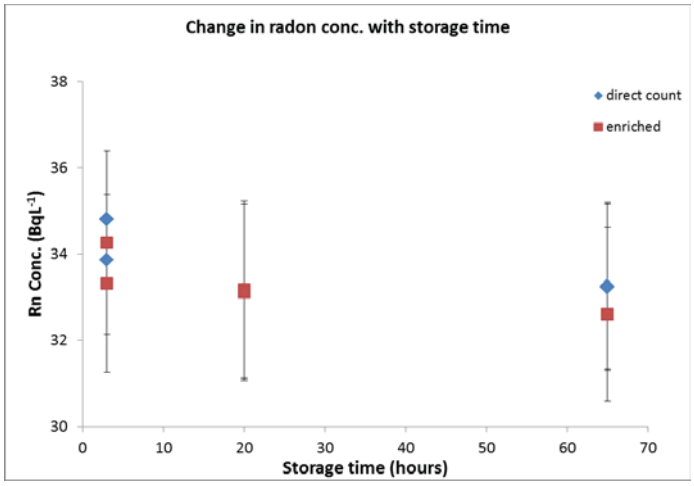

Figure 3.11: Measured radon concentrations from 25 mL direct count and 273 mL enriched samples from the Avalon well wherein samples were prepared and measured for 3 hours, 20 hours and 65 hours after the samples were initially collected.

3.4 Chapter summary

The direct count analysis for measuring ^{222}Rn has a measurement sensitivity suitable for measuring groundwaters. However, the 0.2 BqL^{-1} lower limit of detection for the direct count procedure is not sufficient for accurately measuring the radon concentrations in surface waters with very little radon. To measure the radon concentrations in surface waters several procedures have been developed which use greater volumes of sample water to enrich a small volume of scintillation cocktail, which is then separated from the sample water and the alpha decay is measured using LSC. However, none of these methods fulfil all the criteria of being cost effective, time effective, simple and reproducible so that they can be applied to large scale high sensitivity radon surveys. To fulfil all of these criteria a high sensitivity radon method using a syringing procedure was developed. The procedure involves the collection of a sample in a 273 mL glass flask with an elongated neck of 30 mL volume and a Teflon lined cap. After sample collection, 29 mL of sample water is removed using a syringe and 23 mL of scintillation cocktail is added. The sample is then shaken for 3.5 minutes and then left for 2-4 minutes for the oil and water phases to separate out. 20 mL of the cocktail is then extracted using a syringe and placed in a scintillation vial for measurement in a low level liquid scintillation counter. To calculate the radon concentration from the measured cpm of the high sensitivity samples the enrichment factor is needed. Using this syringing high sensitivity radon method procedure gives an enrichment factor of 14.9 with an error of 2%. This is the same as the sample preparation error for the direct count samples but as the direct count samples have a higher counting error, overall the error of the samples prepared using the high sensitivity radon procedure is much lower. The high sensitivity method developed in this chapter has a total radon transfer efficiency of approximately 60% and a lower limit of detection of 0.006 BqL^{-1}. This is an improvement over some previously published methods and comes close to the lower limit of detection of 0.003 BqL^{-1} published by Leaney and Herczeg (2006). The proposed method also requires no handling of scintillation cocktail in the field, requires a significantly smaller sample volume than the other published methods, making large numbers of samples easier to transport and there is no loss of radon during storage due to diffusion through the sample bottle. The proposed high sensitivity radon method therefore meets the objective of being cost and time effective, reproducible and can easily be applied to large scale radon surveys.

Chapter 4 - Hutt River Case Study

4.1 Introduction and objectives

The Hutt River flows through an urbanised area and is used for recreational swimming in the warmer months of the year. A pedestrian and cycle pathway has been constructed along the river banks where dogs are often walked. During the summer, low flow months, cyanobacteria blooms have formed in the Hutt River. This toxic algae is unwanted by the Regional Council and public as ingestion of the algae can cause death to dogs and human contact with the algae can cause vomiting, diarrhoea and skin irritations (Greater Wellington Regional Council, 2015).

Warm temperatures, sunlight and low river flows are ideal conditions to contribute to cyanobacteria growth. Other contributors to the algae growth are nitrogen and phosphorous concentrations in the river water (Greater Wellington Regional Council, 2013). These nutrient sources can either come from point source surface runoff or from groundwater inputs. An understanding of the groundwater-surface water interaction dynamics in the Hutt River may help to identify the nutrient flow pathways which contribute to the growth of cyanobacteria. Sound management or prevention of these algal bloom outbreaks can only occur if the groundwater-surface water interactions in the river system are understood.

This chapter describes an investigation that was undertaken in the Hutt River with the aim of identifying groundwater surface water interactions and dynamics within the river system. To achieve this aim, groundwater-surface water interaction dynamics are captured using high sensitivity and high spatial resolution radon measurements. These radon measurements enabled the development of radon concentration thresholds to determine what measured radon concentrations in surface waters represent groundwater discharge and possible recharge in the Hutt River. From the development of these thresholds, the radon measurements were then analysed to assess and map the locations where groundwater is discharging into the Hutt River, where the river water is possibly being recharged into the groundwater system and where the river water is neither losing, nor gaining, but instead mixing with the gravel bed of the river. Furthermore, this chapter also assesses the potential of using radon in conjunction with other hydrochemistry analysis and concurrent stream flow gauging to give more insight into the dynamics of the groundwater and surface water interactions within the Hutt River system.

4.2 Study area and its hydrogeological setting

The Hutt River is located in the Hutt Valley, north east of Wellington. The Hutt River catchment lies within the Lower Hutt and the Upper Hutt City boundaries (Fig. 4.1) and is extensive, covering an area of 655 km^2 (Lawrence, Reisinger, Tegg, & Quade, 2011). The catchment area has a topographic range of steep ranges to the north and east of the Valley including the Tararua Ranges and the Rimutaka Ranges, flat land in the alluvial basin of the Hutt Valley floor and raised hills formed by tectonic uplift on either side of the Hutt Valley basin (Greater Wellington Regional Council, 2004; Miskell, 2012). The land directly adjacent to the river, the flat Hutt Valley floor (Fig 4.1), has an urban coverage of 59% with the majority of the 130,000 population residing in this area (Lawrence et al., 2011; Miskell, 2012). However, the majority of the catchment is covered by indigenous and exotic forest (Fig. 4.2).

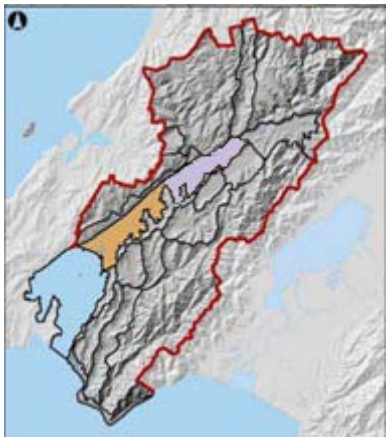

Figure 4.1: The approximate extent of the Hutt Valley floor in which the Lower Hutt (orange) and Upper Hutt (purple) groundwater zones lie within the Upper Hutt and Lower Hutt City boundaries (red). Image retrieved and adapted from (Miskell, 2012).

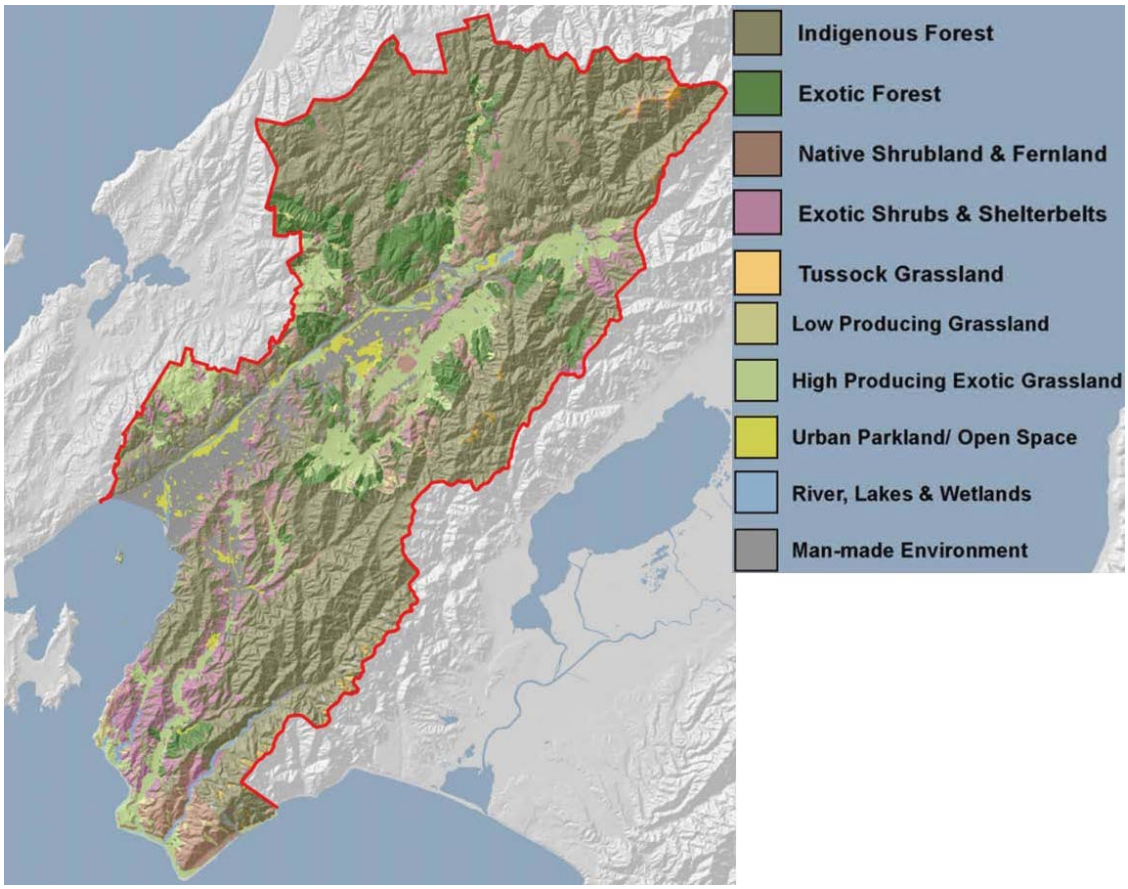

Figure 4.2: Land use type/coverage within the Upper Hutt and Lower Hutt City boundaries. Image adapted from (Miskell, 2012).

Greater Wellington Regional Council collects rainfall data at more than 12 sites within the Hutt Valley catchment (Greater Wellington Regional Council, 2012b). Annual rainfall data collected within the catchment between 2010 and 2014 ranges from 950 to 5000 mm (Greater Wellington Regional Council, 2012b). The Valley floor receives the least amount of rainfall, ranging approximately from

950 to 1350 mm. The Tararua Ranges and Rimutaka Ranges comparatively receive the most rainfall within the catchment.

The hydrogeological setting of the Hutt River can be described in two parts: the Lower Hutt Basin groundwater zone and the Upper Hutt groundwater zone (Fig. 4.1).

The geological setting of the Lower Hutt Valley is strongly influenced by the Wellington fault which has caused a half graben, a geological feature where a fault line lies parallel to depressed block of rock. This wedge shaped basin is confined to the West by the Wellington fault and to the East by greywacke bedrock (Boon, Perrin, & Dellow, 2011; Jones & Baker, 2005). The basin has been in-filled with gravels, sand and silts, deposited by the Hutt River from the Tararua Ranges, and marine sediments, deposited by the effects of rising and falling seas levels. The Basin gravels have a maximum depth of 350 m at the Petone foreshore and shallow northwards until the Taita Gorge, where bedrock is exposed (Boon et al., 2011).

The gravel deposits have led to the formation of aquifers. These aquifers are separated by marine deposit aquitards as far north until just north of the Kennedy Good Bridge in Avalon. The location of the boundary between the confined and unconfined aquifers is shown in Figure 4.3. There are two main confined aquifers between Petone and the Kennedy Good Bridge, the underlying Moera Basal Gravels and the overlying Waiwhetu Artesian Gravels (Jones & Baker, 2005; Phreatos, 2001). The Waiwhetu aquifer is the predominant aquifer within the region. The hydraulic characteristics of the aquifer vary significantly throughout as aquifer material ranges from course gravels to fine clays (Hughes, 1996). Within the Waiwhetu aquifer is a low permeability, fine grained layer that divides the Waiwhetu aquifer into an upper aquifer and a lower aquifer. The upper Waiwhetu aquifer is the most productive, with transmissivity values of up to 35000 $m^2 day^{-1}$, which is about 17 times higher than the lower Waiwhetu aquifer or Moera aquifer transmissivity rates (Wellington Regional Council, 1995). The Waiwhetu aquifer is thought to remain confined until the Wellington harbour entrance, where the aquifer discharges into the sea (Phreatos, 2001).

North of Avalon the aquifers become unconfined until the Taita Gorge. This area is known as the Taita Alluvium Aquifer. The Taita Alluvium is comprised of 10-15 m of gravels and gravels and sands (Boon, Perrin, Dellow, & Lukovic, 2010). Water within the Taita Alluvium flows at a depth of 3-10 m with the depth of flow closely correlated to the stage of the Hutt River and the tide (Phreatos, 2003). This shallow aquifer is recharged from the overlying, directly hydraulically connected, Hutt River (Phreatos, 2003).

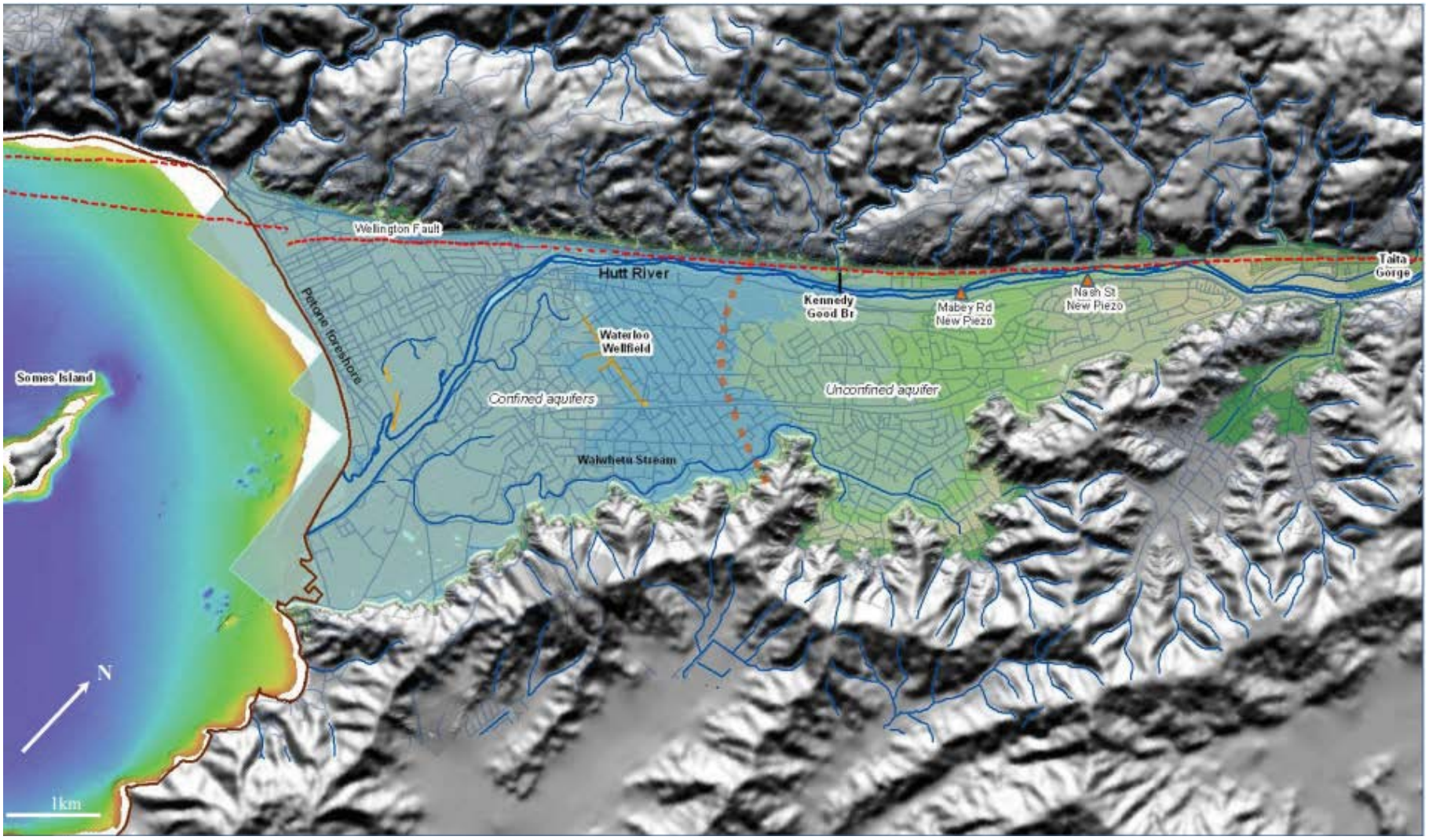

Figure 4.3: Map of the Lower Hutt Valley showing the main geographical features, topography and the location of the approximate boundary between the confined and unconfined aquifers (orange dashed line). Image retrieved from (Gyopari, 2014).

The Upper Hutt Basin, like the Lower Hutt, comprises greywacke bedrock. The geology of the Upper Hutt Basin is very similar to the Lower Hutt but with the exclusion of marine sediment deposits. In an investigative drill site, at a groundwater bore maintained by Greater Wellington Regional Council in the Trentham Park, bedrock was not found until drilling had reached 214 m below ground level (Jones & Baker, 2005). The bore itself is 32 m deep (Greater Wellington Regional Council, 2012a). Despite the large amount of sediment overlaying the bedrock there is little groundwater flow within the Upper Hutt aquifers (Jones & Baker, 2005). There are two recognised aquifers in the Upper Hutt Basin. The first is a shallow unconfined aquifer. The second is a deeper aquifer which is confined at 55 m below ground level by a dense silt layer (Jones & Baker, 2005; Phreatos, 2001). In the Upper Hutt zone the Hutt River strongly influences groundwater levels with river water thought to seep into the aquifer at the upper part of the zone. Groundwater is thought to be discharged back into the river at the base of the Upper Hutt zone due to bedrock outcrop to the surface (Wellington Regional Council, 1995).

The area of the study undertaken in the Hutt River as well as the site numbers for radon sampling sites that will be used from here are detailed in Figure 4.4 below. Site number 1 begins at the Whakatikei confluence in the Upper Hutt. Site 1 was chosen as the northern most sampling site because bedrock underlies the river here. Further downstream the river bed comprises gravels. Sampling further upstream of the bedrock is unlikely to capture any interaction between groundwater and surface water. From Site 1, the next site points were selected based on the criteria of being approximately 500-800 m downstream of the previous sampling site and the accessibility of sampling point. The Ferguson Drive Bridge is located at Site 11 and is a major landmark along the river. At approximately Site 12 there is a large man made weir. At Site 17 the Taita Rail Bridge crosses the Hutt River. The Avalon, also referred to as the Kennedy Goode, Bridge is located a few tens of metres upstream of Site 24. At approximately Site 14, in the Taita Gorge, there is an automated flow gauging station run by the Greater Wellington Regional Council. As a reference, the flow from this gauging station was always recorded when radon sampling surveys were carried out. The river flows referred to in this chapter, other than those using the SonTek flow gauging equipment, were taken from this gauging site. Groundwater samples were also taken as part of this study in the Lower Hutt groundwater zone. These groundwater wells are also identified on Figure 4.4.

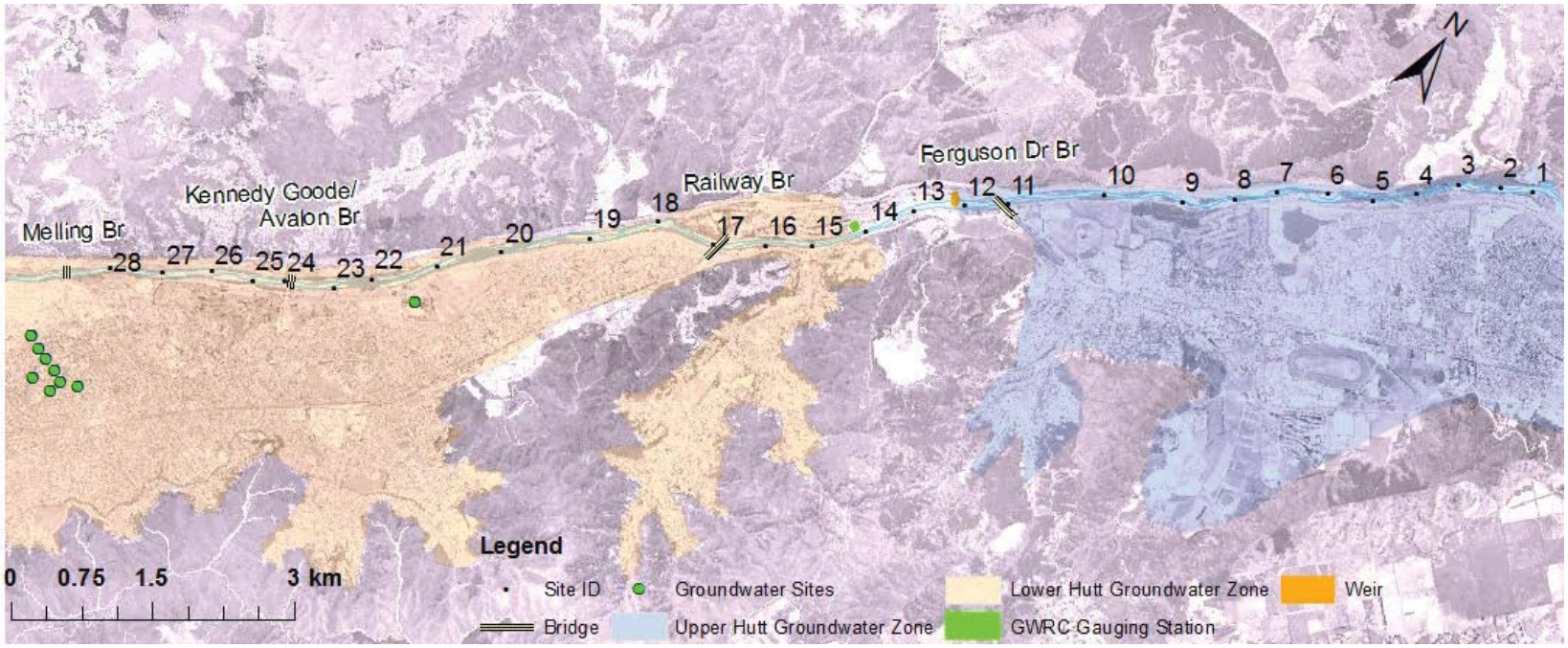

Figure 4.4: Radon sampling sites, groundwater zones and landmarks in this Hutt River study.

4.3 Methods and materials

4.3.1 Hierarchical cluster analysis

The potential of using radon measurements in comparison or combination with hydrochemistry analysis to capture dynamics of groundwater – river water interactions was assessed. To carry out this assessment hydrochemistry data from the Hutt River and surrounding groundwater wells in the Hutt Valley Region were analysed and compared using multivariate statistical methods. Statistical analysis was carried out primarily using Hierarchical Cluster Analysis (HCA). HCA was chosen because it groups water samples taken from different sampling sites into clusters based on the relationships between the variables or analytes used in the analysis. HCA is also advantageous because it does not show bias towards differing numbers or types of analytes used (Daughney & Reeves, 2005; Guggenmos, Daughney, Jackson, & Morgenstern, 2011; Güler, Thyne, McCray, & Turner, 2002). HCA analysis helps to determine any potential relationships between hydrochemical data, geographic locations, aquifer characteristics and groundwater or river water. If such relationships exist then groundwater and surface water chemical parameters could be used as complementary tracers to verify groundwater-surface water interactions indicated by radon concentrations.

Existing hydrochemical data for the HCA analysis was sourced by the Greater Wellington Regional Council (GWRC). It included hydrochemical data for a total of 48 surface water samples, taken from 4 different sites, and 704 groundwater samples, taken from 20 different sampling sites within the Hutt Valley from 1993 to 2014. Prior to any statistical analysis the hydrochemical data needed to be extracted and cleaned. This was done using the following method:

- Only the dissolved concentrations of analytes were used.
- Groundwater datum prior to 2003 was removed as analytes were measured for their total concentrations rather than dissolved. From 2003 onwards dissolved concentrations of analytes were measured as total concentrations of analytes do not represent the actual groundwater chemistry of a sample.
- There was only one year in which a wide range of chemistry data was measured for surface water in the Hutt Valley, 2008. Therefore, only surface water data for 2008 was included in the HCA analysis. Groundwater chemistry data collected between 2003 - 2014 was included. The consequence of analysing only one year of river data is that the HCA cannot investigate seasonal trends as the analysis would be strongly biased with such a limited dataset.
- Where bicarbonate data was not available the alkalinity value was converted to give the concentration of bicarbonate. Bicarbonate data was often missing from the dataset at groundwater sites where the site was sampled twice in one day but at different times, most likely to measure differences in chemistry after pumping the well for several hours. There were 70 samples where the alkalinity was used to calculate bicarbonate. All of these were from groundwater sites.

- Where field pH and electrical conductivity measurements were not available the value measured in the laboratory was used. Like the bicarbonate data, these measurements were not normally taken at groundwater sites where the site was sampled twice in one day. Of the data set used in the HCA, 96 samples, 8 surface water and 88 groundwater samples, had field pH missing. Where laboratory and field pH measurements were both available the difference between the measurements was on average 0.4, with the majority of the laboratory pH values being higher than the field sample. For electrical conductivity, of the dataset used in the HCA, 82 samples, 78 groundwater and 5 surface water samples, had field electrical conductivity missing. Where both field and laboratory measurements were taken the average difference between the two measurements was 7.1 μScm^{-1}, with neither the lab or field measurement consistently greater than the other.

- With the remaining dataset frequency of measurement of the analytes was looked at. If an analyte was measured only a few times in the dataset the analyte was removed from the analysis dataset. Five analytes were removed in total: dissolved cadmium, dissolved copper, dissolved nickel, total reactive silica, and total coliforms. All five of these analytes had measurements for eight or less samples of the entire dataset.

- Derived values were also removed from the dataset. The removed derived values were total anions, total cations, dissolved oxygen percentage saturated (field measurement), total hardness, ionic balance error and total oxidised nitrogen.

The processed hydrochemical dataset after the above described data cleaning process included a total of 378 samples, of which, 48 are surface water samples from 4 different sites (Fig. 4.5). The remaining 330 groundwater samples are from 10 different sites (Fig. 4.5). The analytes included in the analysis are Ca^{2+}, Mg^{2+}, K^{+}, Na^{+}, Cl^{-}, HCO_3^{-}, SO_4^{2-}, Mn^{2+}, NH_3-N, B, DO (dissolved oxygen - field measurement), DRP (dissolved reactive phosphorus), NO_2-N, NO_3-N, TOC (total organic carbon), pH and electrical conductivity. A drawback of the processed dataset is that it does not include any groundwater sites from the Upper Hutt groundwater zone. This prevents any relationships between the groundwater and the surface water in the Upper Hutt zone to be identified.

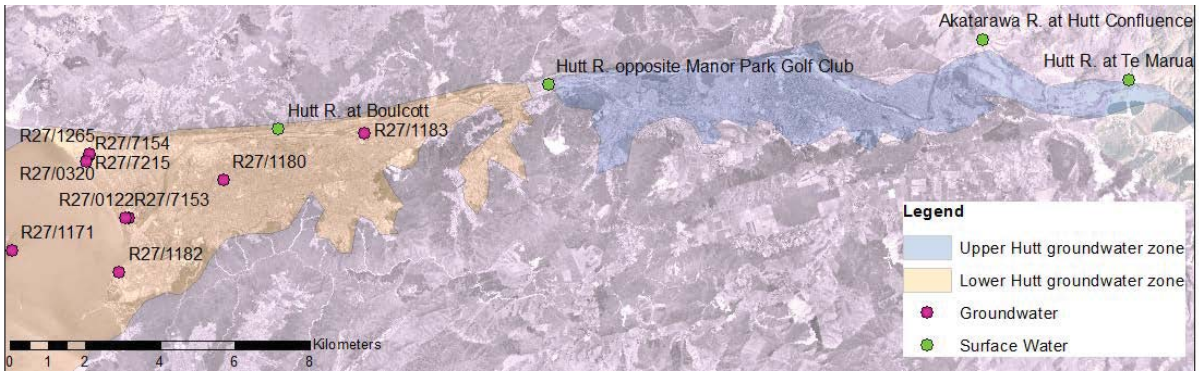

Figure 4.5: Geographical locations of all sampling sites used in HCA after data cleaning.

The data from the 378 samples were then processed using a spread sheet for automatic processing of water quality data (Daughney, 2010). Using this spread sheet, charge balance errors, outliers and median values for all analytes at the 14 different sampling sites were found. No outliers were

removed due to charge balance error as no charge balance error greater than 10% was found for any one sample in the dataset. While Daughney's (2010) spread sheet has the capability to find outliers in datasets for individual analytes, almost none were removed. This is because on closer inspection of the data, apparent outliers were realistic values which could have occurred. Therefore to prevent the creation of any unnecessary bias, outliers were not removed. However, there was one exception to this rule on outlier removal. At location R27/1182 a pH of 509 was recorded for one sample. This is clearly incorrect so the entire sample was removed from the HCA.

Censored values, data above or below a detection limit threshold, are not suitable for multivariate statistical methods (Daughney & Reeves, 2005; Güler et al., 2002). There are several methods to address this to keep the analyte with a censored value in the HCA analysis. For simplicity, the method wherein the detection limit is halved was used (Güler et al., 2002).

The median values for the analytes used in the analysis were checked for normality using the Shapiro-Wilk test, quantile-quantile plots and frequency histograms. Given the small dataset a normal distribution is not expected. Log transformation of the data gave a better fit to a normal distribution therefore the log transformed median values were used for the HCA analysis.

To perform HCA the methodology described by Guggenmos, Daughney, Jackson and Morgenstern (2011) was followed. The log transformed data was plotted on a dendrogram using Statgraphics Centurion XVI software. The nearest neighbour linkage rule, using squared Euclidean as the distance metric, was used initially to plot the dendrogram (Guggenmos et al., 2011). The log transformed data was then plotted using the Ward's Linkage method.

HCA analysis requires that all sample sites have data for all of the analytes being plotted. Guggenmos et al. (2011) only used the analytes Ca^{2+}, Mg^{2+}, K^{+}, Na^{+}, Cl^{-}, HCO_3^{-}, SO_4^{2-} and electrical conductivity. These were likely chosen based simply on their frequency of occurrence in their dataset (Güler et al., 2002). To check that no bias was created in the HCA plots by using only the analytes suggested by Guggonmos et al. (2011), HCA analysis was performed using additional log transformed variables which were in the cleaned dataset for almost all sites. The additional analytes added were Mn^{2+}, NH_3-N, B, DO, DRP, NO_2-N, NO_3-N, TOC and pH. If the two different HCA analyses using different analytes give similar results then it can be assumed that the choice of analytes for the HCA analysis has not provided misleading results.

Following the allocation of clusters from the HCA analysis the median value for chemistry data for each sampling site was plotted on a Piper diagram. Piper diagrams are a tool used to determine the water type of the sample from relative concentrations of major cations and anions in the water. Knowledge of the water type can aid in determining the origin and evolution of the water (Daughney, Meilhac, & Zarour, 2009). Multiple data points from different sites plotted in the same region on the Piper diagram can indicate that those sites are from the same source.

4.3.2 River radon surveys

Radon measurements were used to investigate spatial and temporal trends of the groundwater surface water interaction dynamics of the Hutt River. Between April 2014 and March 2015 thirteen radon surveys were carried out under varying flow conditions between surveys, using different

radon measurement methods and at different resolutions (Table 4.1). Low resolution radon surveys involve the collection of radon grab samples at a distance of 500 – 800 m between each sampling point. The low resolution surveys were undertaken to get a broad snapshot of the groundwater-surface water interactions occurring in the Hutt River. Higher resolution radon surveys, where grab samples were collected 50 m apart, were then used to investigate smaller sections of the river at a more detailed scale. High sensitivity radon surveys were also undertaken to establish radon concentration thresholds to determine radon concentrations which indicate river reaches of groundwater discharge, no discharge or possible recharge, or hyporheic exchange. High sensitivity sampling was also carried out to estimate the rate at which radon degasses in the river system. In addition to the spatial radon surveys, temporal surveys were also undertaken to capture if, or how, the groundwater-surface water dynamics changed over time and under varying flow conditions. The radon surveys also included the measurement of groundwater samples from groundwater wells within the Hutt Valley to be used as a comparison for the river water radon samples measured. Lastly, flow gauging was carried out in conjunction with the radon surveys. The flow gauging was used to compare or verify groundwater surface water dynamics indicated by the radon measurements. The details of how and why these surveys were carried out are described below.

Table 4.1: Radon river surveys undertaken between April 2014 and March 2015

Survey type	Radon measurement method	Date	Location	Flow ($m^3 s^{-1}$)
Low Resolution	Direct Count	04/04/2014	Sites 6 - 28	4.0
River Width/Temporal	Direct Count	04/04/2014	Sites 24, 26A	4.0
River Width/Temporal	Direct Count	11/04/2014	Site 24	41.0
River Width/Temporal	Direct Count	06/05/2014	Sites 24, 26A	16.9
Low Resolution	Direct Count	30/08/2014	Sites 23 - 27	10.0
River Width/Temporal	Direct Count	10/09/2014	Site 24	8.2
Low Resolution	Direct Count	10/01/2015	Sites 1 - 28	5.7
High Resolution	Direct Count	11/01/2015	Sites 23 - 24 & 25 - 26	5.7
River Width/Temporal	Direct Count	18/01/2015	Site 24	3.5
River Width	High Sensitivity	11/02/2015	Site 23	3.9
River Width/Temporal	Direct Count	18/02/2015	Sites 24, 26 & 26A	3.2
Low Resolution	High Sensitivity	20/03/2015	Sites 12 – 20	3.5
High Resolution	High Sensitivity	28/03/2015	Sites 12 - 13	3.2

Two low resolution radon river surveys were carried out over an approximate 16 km stretch of the Hutt River between the Whakatikei confluence (Site 1) in the Upper Hutt to Melling (Site 28) in the Lower Hutt (Fig. 4.4). The purpose of these surveys was to identify approximate locations of groundwater discharge and possible recharge reaches along a large reach of the Hutt River. During these low resolution surveys a radon grab sample was collected every 500-800 m along the river. This sampling distance was chosen as it was the smallest practical sampling distance to enable the river reach surveyed to be sampled in a day. River water grab samples were collected in 25 mL glass vials with aluminium foil lined caps using the field collection procedure described in Chapter 3, Section 3.2.1. At each sampling site the GPS coordinates and the sampling time were recorded. A photograph of the sample site was also captured. At the end of each day of sampling the grab samples were taken to the Water Dating Laboratory at GNS Science, where they were prepared and analysed for radon using the direct count measurement procedure described in Chapter 3, Section

3.2.3, wherein the sample preparation error for the calculation of the radon concentration was 2%. These surveys were carried out on 4 April 2014 and 10 January 2015 with river flows of 4 $m^3 s^{-1}$ and 5.7 $m^3 s^{-1}$ respectively, as measured by the GWRC gauging station at the Taita Gorge. The purpose of carrying out two low resolution surveys was to investigate whether the groundwater-surface water discharge patterns in the Hutt River changed over time. In addition to these two low resolution surveys, a further low resolution survey was carried out between Sites 23 - 27 during winter, 30 August 2014, with a measured river flow of 10 $m^3 s^{-1}$ at the Taita Gorge. The purpose of carrying out this survey was to assess whether groundwater discharge patterns changed under higher flow conditions. Under higher flow conditions a larger volume of surface water runoff in the river will cause the radon signals to be diluted. Therefore, for this low resolution survey radon grab samples were collected every 200 – 300 m. Electrical conductivity was also measured during this sampling event to assess the potential of using it as complementary tool with radon to infer further knowledge of groundwater-surface water interaction.

Using the results of the low resolution radon river surveys, approximate locations of groundwater discharge were identified. Two of these river reaches were further investigated using high resolution radon river sampling. Higher resolution radon samples would provide a more precise snapshot of the locations and patterns of the groundwater-surface water interactions occurring. The first river reach selected was between Sites 23 and 24. At Site 23 the radon concentration was low relative to the results from the two low resolution radon surveys. At Site 24 there was a large increase in radon concentration, indicating a reach where groundwater is discharging. The higher resolution sampling in this area was carried out to more precisely locate where the discharge was occurring and to establish whether the discharge is a slow seep over a large distance or a larger volume of discharge over a small distance. The second river reach where high resolution sampling was carried out was between Sites 25 and 26. Low resolution radon sampling had indicated fairly consistent high radon concentrations and thus groundwater discharge. Radon samples at a higher spatial resolution were collected on 11 January 2015 with a river flow of 5.7 $m^3 s^{-1}$, as measured at the Taita Gorge gauging station. For this sampling, 25 mL radon grab samples were collected every 50 m. In addition, radon river width profiles were also taken at three different locations: Site 24, Site 26 and Site 26a which is 250 m downstream of Site 26. The river width radon profiles were taken to investigate whether the groundwater discharge distributions were different from the eastern to western banks of the river. River width radon profiles were conducted using a tape measure. A sample was taken on the eastern river bank, another sample was taken 2 m inshore from the eastern river bank. Samples were then taken 3 m apart across the width of the river at these sites. Further river width radon profiles were taken at these same three sites over the course of a year, under different flow conditions (Table 4.1). The purpose of taking these temporal river width radon profiles was to identify whether the discharge patterns across the river changed with time and flow conditions. Radon samples were collected and measured using the same techniques as described for the low resolution radon sampling above.

Where the two, full river, low resolution radon surveys showed an approximate 6 km reach where relatively low radon concentrations were measured, 0.3 – 0.7 BqL^{-1}, high sensitivity radon samples were taken. These low concentrations of radon could indicate a reach of the river where no groundwater discharge is occurring and may indicate a possible losing reach of the river. High sensitivity radon sampling was undertaken to show the rate at which the radon degasses. The high

sensitivity samples were also taken to identify radon concentration thresholds to determine what radon concentrations indicate gaining sections, potential losing sections, or non-gaining sections of the river which comprise higher than expected radon concentrations due to hyporheic flow. This is possible because the geology of this reach is well known to be bedrock, where groundwater discharge is not possible. Further downstream the geology then changes to gravels (Boon et al., 2011). In the bedrock section the radon concentrations will decrease as the radon degasses. This will continue to occur until equilibrium is reached between the radon degassing and the radon being emanated from the river bed material. The equilibrium radon concentration will allow a "no groundwater discharge" radon concentration threshold to be identified. On 20 and 28 March 2015 two high sensitivity radon sampling surveys were carried out in the Hutt River, at flows of 3.5 $m^3 s^{-1}$ and 3.2 $m^3 s^{-1}$ respectively, as measured at the Taita Gorge gauging station. In the first of these two surveys eight 273 mL samples were collected at a distance of 600 – 800 m, over an approximate 5 km distance, beginning below the Weir at Site 12 and continuing downstream to Site 20. These samples were collected using a hand held submersible pump. The second of these two high sensitivity radon surveys also began below the Weir at the Ferguson Drive Bridge, Site 12, and ten 273 mL samples were collected, at a distance of approximately 60 m, between the weir and approximately 600 m downstream of the weir.

In addition to these two high sensitivity radon surveys, on 11 February 2015, when the Hutt River was at a flow of 3.9 $m^3 s^{-1}$ at the Taita Gorge gauging station, high sensitivity radon samples were taken across the river width profile 100 m upstream of the Avalon Bridge. These samples were taken using a Bennet pump. Four, approximately 273 mL, samples were collected in conjunction with 25 mL direct count radon grab samples for comparison.

The high sensitivity samples were collected with 273 mL glass volumetric flasks using the following method:

1. Tubing from a pump is place inside a flask and the flask is held underwater.
2. The tubing is connected to a pump. The pump is placed at the point where the sample is to be collected from, near the bottom of the river bed.
3. The pump is turned on and water is allowed to flow from the tubing into the flask. Once the pump has put approximately 1 L of water through the flask, the flask is capped underwater.
4. When the flask is removed from the water the flask is checked for air bubbles. If there are air bubbles present steps 1-3 are repeated. If no air bubbles are present then the cap on the flask is tightened.

The high sensitivity radon samples were then analysed using the high sensitivity method, wherein the enrichment factor, Z, is 14.9 and $\sigma(Z)$ is 2%, established in Chapter 3 and is listed below:

1. 29 mL of sample water was removed and discarded from the sample bottle using a 60 mL syringe.
2. 23 mL of cocktail was then added to the glass flask containing the remaining sample.

3. The sample was then shaken for 6 minutes.

4. After approximately 2-4 minutes, when the sample water and cocktail had separated out into their different phases, 20 mL of cocktail was removed from the sample bottle using a 30 mL syringe and placed in a scintillation vial.

5. The vial was left for three hours before being measured to allow the daughter products of radon to equilibrate.

6. The vial was then measured in a low level scintillation counter (QUANTULUS by PerkinElmer) 10 times for 10 minutes, with a total count time of 100 minutes.

4.3.3 River flow gauging

River flow gauging was carried out to assess whether radon measurements and concurrent flow gauging could be used as complementary techniques to capture dynamics of groundwater – river water interactions. Flow gauging was carried out on 13 January 2015 at and between the locations where the 25 mL higher resolution radon sampling was carried out at Sites 250 m downstream of Site 23, 24, 30 m downstream of Site 24, 100 m downstream of Site 24, 25 and 26. Flow gauging was conducted at these six sites using a Son Tek M9 River Surveyor. The River Surveyor M9 was used to measure about 6 and 10 transects at each site to calculate average river flow at each site. In this procedure, the flow readings which were designated as being outliers by the River Surveyor Software were discarded to calculate the average river flow.

River flow gauging was also carried out on 18 February 2015 in the Hutt River by GWRC between downstream of the Whakatikei confluence in the Upper Hut, Site 4, and the Taita Gorge, Site 14. This flow gauging was carried out using a Son Tek FLOWTRACKER® HANDHELD-ADV®. These river flow gauging recordings were provided by the GWRC.

4.3.4 Groundwater radon samples

Groundwater samples were also collected as part of the radon analysis. This was so that the surface water concentrations of radon measured from the Hutt River could be compared to the concentrations in the groundwater. On February 26, 27 and March 27 2015, a total of ten 25 mL groundwater samples were collected from nine groundwater wells within the Lower Hutt groundwater zone. Samples were collected following the same procedure outlined in Chapter 3, Section 3.2.1, for the collection procedure for samples from a well. The groundwater well locations are shown in Figure 4.4.

4.4 Results and discussion

4.4.1 Hierarchical cluster analysis

The nearest neighbour method for the HCA analysis of the Hutt Valley hydrochemical data showed three possible cluster groupings (Fig. 4.6a). Unlike the suggestions in Guggenmos et al. (2011), no outliers were removed before the dendrogram was plotted using Ward's method (Fig. 4.6b). This is because of the small number of sampling sites in the dataset. Removal of any samples could create significant bias.

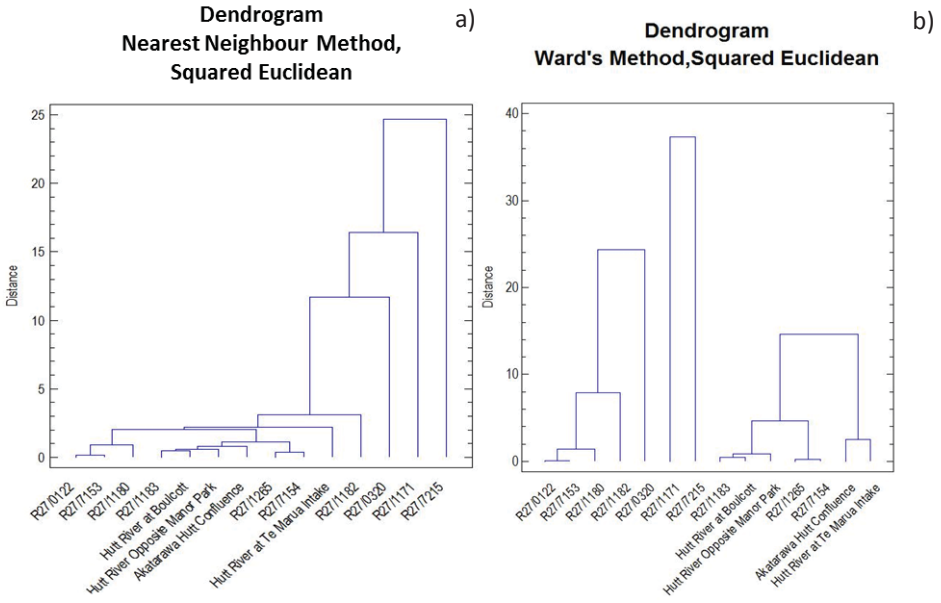

Figure 4.6: HCA analysis using the Nearest Neighbour Linkage rule (a) and Ward's linkage rule (b) with a squared Euclidean distance metric. The parameters used for the dendrogram were the log transformed median values for Ca^{2+}, Mg^{2+}, K^{+}, Na^{+}, Cl^{-}, HCO_3^{-}, SO_4^{2-} and electrical conductivity for all data sampling sites.

Dendrograms (Fig. 4.7) were also prepared using analytes Mn^{2+}, NH_3-N, B, DO, DRP, NO_2-N, NO_3-N, TOC and pH, in addition to those suggested by Guggenmos et al. (2011) (Fig. 4.6).

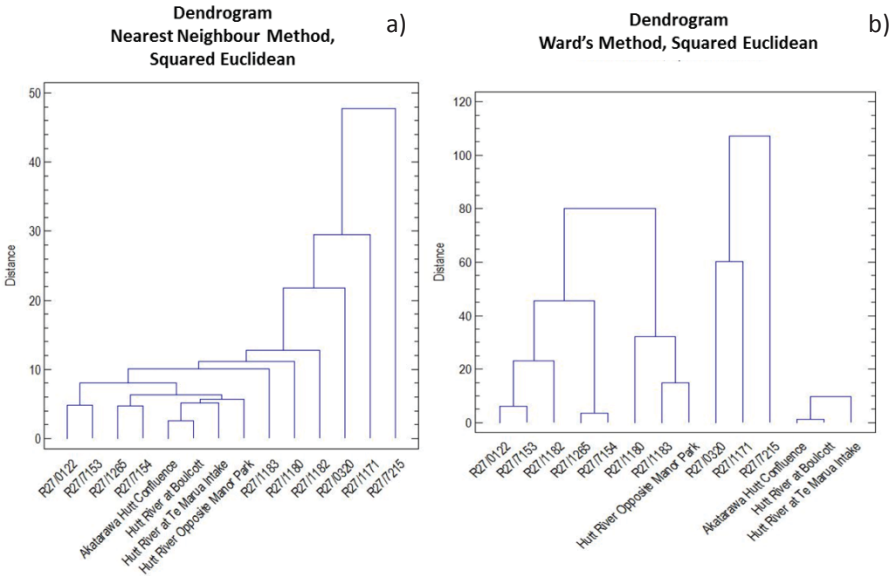

Figure 4.7: HCA analysis using the Nearest Neighbour Linkage rule (a) and Ward's linkage rule (b) with a squared Euclidean distance metric. The parameters used for the dendrogram were pH and the log transformed median values for Ca^{2+}, Mg^{2+}, K^{+}, Na^{+}, Cl^{-}, HCO_3^{-}, SO_4^{2-}, Mn^{2+}, NH_3-N, B, DO, DRP, NO_2-N, NO_3-N, TOC and electrical conductivity for all data sites.

Table 4.2 summarises the clusters of the sampling sites, the locations of which are shown in Fig. 4.5, designated by the two dendrograms using Ward's linkage method and different analytes. Five of the 14 sampling site locations have different cluster designations when 18 analytes are used for HCA instead of 8. Interestingly, cluster 2 has the least amount of change when different analytes are used to assess HCA.

Table 4.2: HCA clusters designated by dendrograms using Ward's linkage method and with analytes suggested by Guggenmos et al. (2011) and analytes suggested by Guggenmos et al. (2011) with 9 additional analytes.

Label	Cluster Grouping using 8 analytes suggested by Guggenmos et al. (2011)	Cluster Grouping using 18 analytes.
R27/0122	1	1
R27/0320	1	2
R27/1180	1	1
R27/1182	1	1
R27/7153	1	1
R27/1171	2	2
R27/7215	2	2
R27/1183	3	1
R27/1265	3	1
R27/7154	3	1
Akatarawa River at Hutt Confluence	3	3
Hutt River Opposite Manor Park Golf Club	3	1
Hutt River at Boulcott	3	3
Hutt River at Te Marua Intake Site	3	3

To investigate why the dataset was grouped into these clusters the HCA cluster groupings, using the analytes suggested by Guggenmos et al. (2011), were first compared against the data sources, groundwater or surface water, aquifer name and well depth (Table 4.3). Table 4.3 shows no correlation between cluster grouping and aquifer, nor cluster grouping and screen depth. The surface water sites are, however, all clustered together in group 3 as well as three other groundwater sites, R27/1265, R27/7154 and R27/1183, located in the Waiwhetu aquifer.

Table 4.3: Compilation of surface water and groundwater samples locations used in HCA analysis with cluster groupings, aquifer/river source, aquifer name and well screen depth.

Label	Cluster Grouping	Aquifer	Screen Depth (m)	Well Name
R27/0122	1	Waiwhetu	26.2	McEwan shallow
R27/0320	1	Moera	114.3	IBM1
R27/1180	1	Waiwhetu	39	Willoughby St
R27/1182	1	Waiwhetu	24.7	SeaView Wools
R27/7153	1	unknown		McEwan Deep
R27/1171	2	Waiwhetu	21.2	Somes Island
R27/7215	2	unknown		Tamatoa Deep
R27/1183	3	Waiwhetu	25	Avalon Studios
R27/1265	3	Waiwhetu	48.3	IBM2
R27/7154	3	Waiwhetu		Tamatoa Shallow
Akatarawa River at Hutt Confluence	3	Hutt River		
Hutt River Opposite Manor Park Golf Club	3	Hutt River		
Hutt River at Boulcott	3	Hutt River		
Hutt River at Te Marua Intake Site	3	Hutt River		

The clusters were investigated to see if their groupings are geographically related (Fig. 4.8). With the exception of all the surface water sites belonging to the same cluster group, there is no correlation shown between geographical location and cluster group. This is particularly evident on the enlarged map showing the Petone foreshore area, where all three cluster groups are located (Fig. 4.9).

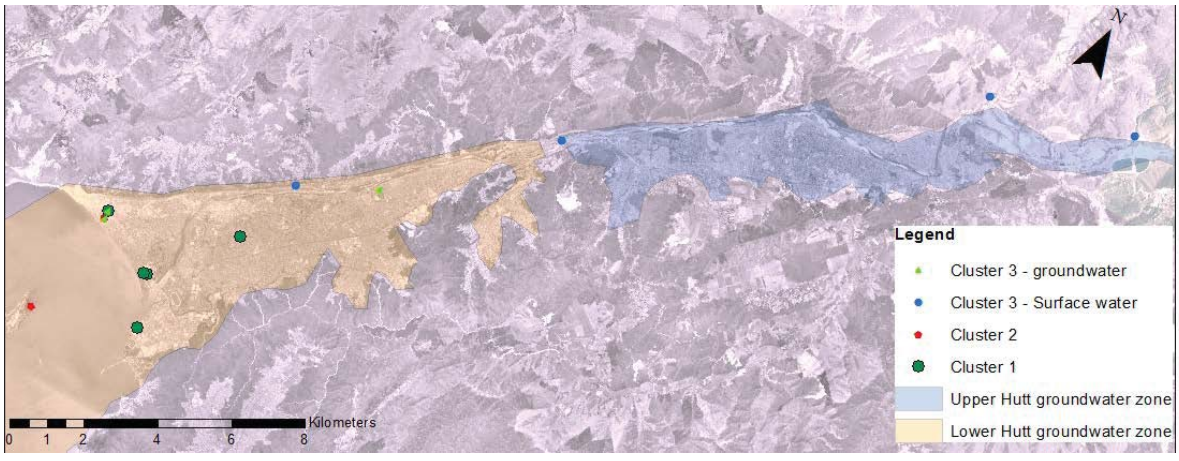

Figure 4.8: Geographic locations of the cluster groupings found in the HCA analysis of the Hutt Valley.

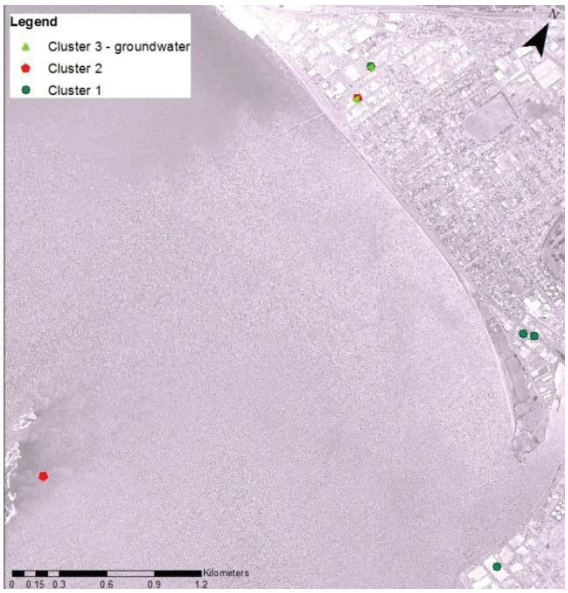

Figure 4.9: Geographic locations of the cluster groupings found in the HCA analysis of the Hutt Valley at Petone foreshore.

The chemistry was also compared between each cluster. Using the three clusters designated by Ward's linkage method for HCA analysis, Piper diagrams were plotted for both sets of cluster allocations in Table 4.2, giving very similar results. The Piper diagram (Fig. 4.10) shows that clusters 1 and 3 indicate hydrochemistry of shallow, fresh groundwaters or surface water, while cluster 2 hydrochemistry has a stronger sodium bicarbonate signal and thus indicates older groundwaters.

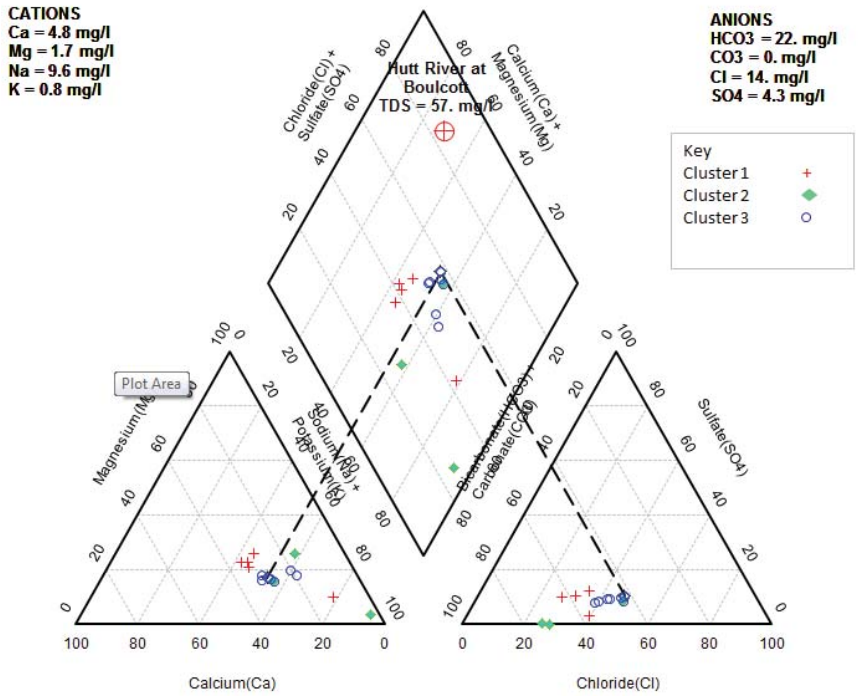

Figure 4.10: Piper Diagram displaying the chemistry of the three different clusters found using HCA which was computed with the 8 analytes suggested by Guggenmos et al. (2011).

To look at the differences in hydrochemistry between the clusters in more detail the log centroid values used in the dendrograms for HCA analysis were inverted to non-log values and compared (Table 4.4). Furthermore, the surface and groundwater centroid values from cluster 3, where all surface water sites are clustered, were separated out to further distinguish differences between the two water sources (Table 4.5).

Table 4.4: Median values for each analyte of each cluster used in the HCA analysis using Ward's Linkage method and the analytes suggested by Guggenmos et al. (2011).

Cluster	Ca^{2+} (gm^{-3})	Mg^{2+} (gm^{-3})	K^{+} (gm^{-3})	Na^{+} (gm^{-3})	Cl^{-} (gm^{-3})	HCO_3^{-} (gm^{-3})	SO_4^{2-} (gm^{-3})	Electrical Conductivity (μScm^{-1})
1	8.2	3.7	1.2	16.8	18.3	55.6	6.4	170.9
2	2.0	1.9	2.2	25.8	15.8	74.3	0.1	169.4
3	4.5	1.8	0.8	10.4	13.4	25.2	3.9	93.8

The data in Table 4.4 shows some differences in the hydrochemistry of the cluster groups. The concentrations of the calcium, magnesium and sodium cations, as well as the anion sulphate show some variability between the clusters. Electrical conductivity is similar between clusters 1 and 2 but is significantly lower for cluster 3. Likewise, bicarbonate is significantly lower for cluster 3 than the other 2 clusters. This is not unexpected as the third cluster includes all of the surface water sampling sites. Groundwaters generally have higher concentrations of bicarbonate as water which percolates through soils and gravels to the groundwater zone often become enriched in CO_2, promoting the dissolution of calcite to form bicarbonate. Electrical conductivities are also generally higher in groundwaters as the concentrations of dissolved ions are higher. Thus surface waters which show an increase in electrical conductivity or bicarbonate concentrations can indicate groundwater discharge. In Table 4.5 there are very little differences in the hydrochemical parameters between groundwater and surface water. Only bicarbonate and electrical conductivity show any significant differences between the two water sources.

Table 4.5: Median values for each analyte of surface water and groundwater from cluster 3 used in the HCA analysis using Ward's Linkage method and the analytes suggested by Guggenmos et al. (2011).

Cluster sample type	Ca^{2+} (gm^{-3})	Mg^{2+} (gm^{-3})	K^{+} (gm^{-3})	Na^{+} (gm^{-3})	Cl^{-} (gm^{-3})	HCO_3^{-} (gm^{-3})	SO_4^{2-} (gm^{-3})	Conductivity (μScm^{-1})
Surface Water	4.6	2.2	0.7	9.3	13.1	21.5	3.7	83.5
Groundwater	4.6	1.0	0.9	12.6	14.2	31.0	4.3	111.4

The chemistry data of cluster 2 shows a more strongly sodium bicarbonate water type influence, and is thus more evolved than the other two clusters. The waters of the other two clusters (1 and 3) have more of a calcium bicarbonate influence which is an indication of surface or shallow groundwaters. The similarities in water signatures of cluster groupings 1 and 3 are reinforced by the results of the second HCA analysis conducted with the additional analyte parameters. When comparing the two HCA results cluster 2 remained fairly constant while clusters 1 and 3 were interchangeable (Table

4.2). Cluster 2 remained constant between the two HCA analyses with the exception of site R27/0320 which was converted from cluster 1 to cluster 2. This is the only site sampled from the Moera Aquifer. The Moera aquifer has lower transmissivity values than the Waiwhetu aquifer leading to the mean residence time of the water in the ground to be longer, creating more evolved waters. The age of the water in the groundwater system could be one significant factor contributing to the cluster analysis. The age of the water at Somes Island (R27/1171) is approximately 20 years old (Stewart & Morgenstern, 2001). Age data also suggests that the water from the Moera Gravel Aquifer is also comparably old. One can assume that the Tamatoa Deep well is older than the Tamatoa Shallow well, giving it a more evolved hydrochemical signature and separates this site into cluster 2. The remaining sampling sites all have relatively young waters, ranging from 0 years to 3.5 years (Stewart & Morgenstern, 2001). Thus for groundwater sites in clusters 1 and 3 the residence time between water infiltrating the groundwater and being discharged back to the surface is not long enough to significantly change the hydrochemical signature of the infiltrating surface water. This is confirmed by the results of Table 4.4, where there is little difference between the signature of the ground and surface waters from cluster 3.

The purpose of performing HCA was to determine whether there were distinguishing hydrochemical tracers or analytes that could be used to compliment the radon technique in identifying groundwater and surface water interaction. A measured elevated hydrochemical parameter in surface waters could indicate groundwater discharge and thus verify the findings of the radon measurements. However, there was a significant limitation of the HCA undertaken which puts in to question using any of the analytes in conjunction with the radon analysis. The cleaned dataset used for the HCA analysis was very small in terms of the number of samples and sampling sites used. This can skew or create bias within the results of the dataset. Of the limited HCA undertaken, HCA was able to identify three possible clusters within the river system. One of these clusters, Cluster 3 (Table 4.3), included all of the surface water sites and three groundwater sites. However, only bicarbonate and electrical conductivity show any significant differences between the two water sources (Table 4.5). The groundwater bicarbonate and electrical conductivities ranged from 25 – 74 g m^{-3} and 97 – 202 µS cm^{-1} respectively, with no geographical pattern in the distribution of concentrations. The average electrical conductivity for each surface water site ranged from 68 µS cm^{-1} to 99 µS cm^{-1}, with electrical conductivity slightly increasing at each site as you go downstream. The same trend in surface water sites was seen with bicarbonate concentrations, with concentrations increasing from the most upstream site, 19 g m^{-3}, to the most downstream site, 25 g m^{-3}. This trend likely occurs due to the cumulative effect of groundwater discharge occurring through the river.

Electrical conductivity was measured during the sampling event carried out in August 2014 in the Hutt River in the Lower Hutt. Electrical conductivity measurements were taken in four locations, one upstream of the Avalon Bridge at Site 23, where there is little or no groundwater discharge and three sites, Sites 24, 26 and 27 where higher radon concentrations have been measured and thus where groundwater discharge is thought to occur downstream of the Avalon Bridge. There was no significant difference in the conductivities measured, with the four conductivities measured being between 95.3 ± 4.8 µS cm^{-1} and 97.2 ± 4.9 µS cm^{-1}. This absence of a significant gradient in electrical conductivities shows the limitations of using electrical conductivity as an indicator for locating groundwater-surface water interaction. Where groundwater discharge from upstream dominates the flow downstream during low flow conditions the gradient between surface water and

groundwater becomes too small to differentiate the source of the groundwater discharge. This same trend is likely be seen for other hydrochemical analytes, such as nitrate, which showed differences between the concentrations in the surface water in the Upper reaches of the Hutt River to the groundwater in the Lower Hutt groundwater zone.

The HCA analysis indicated limited benefits for measure hydrochemical analytes in conjunction with the radon surveys. The only two analytes which showed any potential from the HCA as being suitable as a complementary tracer with the radon sampling was electrical conductivity and bicarbonate. The results of the in-stream sampling of electrical conductivity in sites known to have no groundwater discharge as well as those known to have groundwater discharge show the electrical conductivity does not capture any information on the dynamics of groundwater surface water interactions. Therefore no further hydrochemical parameters were measured and used in combination with the radon sampling to assess surface water-groundwater interactions in the Hutt River system.

4.4.2 Groundwater radon samples

Groundwater samples were measured for radon in order to compare the radon concentrations measured in the Hutt River to the concentrations present in the groundwater. The concentration of radon in a river water sample divided by the radon concentration in discharging groundwater gives a minimum ratio of groundwater contribution in the river at a discrete site (see Section 4.4.4). Samples were taken from the Lower Hutt only due to the accessibility of the wells. The radon concentrations were very similar, ranging from 28 to 37 BqL^{-1} between the nine groundwater wells. The geographical location of the groundwater wells are shown in Figure 4.4.

4.4.3 Longitudinal low resolution radon sampling

Three low resolution radon surveys were carried out in the Hutt River. The radon concentrations for all of the low resolution surveys are tabulated in appendix 1 and plotted in Figures 4.11-4.13. The scaling of the radon concentrations in Figures 4.11-4.13 were determined by plotting the frequency of radon concentration occurrence for all low resolution surveys sites between the Whakatikei confluence and the Melling Bridge in quantile plots. The percentiles were then determined from the quantile plots and used to scale the results. The radon concentrations collected in the August 2014 sampling survey were not included in the frequency calculations as the flow was approximately twice that of the other low resolution surveys which would likely dilute the radon concentrations.

The first survey was undertaken in April 2014 (Fig. 4.11) from approximately 1.5 km downstream of the Whakatikei confluence, at the Upper Hutt, to Melling, in the Lower Hutt. The survey results indicate strong groundwater discharge circa. 1.5 km upstream of the Ferguson Drive Bridge, Site 11, with radon concentrations of 2.7 BqL^{-1} measured. Further downstream at the weir, Site 12, near the Ferguson Drive Bridge, radon concentration decreased steadily, from 1.0 BqL^{-1} to 0.5 BqL^{-1}, indicating that no interaction is occurring as the radon degasses or possibly there is groundwater recharge. Groundwater discharge is also strongly indicated downstream of the Avalon Bridge, Site 24, to Melling, Site 28, where radon concentrations increased from 0.5 BqL^{-1}, at Site 23, to 4.8 BqL^{-1} at Site 24, and remain consistently high, between 1.7 BqL^{-1} and 3.0 BqL^{-1} to the Melling Bridge. The flow for

this April survey, measured by the GWRC gauging station at the Taita Gorge, was approximately 4 $m^3 s^{-1}$.

The second low resolution survey was undertaken on 30 August 2014, with a flow of 10 $m^3 s^{-1}$ at the Taita Gorge gauging station (Fig. 4.12). This survey was conducted over an approximate 2 km distance starting 200 m upstream of the Avalon Bridge going downstream. The relative differences in measured radon concentrations again suggest significant groundwater discharge downstream of the Avalon Bridge as the radon concentration increases from 0.6 BqL^{-1} 250 m downstream of Site 23, to 1.4 BqL^{-1} at Site 24.

The third low resolution survey was undertaken on 10 January 2015, with a flow of 5.47 $m^3 s^{-1}$ at the Taita Gorge (Fig. 4.13). This survey began 2 km further upstream from the first survey undertaken in April 2014 and was carried out from the Whakatikei confluence, Site 1, in the Upper Hutt to Melling, Site 28.

The survey undertaken on 10 January 2015 found the same groundwater discharge trends as the previous surveys in April 2014 (Fig. 4.11) and August 2014 (Fig. 4.12). At the Whakatikei confluence bedrock is observed and radon concentrations are almost negligible, at 0.1 BqL^{-1}, indicating no groundwater discharge until approximately 2 km downstream, Site 5, where the river bed changes to gravels. At Site 5 radon concentrations increase steadily to 0.7 BqL^{-1}, and continue to increase to levels exceeding 2 BqL^{-1}. Downstream of Site 12, after the weir, radon concentrations decrease to concentrations of 0.7 BqL^{-1} and lower through the Taita Gorge until Site 23. The lower radon concentrations are an indication that there is no groundwater discharge through this area and are possibly representative of a groundwater recharge zone. At the Avalon Bridge, Site 24, the sharp increase in radon concentrations indicates a river reach of groundwater discharge, which continues to the Melling Bridge, Site 28. This radon distribution pattern from the Avalon Bridge to the Melling Bridge is also observed under higher flow conditions (Fig. 4.12).

These findings from radon measurements in groundwater discharge patterns are supported by a previous groundwater modelling study of the Waiwhetu aquifer by Gyopari (2014) (Fig 4.14). Moreover, the model supports the idea that the low radon results found through the Taita Gorge, from Site 13, indicate that there is groundwater recharge.

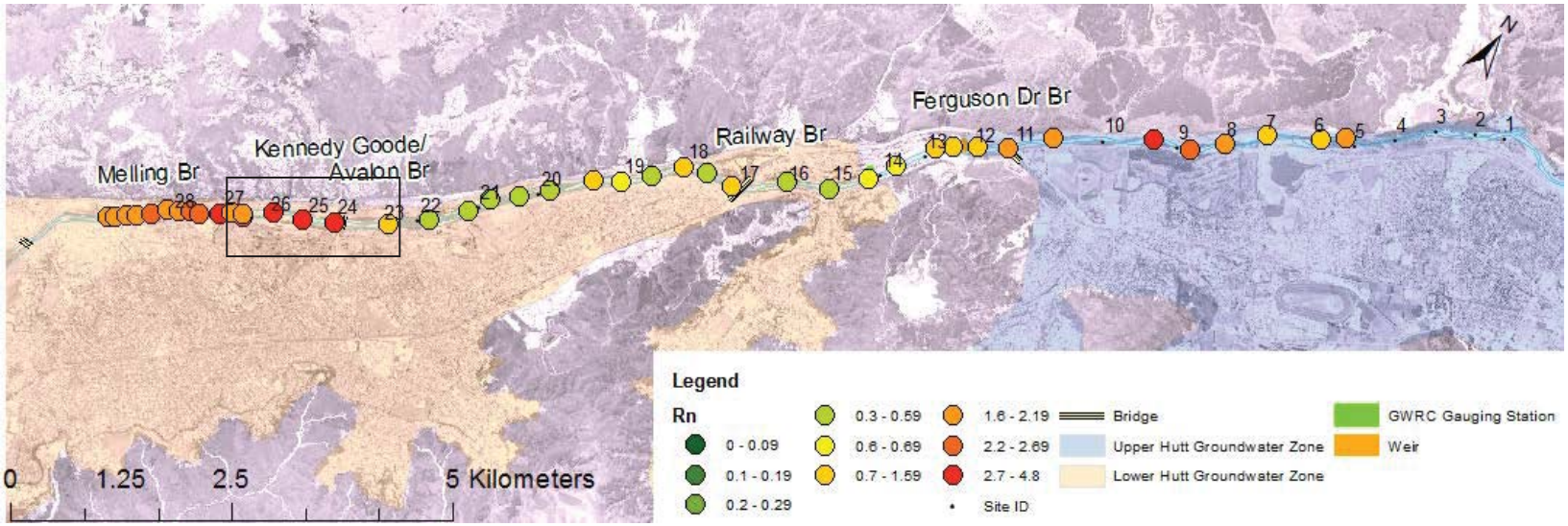

Figure 4.11: Measured radon concentrations in the Hutt River at low flow (4 $m^3 s^{-1}$) on 4 April 2014: The colour denotes radon concentrations in BqL^{-1}. The black rectangle indicates the river reach sampled on 30 August 2014 in Figure 4.12 below.

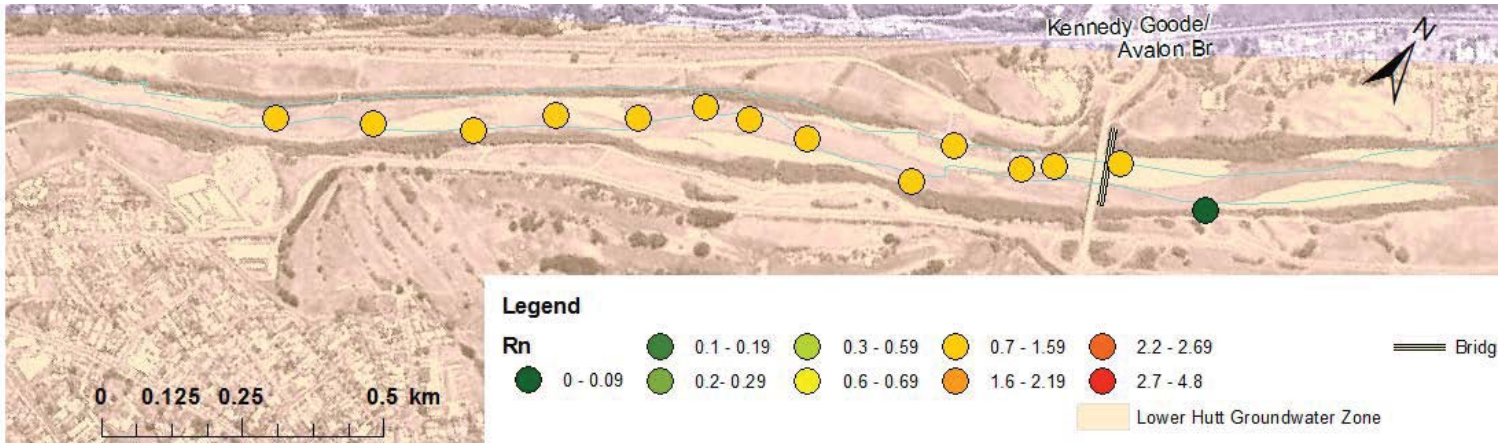

Figure 4.12: Measured radon concentrations in the Hutt River at medium flow (10 $m^3 s^{-1}$) on 30 August 2014. The colour denotes radon concentrations in BqL^{-1}.

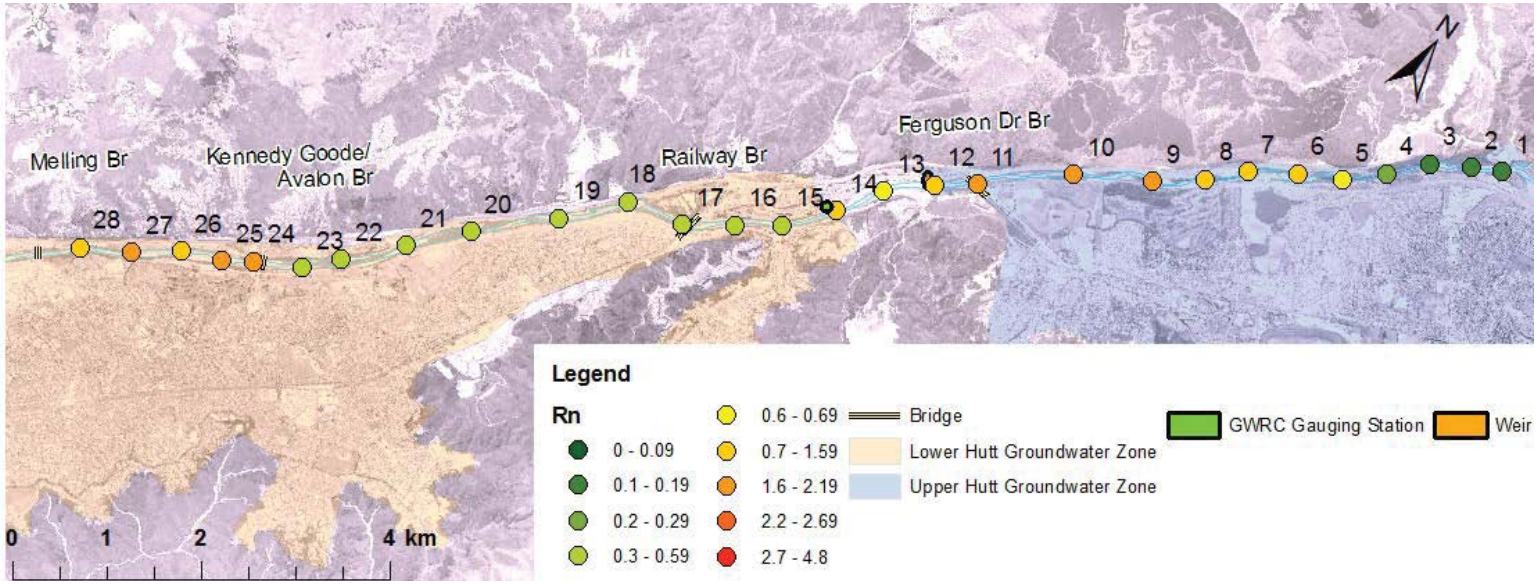

Figure 4.13: Measured radon concentrations in the Hutt River at low flow (5.7 $m^3 s^{-1}$) on 10 January 2015. The color denotes radon concentrations in BqL^{-1}.

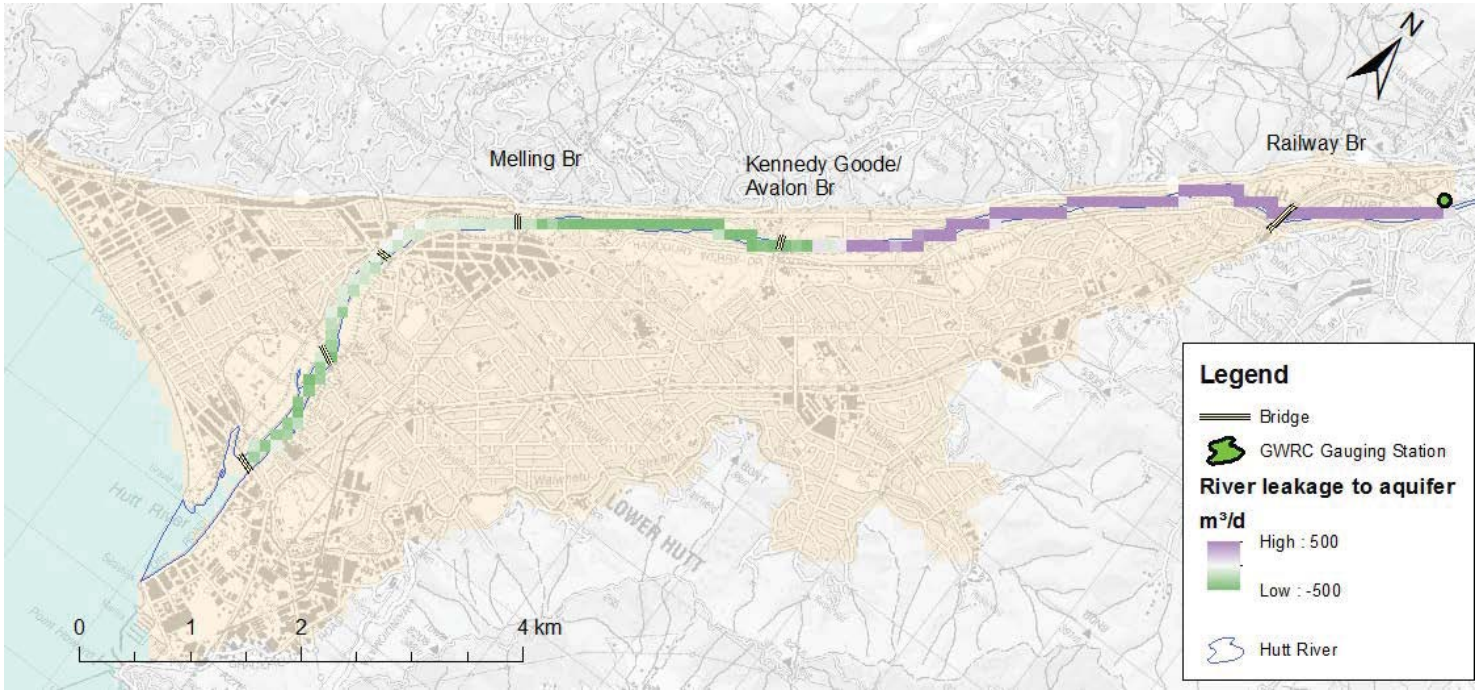

Figure 4.14: Transient MODFLOW model simulates groundwater exchanges with the Hutt River, as well as other hydraulic boundaries and pumping wells. Results from the simulated river leakages along the Hutt River show a transition from aquifer gaining (positive flux) to river gaining (negative flux). Image adapted from Gyopari (2014).

4.4.4 Lower Hutt - high resolution radon sampling, temporal radon sampling and river flow gauging

The low resolution radon sampling surveys have provided a good initial snapshot of potential groundwater-surface water interaction dynamics in the Hutt River system. However, a limitation of the survey is the low resolution. Samples were taken between 500-800 m apart. While this has allowed for reaches of the river which are thought to be gaining and possibly losing to be identified it does not capture potential interactions between these sampling sites. Furthermore, it does not give insight into whether the high radon concentrations measured are from groundwater discharge sources close by or carried downstream from an upstream discharge source. To investigate these groundwater surface water interaction dynamics further higher resolution radon measurements were conducted.

Two low sensitivity, high resolution, radon surveys were undertaken, in January 2015. The first high resolution survey undertaken was around the Avalon Bridge. Just downstream of the bridge, Site 24, there was measured a large increase in the radon concentrations during the low resolution surveys (Fig. 4.11-4.13). However, approximately 500 m upstream there was an almost negligible concentration of radon. During the high resolution survey, a total of ten samples were taken 50 m apart between Site 24 and Site 23. The results show that the radon concentration started to increase gradually from approximately 100 m upstream of the bridge, reaching a high radon concentration, or greater groundwater discharge, approximately 100 m downstream of the bridge (Fig 4.15). High radon concentrations measured downstream of the bridge indicate a large groundwater discharge at that site, rather than an accumulation of radon from slight groundwater discharges starting from 100 m upstream of the Avalon Bridge. This assumption is made because in April 2014 a radon sample measured from this site found a concentration of 4.8 BqL^{-1} (Fig 4.11). Given that the concentration of radon in the groundwater is approximately 30 BqL^{-1}, a measured radon concentration of 4.8 BqL^{-1} in the river indicates that the groundwater contribution at Site 24 was a minimum of 16%. Radon concentrations this high would not be achieved without a significant groundwater contribution.

The second high resolution survey, between Sites 25 and 26, showed less variable results. Very little changes in radon concentrations were observed across the eight points sampled, with the radon concentrations ranging from 1.2 BqL^{-1} to 1.7 BqL^{-1}. Starting from the most upstream site, the radon concentration decreased slightly, then increased, and then decreased again. While it can be assumed that there is groundwater discharge at the site where radon increases, the river flow gauging results could suggest otherwise. This is further discussed below.

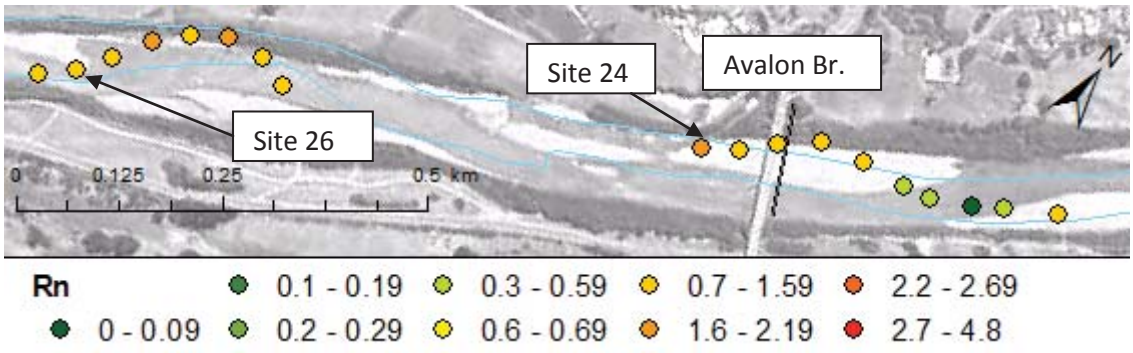

Figure 4.15: Measured radon concentrations in the Hutt River at low flow (5.7 $m^3 s^{-1}$) on 11 January 2015. The colour denotes radon concentrations (BqL^{-1}).

River width radon profiles were taken at Sites 24 and 26 (Fig. 4.16b and 4.16a). A river width radon profile was also taken at Site 26A, located 250 m downstream of Site 26 (Fig. 4.16c). These sites were selected for across width radon profiles as the low resolution surveys identified them as areas where groundwater discharge is occurring. Site 24 has significantly higher radon concentrations on the eastern side of the river bank, with concentrations decreasing towards the western side of the river. This trend was observed consistently under varying river flow rates from 3.2 to 8.2 $m^3 s^{-1}$ (Fig. 4.16b). Sites 26 and 26A have a similar trend in radon concentration distribution across the width of the river to Site 24. This suggests groundwater discharge from the east but not, or to a lesser extent, from the west of the river. This spatial distribution in radon concentrations across the width of the river fits with the geology of the area as the aquifer extends to the east, and ends in the west with the fault and bedrock only a few meters away (Boon et al., 2011; Jones & Baker, 2005). Groundwater discharge is therefore expected from the eastern side of the river. Furthermore, the radon river width profiles show that the radon signature is best apparent at lower flows, when the signal is less diluted by surface water.

As a comparison, high sensitivity samples were taken across the river width profile at Site 23, where no groundwater discharge was thought to be occurring. This survey aimed to measure whether the same trend in groundwater seepage from the eastern side of the river bank occurred in areas where the concentration of radon was very low. The results from this survey showed that, the radon concentration distribution across the river width was predominantly uniform (Fig. 4.17).

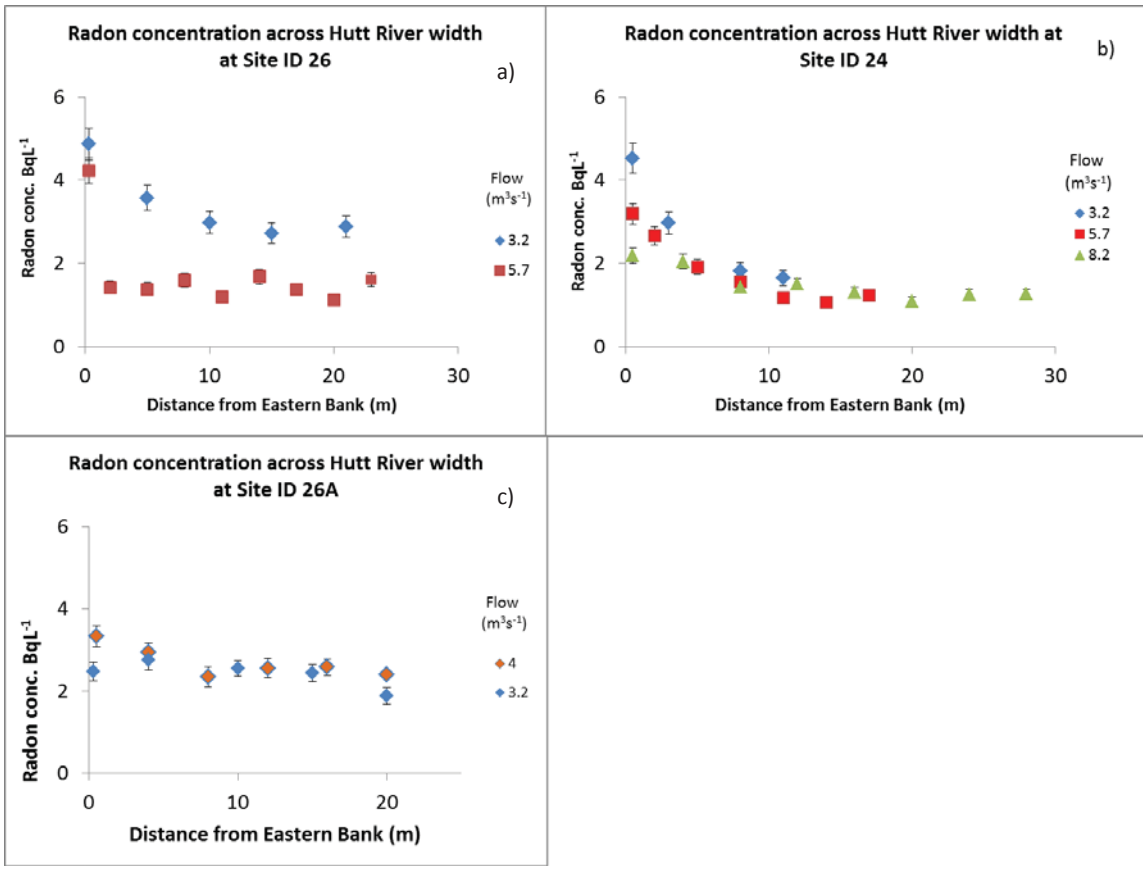

Figure 4.16 : Measured radon concentrations across the width of the Hutt River at Sites 26 (a), 24 (b), and 26A (c) at varying flow rates.

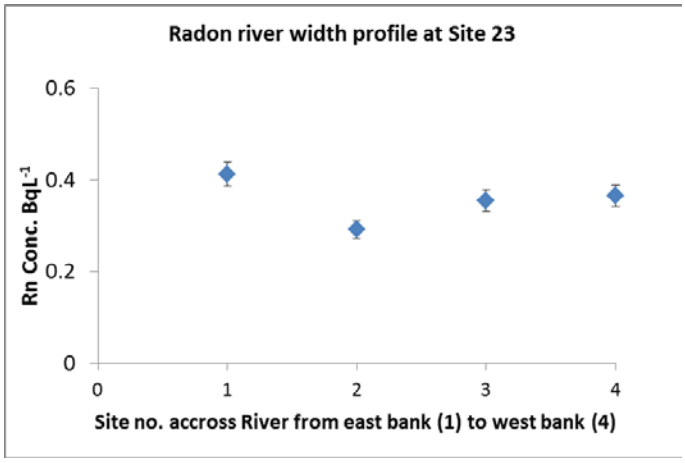

Figure 4.17: Radon concentrations from high sensitivity samples collected across the width of the Hutt River at Site 23, upstream of the Avalon Bridge.

The variation in radon concentrations of the grab samples taken at Site 24, 26 and 26A with varying flow conditions are also compared (Fig. 4.18a-c). The measured radon concentrations all decrease with increasing flow, except for one sampling event at site 26A. The radon, or groundwater discharge, consistently discharges in from the eastern river bank (Fig. 4.16a-c). The temporal variation in the river width profiles shows that radon concentration increases as the flow decreases. This is likely due to there being more groundwater relative to surface water as the river levels fall to

base flow. Though, there is one exception to this finding. At Site 26A two radon river width profiles were taken under different flow conditions, 4.0 $m^3 s^{-1}$ and 3.2 $m^3 s^{-1}$. It is expected that higher radon concentrations would be measured in the lower of the two flows. However, at Site 26A the opposite occurred with the radon concentrations being measured higher at the higher flow (Figure 4.18c). This highlights an important limitation of the study. All radon sampling points were measured using a Garmin GPS. It has an accuracy of 4 m. It is highly probable that samples in the temporal study were not taken in precisely the same location every time due to the error of the GPS. This may account for the discrepancy between radon concentration and river flow. Another possibility is that the position of the groundwater discharge moved over time. The Hutt River is a gravel bed river which can easily have sediment movement or slumping over time during high flow conditions. Given that there was a period of approximately 10 months between the two sampling events the movement of the river sediment and/or gravels over time could have impacted the location and rate of the groundwater discharge. Such changes in radon concentration over time due to river bed changes have been reported in other studies (Hammond et al., 1977). However, from photographs taken during both sampling surveys, no noticeable change in streambed was observed at this site. A further possibility for this unexpected finding at Site 26A could be related to the turbulence. If the river is more turbid, due to wind or flow conditions, the radon will degas faster. However, no wind measurements were taken during sampling so this cannot be confirmed as being a reason for the difference in the radon concentrations.

Interestingly, the river width profile at Site 26, in the Lower Hutt, did not show the same radon concentration profile as measured upstream at Site 24 during the higher flow of 5.7 $m^3 s^{-1}$. Apart from the one very high radon concentration measurement on the Eastern bank, the radon concentration across the Site 26 profile is relatively consistent (Fig. 4.16a). However, at a lower flow of 3.2 $m^3 s^{-1}$ the radon concentration across the profile follows the same trend as that upstream at Site 24. This suggests that the groundwater is being discharged at the eastern bank but in the higher flow is being diluted across the river width. Under lower flow conditions the effect of the radon being diluted by surface water is greatly reduced.

The consistent trend from the temporal and across river width radon surveys is that groundwater predominantly discharges from the eastern side of the river bank. This groundwater discharge pattern is mainly governed by the geological setting of the area where the aquifer extends to the east, and ends in the west with the fault and bedrock only a few metres away (Boon et al., 2011; Jones & Baker, 2005). It is unlikely that groundwater is being discharged from the bedrock on the western river bank.

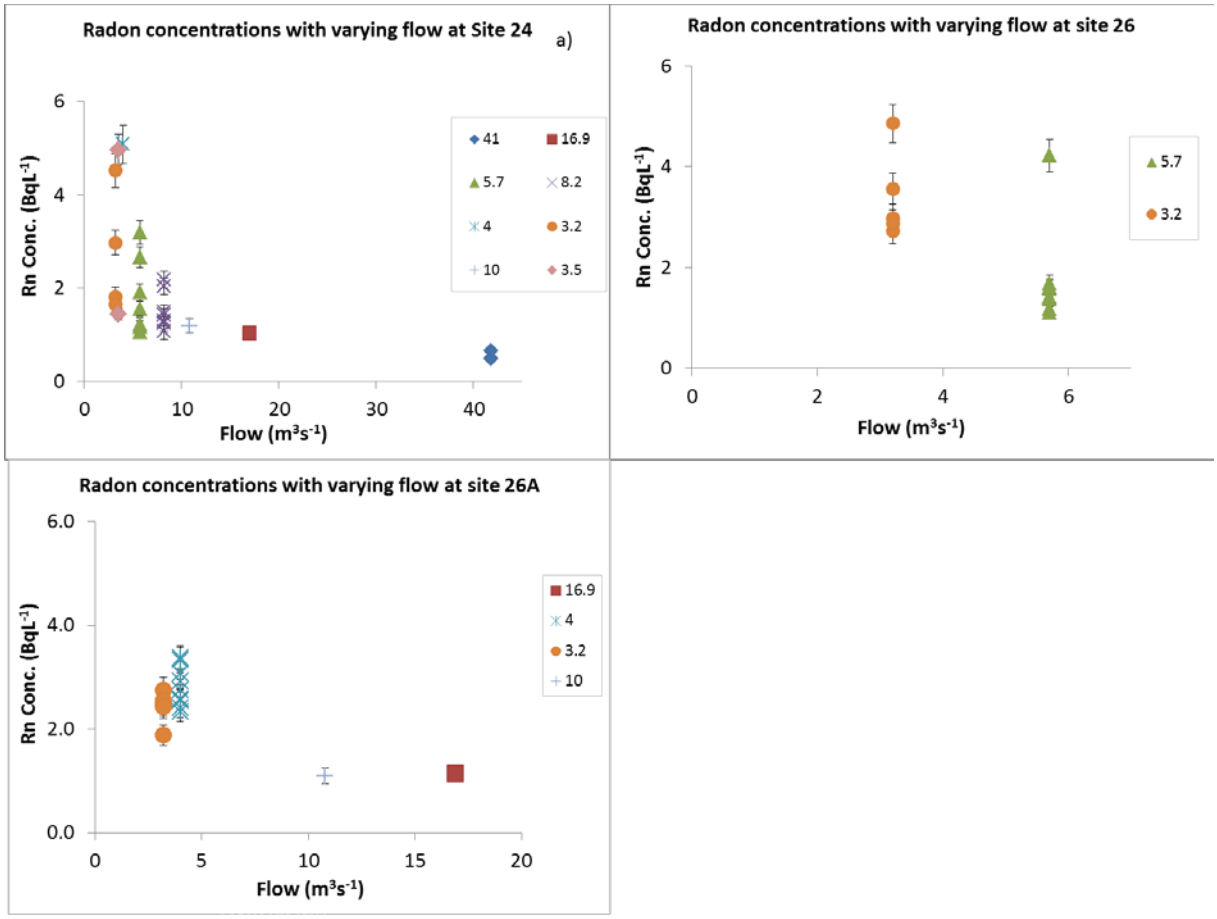

Figure 4.18: Variation in radon concentrations at Site 24 (a), 26 (b) and 26A (c) with varying river flows rates. Points on each graph with the same colour/shape were taken on the same day in a different section of the river width.

The concurrent river flow gauging results, as well as the gauging location site names, collected from the surveys in the Lower Hutt are tabulated in Table 4.6. Flow gauging measurements were taken at 6 sites over a distance of aprroximately 1 km, from 300 m downstream of Site 23 to Site 26. The distance between flow gauging sites was between 150 m – 350 m, with the exception of one site, d/s speedy ck (Table 4.6), 10 m downstream of Site 24. Speedy Creek is the only tributary that flows into the Hutt River over the 1 km reach of river that was gauged. Due to the creek being too shallow to measure the flow with the Son Tek M9 River Surveyer, the flow was measured upstream and downstream of the tributary to take into account the Creek's influence on the Hutt River flow. The most upstream flow gauging site, 300 m downstream of Site 23, and Site 24 were chosen for gauging to identify whether the river flow increased between the two sites, and correlated to the increased radon concentrations, indicating groundwater discharge. The remaining three flow gauging sites were selected to determine whether the high radon concentrations measured between Sites 24-26 were due to increased groundwater discharge or whether the radon measured downstream could be residual radon from that being discharged at Site 24.

Table 4.6: Flow gauging measurements taken in the Hutt River in the Lower Hutt on 13 January 2015 in order of most upstream site to most downstream site.

Site Name	Easting	Northing	Flow ($m^3 s^{-1}$)	std. dev.
300 m d/s Site 23	1762064	5438196	3.871	0.049
Site 24	1761835	5438092	5.125	0.090
d/s speedy ck	1761812	5438076	5.162	0.034
before 1st meander	1761763	5438026	5.134	0.113
after 1st meander	1761437	5437823	3.849	0.100
26	1761155	5437718	4.309	0.134

The results of the river flow gauging measurements are compared to the radon concentrations measured in the high resolution survey (Fig. 4.19).

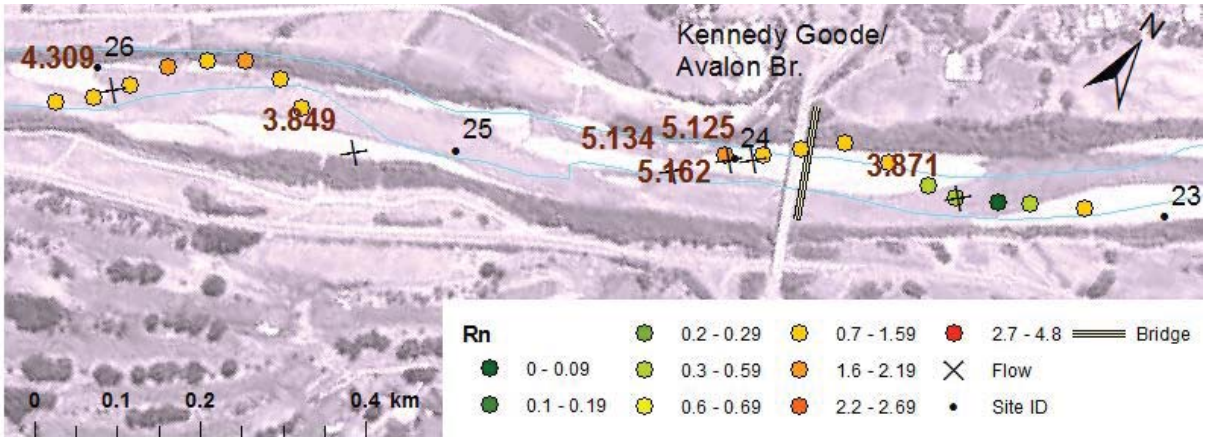

Figure 4.19: Measured river flows (as written on figure) in $m^3 s^{-1}$ comparitive to the measured radon concentrations, where the colour denotes the radon concentration in BqL^{-1}. Flows were taken on 13 January 2015 and radon was measured on 11 January 2015.

The radon survey showed an increase in measured radon concentrations between 200 m downstream of Site 23 and Site 24, indicating groundwater discharge between these two sites. The concurrent river flow gauging also showed a signicant increase in river flow, from 3.871 $m^3 s^{-1}$ to 5.125 $m^3 s^{-1}$, from upstream of the Avalon Bridge, 300 m dowsntream of Site 23, to downstream of the Avalon Bridge, Site 24. Here the radon and flow gauging techniques have shown to complement one another. However, the two most downstream flow gauge sites, Site after 1st meander (Table 4.6) and Site 26, measured lower river flows than expected. Given that the low resolution radon sampling survey shows a relatively consistent concentration of radon to be present and the high resolution radon measurements indicated some groundwater discharge, the flow is expected to be very similar to that taken at Site 24, if not a little higher due to further groundwater discharge. However, the flow measured at Site after 1st meander (Table 4.6) was lower than at Site 24. The standard deviations of the flow measurements for the three most downstream sites were relatively high due to the depth of the river at these gauging points. The Son Tek equipment is less suited for shallower water and can give ambiguous results if the water depth is less than approximately 30 cm. However, the variability caused by the shallow water does not discount the trends in river flow from the

gauging survey as the differences in measured flows between sites, 300 m d/s Site 23, Site 24, Site after 1st meander and Site 26 are greater than the standard deviations.

This variation and inconsistencies between measured flows and radon concentrations may be explained by the shape of the river (Fig. 4.20). After the Avalon Bridge the river flow remains relatively consistent between Sites 24 and Site before 1st meander (Table 4.6). This combined with the high radon concentration measured at Site 24 suggests that there is a large groundwater discharge at Site 24. The river then meanders eastwards, with a shallow rapid. After this first meander the river straightens. The fifth flow gauge was taken where the river straightens, Site "after 1st meander" (Table 4.6). The flow at this site significantly decreased from Sites 24, Site d/s speedy ck (Table 4.6) and Site before 1st meander (Table 4.6), measured downstream of the Avalon Bridge. This suggests that the high radon concentration measured downstream of Site 25 is due to residual radon carried downstream, rather than groundwater discharge. After the second meander (westwards), downstream of the Avalon Bridge, (Fig.4.21) the last gauge was measured at Site 26. Here the river flow increased slightly. Radon concentrations at Site 26 were also relatively high, 1.3 BqL^{-1}. The combined radon and flow gauging data suggest that there is groundwater discharge at Site 26. While this potential groundwater discharge has been shown to come from the eastern river bank (Fig. 4.16a), the radon signal measured at Site 26 could also have contributions from radon picked up from hyporheic flow, as the reduced flow measurement at Site "after 1st meander" suggest that the river water flows beneath the gravels avoiding the meander and re-enters the river when the river straightens out again at Site 26.

Figure 4.20: Photograph of Hutt River downstream of the Avalon Bridge. Icon (1) indicates the location of the Avalon Bridge. Site Name "300 m d/s Site 23" was taken upstream 200 m of this bridge. Site 24 was taken 70 m downstream of this bridge. Site Name "d/s speedy ck" was taken approximately 10m downstream of Site 24. Icon (2) indicates where the first meander occurs after the Avalon Bridge. Site Name "before 1st meander" was taken just before this meander. Icon (3) indicates where the 5th flow gauge was taken, Site Name "after 1st meander".

Figure 4.21: Photograph of Hutt River downstream of the Avalon Bridge. Icon (3) indicates where the 5th flow gauge was taken, Site Name "after 1st meander". Icon (4) indicates where the second meander occurs and where the high radon concentration was measured during the high resolution sampling. Icon (5) indicates where the final flow gauge was measured, Site 26, and where the second river width radon profile was taken.

The concurrent river flow gauging was further compared with the radon concentrations measured in the winter survey in August 2014 (Fig 4.22). During the winter the river flow measured at the Taita Gorge gauging station was 10 m^3 s^{-1}. This flow is much higher than flow conditions when other spatial radon sampling in the Hutt River was undertaken. The effect of sampling in higher flow conditions is that the radon concentration is diluted. Thus because of the dilution of the radon, locations of groundwater discharge are more precisely determined because any measured radon is more likely to be directly from the groundwater source as opposed to residual radon carried downstream from an upstream groundwater discharge source. The winter radon survey identifies a large discharge at Site 24, which correlates to the increase in measured river flow at this site. After the first meander, measured radon concentrations, of 1.0 BqL^{-1}, indicate some groundwater discharge. This is contrary to the river flow measured at this site, which decreases, indicating groundwater recharge. This suggests that groundwater is continually being discharged at the meander, even though the flow gauging identifies a decrease in flow.

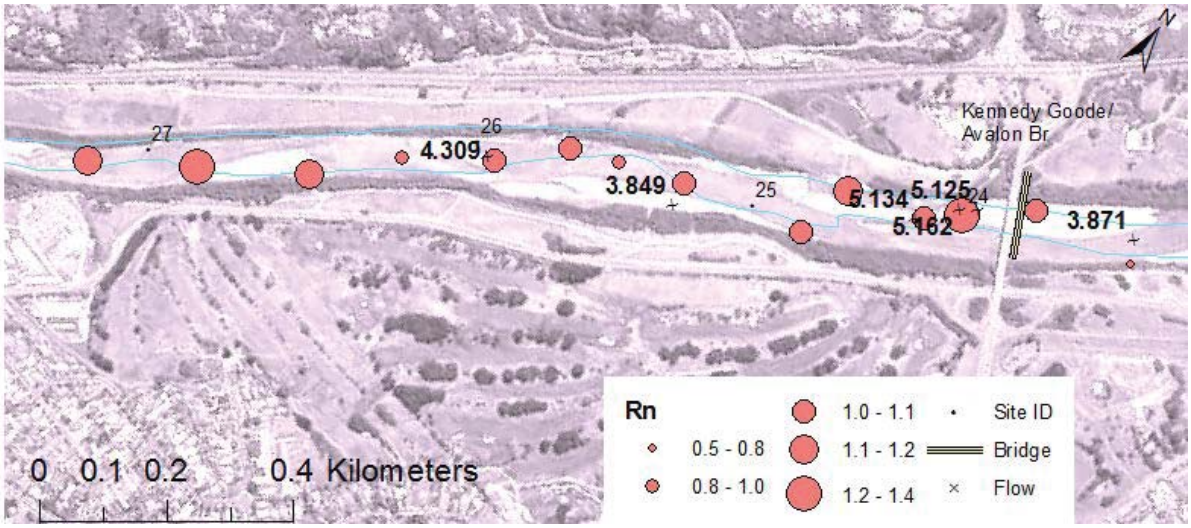

Figure 4.22: Measured flows (as written on figure) in $m^3 s^{-1}$ in bold comparitive to the measured radon concentrations in BqL^{-1}, where the radon concentrations are denoted by the coloured symbol size where the smallest symbol is equal to the lowest measured radon concentrations, 0.5 – 0.8 BqL^{-1}, and the largest symbol is equal to the largest measured radon concentrations 1.2 - 1.4 BqL^{-1}.

From the combination of the concurrent flow gauging and high resolution radon measurements the following groundwater-surface water dynamics in the Lower Hutt are suggested:

- Groundwater discharges into the Hutt River at the Avalon Bridge. This is indicated by the measured increase in flow and higher measured radon concentrations.

- Radon concentrations are measured higher on the eastern side of the river, where discharge would be expected to occur.

- From Speedy Creek to the first meander after the Avalon Bridge, Site before 1st meander, groundwater discharge occurs. This is despite the flow remaining consistent between Speedy Creek and the flow measured just before the first meander. The radon concentrations measured in the winter radon survey remain relatively high until the first meander. This indicates groundwater discharge is still occurring as the effects of residual radon carried downstream are likely to be minimal as the higher winter flow dilutes the radon signal. It is likely that there is a high level of exchange between the groundwater, hyporheic zone and surface water occurring for the flow to remain stable while radon identifies groundwater as being discharged at the same time.

- There is some groundwater discharge between the first and second meander, between Sites before 1st meander and after 1st meander. This is indicated by radon concentrations of 1.0 BqL^{-1} being measured. However, the decrease in flow through this reach of river indicated that two processes were likely occurring: groundwater discharge, as indicated by the measured radon, and underflow beneath the gravels at the first meander, as indicated by flow measurements.

- At the site where the flow increased after the second meander, Site 26, in the section of river gauged, a correlating increase in radon concentration was observed. This is likely due

to a combination of groundwater discharge and discharge of water from the hyporheic zone due to underflow of river water at the gravels between the meanders. The reasons for this hypothesis are:

- The river flow decreases directly after the first meander.
- Radon concentrations increase after the second meander. The second meander finishes directly in line with where the Hutt River ran before the first meander.
- The flow increases after the second meander.

4.4.5 Upper Hutt – river flow gauging and high sensitivity radon sampling

Unlike the flow gauging surveys undertaken in the Lower Hutt, in the Upper Hutt a Son Tek FLOWTRACKER® HANDHELD-ADV® was used for river flow measurements. Only one transect was taken at each measurement site because the flow tracker takes a 20 second measurement at each vertical across the river and then averages the velocity. Vertical velocity measurements, which do not comprise more than 10% of the total streamflow discharge, are taken at each flow measurement site so that an accurate area, bed picture and velocity can be measured. Using this model of flow gauging equipment allows for shallower, smaller streams to be gauged. Thus any tributaries flowing into the Hutt River in the section of the river surveyed were also measured. Flow gauging results collected from the survey in the Upper Hutt between the Whakatikei confluence and approximately 2 km downstream of the Ferguson Drive Bridge are tabulated in Table 4.7. The measured river flows, which ranged 2.1 to 2.8 $m^3 s^{-1}$, have been used to estimate which reaches between gauging sites are gaining or losing, where tributary gains have been taking into account (Table 4.7). The river gains and losses, as indicated by flow gauging, are compared with the measured radon concentrations (Fig. 4.23). The measured river flow decreases between the most upstream site, Hutt River at Moonshine Bridge, 170 m downstream of Site 4, to approximately Site 7, Hutt River at Heretaunga Golf Course north boundary. This groundwater recharge reach indicated by the flow gauging contradicts the groundwater-surface water interaction patterns indicated by the measured radon concentrations as between Sites 4-7 the radon concentration increases from 0.2 BqL^{-1} to 1.1 BqL^{-1}, indicating a river reach of groundwater discharge. Between Sites 8-10, Hutt River at Heretaunga Golf Course 1 to Hutt River at Heretaunga Golf Course, a river reach of groundwater discharge is indicated by both an increase in the measured flow and high radon concentrations. At Site 11, the Ferguson Drive Bridge, the measured flows again contradict the discharge pattern indicated by the measured radon concentration, as the reduced flow indicates groundwater recharge yet the radon concentration is high, indicating groundwater discharge. This contradiction between the radon and flow gauging methodologies is again observed at the final gauging site, Site 14, as the measured radon concentrations are relatively low 0.6 – 0.7 BqL^{-1}, indicating no groundwater discharge, but the measured flow shows an increase in flow from the upstream site.

Table 4.7: Flow gauging measurements taken in the Hutt River (black) and inflowing tributaries (green) in the Upper Hutt on 18 February 2015 starting from the most upstream site to the most downstream site.

Site Name	Easting	Northing	Flow ($m^3 s^{-1}$)	Estimated flow gain/loss ($m^3 s^{-1}$)
Hutt River at Moonshine Bridge	1771010	5445624	2.756	
Moonshine Stream at Hutt Confluence	1770893	5445605	0.009	
Hutt River opposite Moonshine Hill Road	1770619	5445312	2.431	- 0.334
Hutt River at Trentham Memorial Park	1770123	5445046	2.431	0
Hutt River at Heretaunga Golf Course north boundary	1769865	5444836	2.061	- 0.37
Hutt River at Heretaunga Golf Course1	1769406	5444415	2.524	+ 0.463
Hutt River at Heretaunga Golf Course	1769049	5444207	2.600	+ 0.76
Unnamed Hutt tributary at Heretaunga Golf	1768812	5444036	0.002	
Unnamed Hutt tributary at Heretaunga Golf Course1	1768565	5443842	0.006	
Unnamed Hutt tributary at SH2 bridge 9581	1768397	5443864	0.016	
Mawaihakona 1 Stream at Hutt confluence	1768141	5443550	0.075	
Hutt River opposite St Patricks College	1768343	5443787	2.796	+ 0.097
Hutt River at Ferguson Drive Bridge	1767616	5443211	2.596	- 0.203
Hulls Creek at Hutt Confluence	1767339	5442815	0.016	
Hutt River at Taita Gorge	1766532	5441959	2.763	+ 0.151
Hulls Creek at Hutt Confluence	1767339	5442815	0.016	

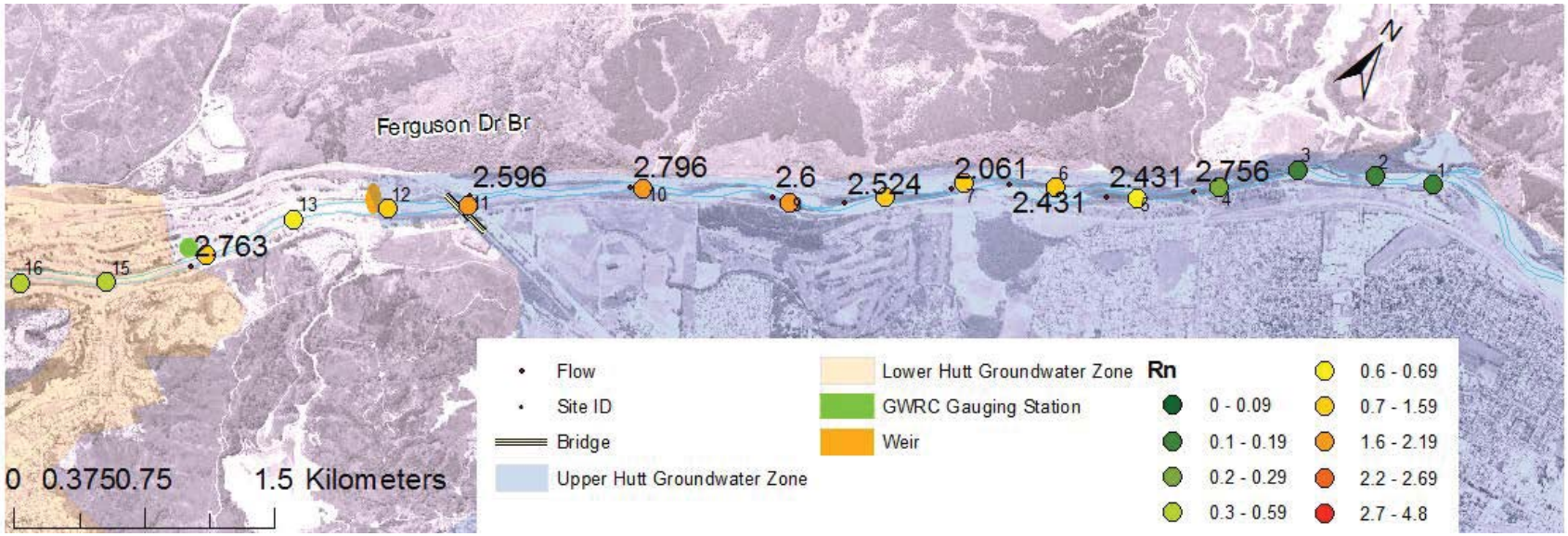

Figure 4.23: Measured flows (as written on figure) in $m^3 s^{-1}$ comparitive to the measured radon concentrations (BqL^{-1}), where the colour denotes the radon concentration.

High sensitivity radon sampling was conducted in selected sections of the Hutt River in the Upper Hutt. Two high sensitivity radon surveys were carried out from the weir downstream of the Ferguson Drive Bridge, Site 12. The purpose of these surveys was to estimate the rate at which radon degassed from the river water and to establish radon concentration thresholds to determine the concentration of radon which indicates groundwater discharge, possible groundwater recharge, and where parafluvial flow may be occurring. Determination of the rate at which radon degasses from the river will also help to remove ambiguity in areas of higher radon concentrations where it is difficult to decide whether the high radon concentration measured is indicative of groundwater discharge or if it is simply due to radon being carried downstream from an upstream groundwater discharge source. Directly below the weir lies bedrock. Because of the geology of this section of the river it could be assumed that any reduction in radon concentration is due to the isotope degassing. After this bedrock section, gravels resume where a previous study showed this gravel reach to be a losing section of the river (Gyopari, 2014). Thus any slight increase in radon concentration or lack of reduction in radon concentration can be assumed to be due to parafluvial interchange in the hyporheic zone. The effect of radioactive decay is ignored because its contribution over small distances of the river is minimal.

The first high sensitivity survey was conducted on 20 March 2015, at river a flow of 3.5 $m^3 s^{-1}$ as measured at the Taita Gorge gauging station, over a distance of approximately 5 km downstream from the weir, Site 12. A total of eight high sensitivity radon samples were collected at a spatial resolution of 600 m – 1000 m. The radon concentration decreased at a consistent rate until 1000 m downstream of the weir before levelling out 2500 m downstream of the weir. The bedrock is exposed in this section of the river, preventing any groundwater discharge and thus the radon concentrations are expected to decrease as the radon degasses. The radon concentrations measured 2500 m downstream of the weir where the concentrations plateau, 0.3 – 0.4 BqL^{-1}, is assumed to be the concentration threshold which indicates no groundwater discharge and simply radon emanating from the river bed material. After this section of bedrock gravels are exposed and the radon concentrations then increase slightly before decreasing at the last site sampled (Fig. 4.24). It is assumed from the study by Gyopari (2014), that there is no groundwater discharge through this reach of gravels in the river. Therefore the increased radon concentrations measured 3200 – 4000 m downstream of the weir are likely due to hyporheic exchange. Furthermore, at low flows of below 4 $m^3 s^{-1}$, when these surveys were carried out, you would expect to see a large increase in radon concentrations if there was any seepage of groundwater throughout this survey site as the groundwater radon concentration is approximately 30 BqL^{-1}. However, only a slight increase, 0.11 BqL^{-1} is measured. An increase this small could be an indication of parafluvial exchange within the gravels.

The second survey was performed at a higher resolution with ten 273 mL samples collected over approximately 600 m downstream of the weir at Site 12. The measured river flow at the Taita gorge gauging station was 3.2 $m^3 s^{-1}$, which was lower than the first high sensitivity survey. The radon concentration remains relatively consistent over this distance, decreasing by only 0.15 BqL^{-1} over the distance of the entire survey (Fig. 4.24). The measured radon concentrations in this second survey were almost double that of the first high sensitivity survey yet the flow was only 10 % lower. One possible explanation for this phenomenon is that the source of groundwater discharge is a long distance upstream. The measured radon concentrations below the weir are simply residual

concentrations from upstream wherein the higher the flow, the higher the degassing rate, thus accounting for the large differences in concentrations.

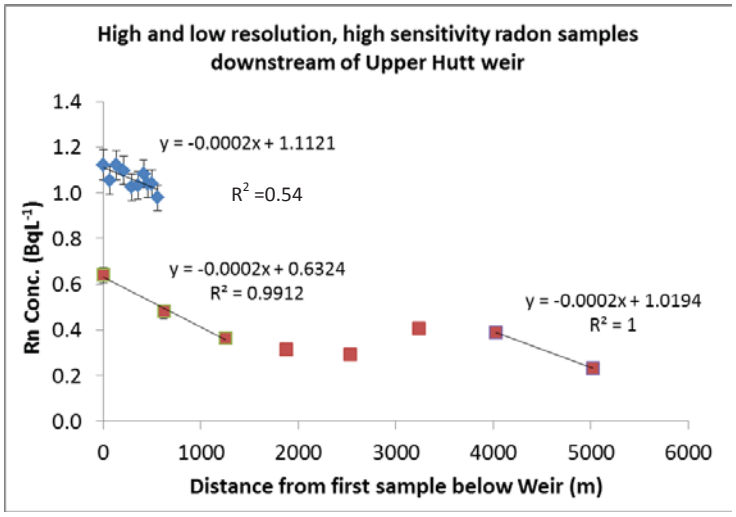

Figure 4.24: Measured high sensitivity radon concentrations downstream from the weir at Upper Hutt at a measured flow of 3.5 m^3 s^{-1} (red) and 3.2 m^3 s^{-1} (blue). The linear trend lines and associated gradient indicate the rate of loss of radon with distance.

To estimate an approximate rate at which radon degasses from the river water the gradients of radon decay from the two high sensitivity surveys are compared. There are two sections of the river surveyed using high sensitivity, under flow conditions of 3.5 m^3 s^{-1}, which decrease in radon concentrations at the same rate (Fig 4.24). They occur immediately after the weir and approximately 4000 m downstream of the weir. While the maximum radon loss over distance has been shown to be 0.0002 BqL^{-1} m^{-1}, this is subject to change. The rate of radon loss is effected by water depth, wind and water turbulence (Dulaiova & Burnett, 2006). This is probably why the second higher sensitivity survey, taken under lower flow conditions, gives a more variable result of the slope gradient with an R^2 value of 0.54. No survey in the Hutt River in this study was carried out during strong winds to avoid ambiguity in radon concentrations caused by excessive degassing through wind turbulence.

Using the estimated rate of radon degassing of 0.0002 BqL^{-1} m^{-1}, the measured radon concentrations taken during the low resolution, January 2015 survey were re-examined to see which measured radon concentrations indicate groundwater discharge, possible groundwater recharge or hyporheic exchange (Fig. 4.25 and 4.26). For this re-examination it is assumed that the rate of degassing remains steady, even though this is unlikely due to varying flow conditions taken between the radon surveys. The radon concentration loss due to degassing was calculated for each sampling point by multiplying the distance between the measured sampling point and the sampling point upstream, with the calculated rate of radon loss through degassing, 0.0002 BqL^{-1} m^{-1}. A losing or no groundwater-surface water interaction section of the river will have a radon loss approximately equal to the calculated loss. A gaining section of the river will have an increase in the radon concentrations of greater than 0.2 BqL^{-1}. This radon concentration threshold for a gaining section was determined by two factors: a radon concentration increase of 0.2 BqL^{-1} is a gain greater than the sensitivity of the direct count analysis and the high sensitivity survey measured that gains of

0.1 BqL^{-1} were likely due to the radon signal from hyporheic exchange. Where there is no or minimal difference in radon concentrations between adjacent sampling sites the rate of degassing is equal to the rate of radon entering the river system. The process dominating in such instances is assumed to be parafluvial interchange in the hyporheic zone.

The sections of the Hutt River in the Upper Hutt which are calculated to be gaining, non gaining and possibly losing or undergoing parafluvial exchange were compared to the flow gauging results to see whether a closer correlation between the two datasets could be observed (Fig. 4.25). However, the two datasets do still not show the same trends. Interpreted radon data indicates significant groundwater discharge after the Whakatikei confluence. However, the river flow gauging data showed a decrease in flow from 2.756 $m^3 s^{-1}$ to 2.061 $m^3 s^{-1}$ over approximately 1500 m. At the Ferguson Drive Bridge, Site 11, to downstream past the weir, Site 14, geological and radon data indicate that the river flow from the weir should remain stable. However the flow gauging data shows an increase in flow of 0.151 $m^3 s^{-1}$ once contributions from tributaries have been accounted for. These discrepencies between flow gauging data and radon concentrations could indicate the occurance of underflow of the river beneath the gravels upstream of the weir. The discrepencies between the data sets from the two methodologies also highlights the ambiguity created when using flow gauging during low flow, as the differences in measured flow between gauging sites have the potential to be smaller than the uncertainty of the measurements.

The spatial distribution of reaches of groundwater discharge, possible recharge or hyporheic exchange in the Hutt River, established in Figure 4.26, indicate that the groundwater-surface water interaction patterns are closely related to geology.

- Above the Ferguson Drive Bridge, Site 11, in Upper Hutt radon concentrations are relatively high. In this area the Upper Hutt groundwater zone ends with bedrock outcrop to the surface (Wellington Regional Council, 1995), and the elevated radon concentrations are likely caused due to seepage of upwelling groundwater at the end of the Upper Hutt groundwater system.

- Downstream from the start of the Upper Hutt bedrock outcrop, Site 12, radon concentrations quickly decrease. This indicates that radon discharged into the river from the Upper Hutt groundwater seepage quickly degasses from the river into the atmosphere, and that there is no groundwater influx into the river in this zone which would cause elevated radon.

- As the flow of the river moves downstream from the Upper Hutt bedrock outcrop and into the upper part of the gravel outcrop area, radon concentrations remain low. This indicates absence of groundwater seepage into the river. In addition, it probably indicates that the river is losing water in this area. Slight elevations in radon concentrations of 0.1 BqL^{-1} observed in this reach are likely due to exchange in the hyporheic zone.

- Slightly downstream of the Avalon Bridge, Site 24, radon sharply increases. This is likely due to large groundwater influx at this point. The reason may be confining layers in the aquifer forcing the groundwater back to the surface.

- Downstream from the Avalon Bridge, the river maintains elevated radon concentrations, indicating continued groundwater seepage.

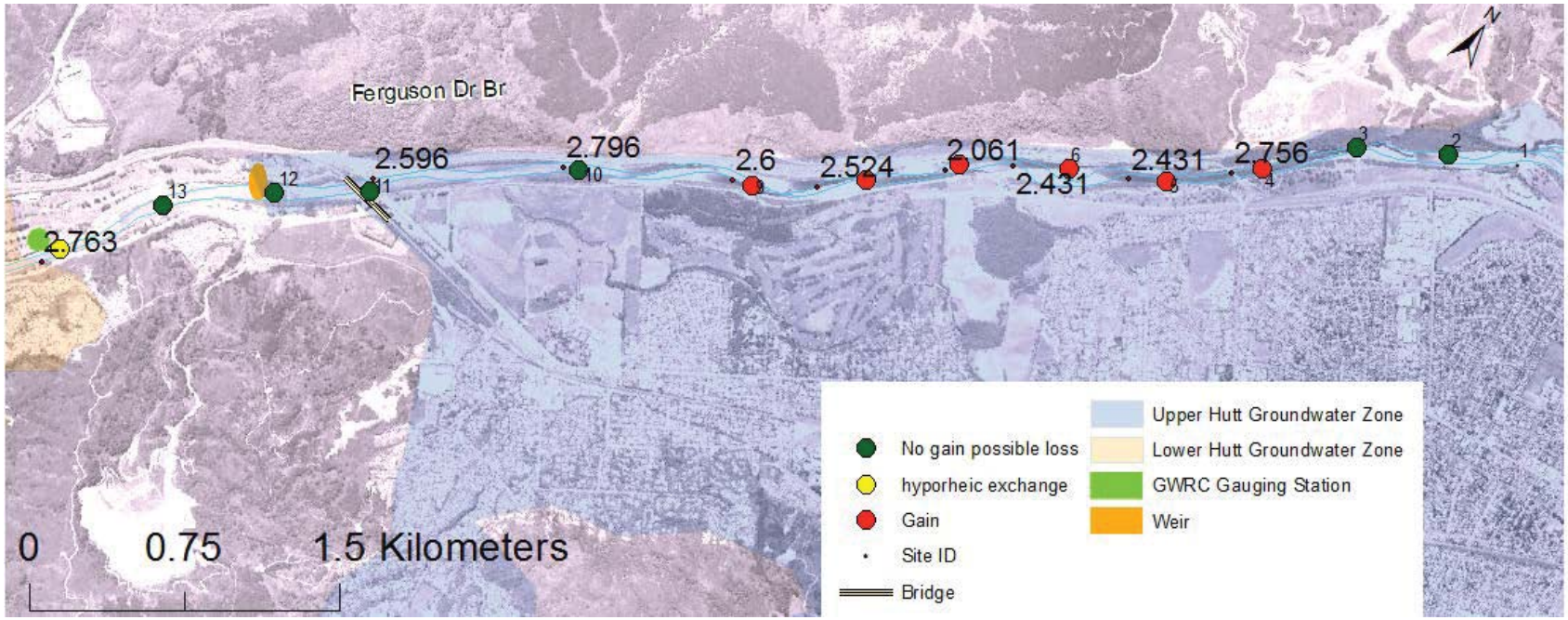

Figure 4.25: Map of groundwater-surface water interactions from radon concentrations occuring in the Upper Hutt of the Hutt River in comparison to flow gauging data. Where the measured flows are written on the figure and the coloured circles are the interaction process indicated by radon concentrations.

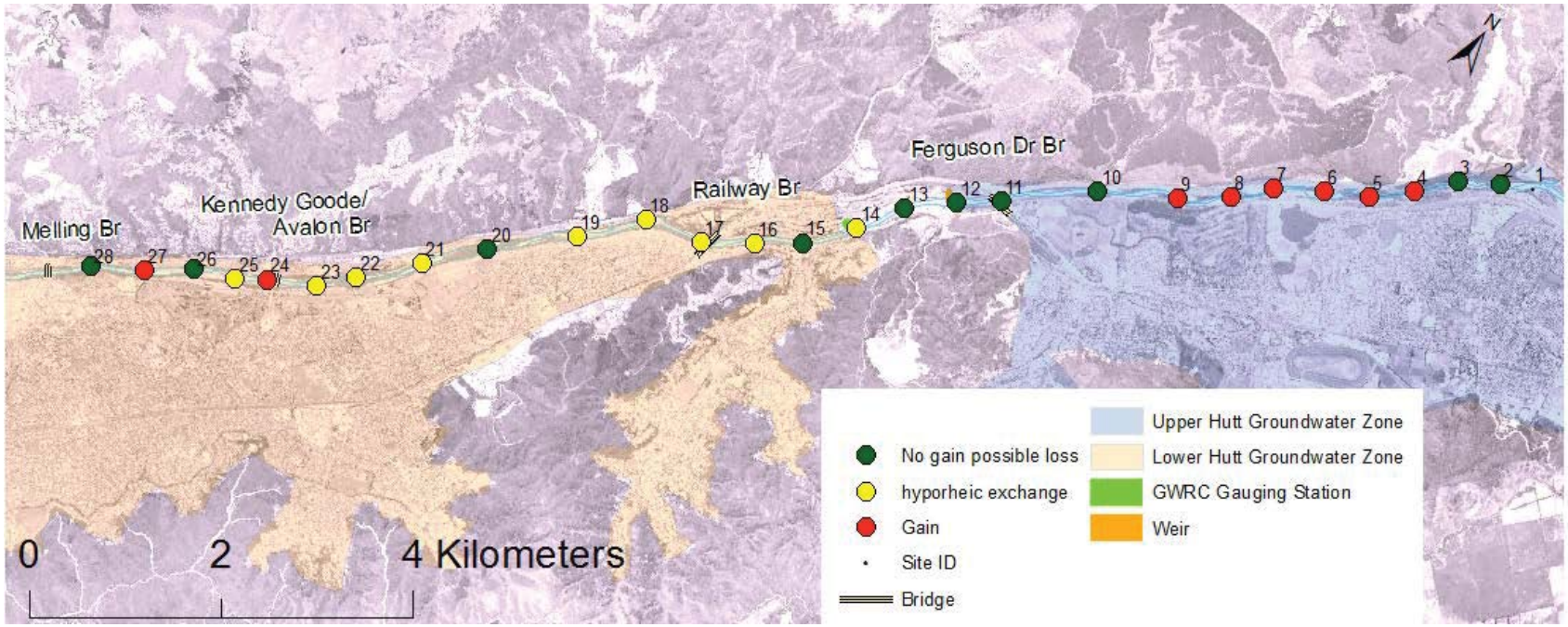

Figure 4.26: Map of groundwater-surface water interactions occuring in the Hutt River as indicated by radon data.

4.5 Chapter summary

Groundwater-surface water interaction dynamics in the Hutt River system were observed using low resolution, high resolution, high sensitivity, spatial and temporal radon studies in combination with concurrent flow gauging. Low resolution radon sampling showed groundwater discharges are occurring approximately 1.5 km upstream of the Ferguson Drive Bridge, Site 11, and between the Avalon Bridge, Site 24, and Melling, Site 28. These discharges between the Avalon Bridge and Melling were further investigated and confirmed using higher resolution radon sampling. Furthermore, the higher resolution radon sampling showed that the interaction between the groundwater and the surface water in the Hutt River system is dominated by its geological surroundings, where groundwater is preferentially being discharged on the eastern side of the river in the Lower Hutt.

High sensitivity radon sampling was able to approximate the rate of radon degassing to be 0.0002 BqL^{-1} m^{-1}. Establishment of the radon degassing rate enabled radon concentration thresholds to be calculated. This allowed the measured radon concentrations to be interpreted as indicating groundwater discharge, possible recharge or non-discharge or hyporheic flow.

The radon study also highlighted the ambiguity surrounding the use of flow gauging in gravel bed rivers for mapping river gains and losses. In sections of both the Upper and Lower Hutt the concurrent flow gauging data indicated areas of both groundwater recharge and discharge where the radon data showed the opposite process to be occurring. This has led to the conclusion that underflow beneath the gravels and other parafluvial exchange processes in gravel-bed rivers could cause the interpretation of concurrent flow gauging results to be misleading. A combined use of river flow gauging with radon sampling has the potential to provide a more robust picture of the groundwater and river water interaction processes in gravel-bed rivers.

Chapter 5 - Mangatainoka River Case Study

5.1 Introduction and objectives

The Mangatainoka River, part of the Manawatu Catchment in the Horizons Region, like the Hutt River, suffers from substantial cyanobacteria growth (McArthur & Clark, 2007). Not only is this growth adverse to human and stock health (Greater Wellington Regional Council, 2013), but it is also unfavourable politically (Norman, n.d), has clogged irrigation (McArthur & Clark, 2007) and has reduced biodiversity with fish stocks declining substantially over the past 20 years (Horizons Regional Council, 2011).

In the Mangatainoka River, the nutrients which support this algal growth predominantly enter the river through groundwater inputs, as the river load of soluble inorganic nitrogen (SIN) is greater than 15 times that of the point source inputs (McArthur & Clark, 2007). This statistic, coupled with studies showing that 30-80% of SIN leached from the root zone in this catchment enters the river (Singh et al., 2014), highlights the need to understand the groundwater surface water interaction dynamics in the Mangatainoka River.

Very little is known about the hydrological processes in the Mangatainoka catchment and river system (Rawlinson & Begg, 2014). The Hutt River study, described in Chapter 4, showed the potential use of using radon as a tool to map groundwater-surface water interactions. With the radon concentration thresholds established from Chapter 4, this Chapter uses low and high resolution radon surveys to map the groundwater discharge locations across the entire Mangatainoka River.

Groundwater discharge patterns identified from concurrent flow gauging measurements are compared to radon concentration measurements taken throughout the Mangatainoka River. This is done to assess if the same discrepancies between the discharge patterns shown by flow gauging measurements and the radon concentrations, as in the Hutt River, are observed in the Mangatainoka River. Furthermore, to give more insight into the dynamics of the groundwater and surface water interactions within the Mangatainoka River system, the potential of using radon measurements in conjunction with nitrate measurements is assessed. Due to high SIN loads being inputted in the groundwater system, elevated nitrate concentration measured in the river water could indicate groundwater discharge. Likewise, electrical conductivity is assessed as a complementary tool to radon which, as described in Chapter 4, Section 4.4.1, elevated conductivity levels in the surface water can indicate groundwater discharge.

5.2 Study area – hydrogeological setting

The Mangatainoka River lies to the east of the Tararua ranges between Ekatahuna and Pahiatua. The river flows from the headwaters south west of Ekatahuna to the north east before joining the Tiraumea River and ultimately flowing into the Manawatu River. The river catchment area (Fig. 5.1) is approximately 440 km^2 (Brougham, 1987; Taylor et al., 2015) where the land is predominantly used for agriculture, in particular sheep and beef (47%) and dairy (30%) (Horizons Regional Council, 2011).

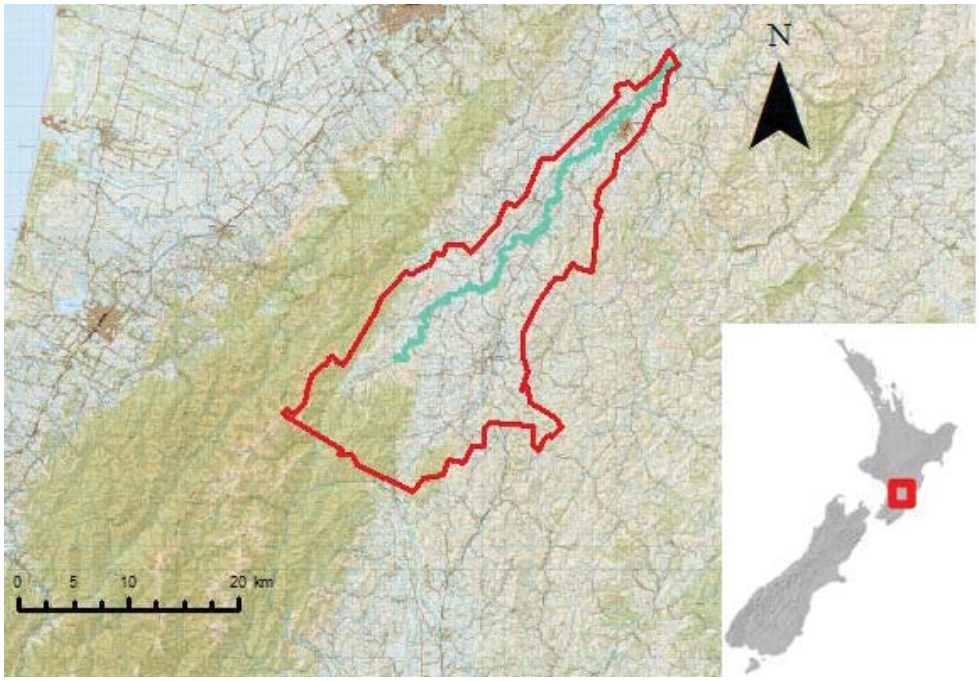

Figure 5.1: Mangatainoka Catchment area (designated by red boundary line) and the Mangatainoka River (designated by blue line).

The Tararua Ranges, on the west of the Mangatainoka catchment, has a large impact on the distribution of rainfall in the area. Annual rainfall within the catchment varies from approximately 1000 mm to 2425 mm (Taylor et al., 2015). The higher annual rainfall occurs in the south west of the catchment and decreases heading north in the catchment and to a lesser extent also decreases to the east of the catchment (Brougham, 1987). The rainfall in the catchment also varies in different months of the year. In general, the highest rainfall month tends to occur in July with February receiving the least rainfall (Brougham, 1987). Because of this, low flow of the Mangatainoka River typically occurs in February/March.

The geology surrounding the Mangatainoka River comprises a highly faulted greywacke basement rock (Rawlinson & Begg, 2014) formed from the Tararua Formation. Tertiary Miocene and Pliocene rock deposits are also found, trending younger in age in a westerly direction (Brougham, 1987). The tertiary rock groups include the Mangaheia Group and the Tolaga Group. The Tolaga Group, approximately 400-500 m thick, is formed from Miocene marine sedimentary rocks and is largely made up of calcareous sandstone, mudstone, basal conglomerates, with some bioclastic limestone present (Rawlinson & Begg, 2014). The younger Mangaheia Tertiary Groups is also made up of sandstones, limestone and mudstones, but also includes conglomerates (Rawlinson & Begg, 2014). This geological unit has the potential to store large volumes of water. This hydrogeological feature is taken advantage of with many wells drilled into this geological unit. However, it is unclear whether the water is for the wells is drawn from the Mangaheia group or the geological unit below (Rawlinson & Begg, 2014). Overlaying some of the Tertiary units lies a Quaternary unit of aggregated gravels and sands (Brougham, 1987). The Quaternary deposits have a maximum thickness of 227.7 m (Rawlinson & Begg, 2014). The distribution of these rock formations are illustrated in Figure 5.2.

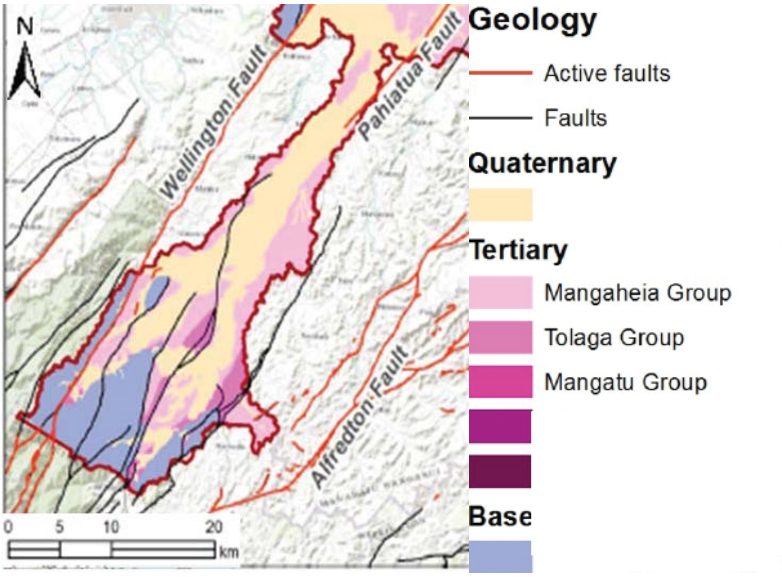

Figure 5.2: Simplified geological map of the Mangatainoka catchment. Image retrieved and adapted from (Rawlinson & Begg, 2014).

The geology provides some limited insight into the groundwater dynamics of the area, which little is known about. The quaternary deposits are more suitable for groundwater storage and extraction as they are closer to the surface and have a higher porosity. (Brougham, 1987; Rawlinson & Begg, 2014). However, poor well log data is unable to distinguish whether the wells drilled into the quaternary deposits are drawing form this geological unit or are draw down further into tertiary units.

Surface water hydrological processes are much more easily observed and thus have greater documentation than the groundwater. There is thought to be major stream flow losses in the upper parts of the Mangatainoka River downstream of the Larsons Road Bridge (Fig. 5.3) with further significant stream flow losses at the Browns road (Brougham, 1987) (Fig. 5.3). The stream flow loss is thought to transfer to the neighbouring Makakahi River (Brougham, 1987). Groundwater discharge in the Mangatainoka River is thought to occur in the middle reaches near the Konini Road Bridge (Brougham, 1987) (Fig. 5.4). However, there is a need to further improve the knowledge of surface water – groundwater interactions to help better manage water and nutrient flow pathways in the catchment.

The Mangatainoka River flows predominantly along private land. Access to the river was therefore limited. To enable data collection, access points to the river designated by Fish and Game were used. The site access numbers and road names used as reference points for accessing the Mangatainoka River as used by Fish and Game, will be referred to throughout this study. Access Sites 1-6 are located in the upper reaches of the Mangatainoka River (Fig. 5.3). Access Sites 7-13 are found in the middle reaches of the Mangatainoka River (Fig. 5.3-5.4). The lower reaches of the river passes through the township of Pahiatua and the Tui Brewery in Mangatainoka, where the river can be accessed at sites 14-18 (Fig. 5.4). Access Site 1, at the Larsons Road Bridge, and 15, at the Pahiatua Town Bridge, have continuous flow gauging monitoring sites, maintained by the Horizons Regional

Council. The Mangatainoka River ends shortly after Site 18, where it joins the Tiraumea before entering the Manawatu River.

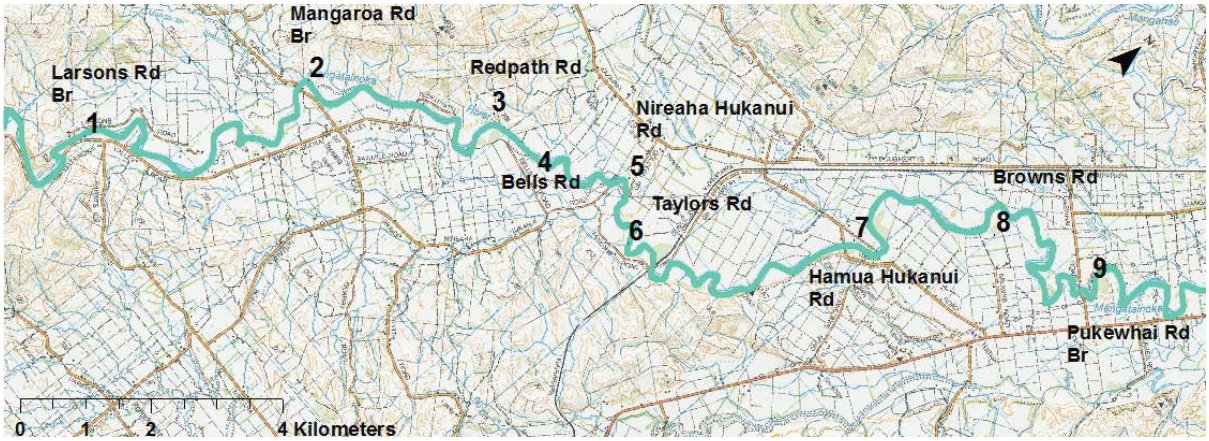

Figure 5.3: Mangatainoka River upper and middle reaches access sites and numbers (bold).

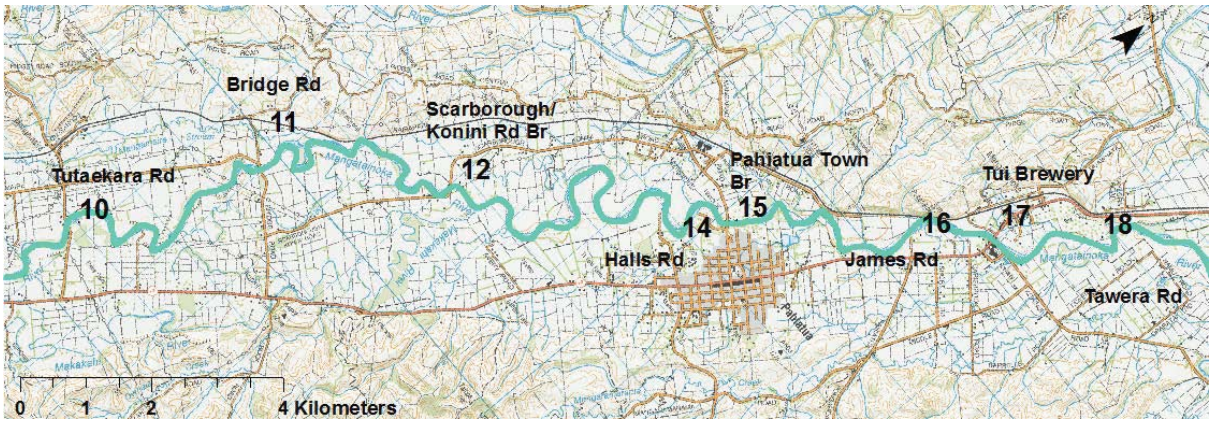

Figure 5.4: Mangatainoka River middle and lower reaches access sites and numbers (bold).

5.3 Methods and materials

5.3.1 River radon surveys

During low flow conditions of approximately 1.1 $m^3 s^{-1}$, a low resolution radon river survey was carried out over the entire, approximate 70 km, reach of the Mangatainoka River. During this survey a 25 mL radon grab sample was collected every 500 m - 800 m along the river. This sampling distance was chosen as the earlier Hutt River study demonstrated that this distance between grab samples was large enough without the risk of missing any major groundwater discharges indicated by radon. However, due to site accessibility, a few samples were collected approximately 1000 m from one another. To assess the potential of using radon measurements in conjunction with other water quality indicators to gain further insight into groundwater-surface water dynamics, at each sampling site a river water sample for nitrate-nitrogen measurement was also collected. Electrical conductivity was also measured, using HACH or YSI field meters, at each sampling site. The GPS coordinates and the sample collection time was also recorded at each site. A photograph of the area in which the sample was taken was also captured. This survey was carried out on 2 February 2015. A 6 km section, between the Tutaekara Road Bridge and Scarborough/Konini Road Bridge, in the middle reaches of the river was not surveyed on 2 February due to loss of daylight and was sampled the following day.

To compare the low resolution results, all the samples need to be collected under similar flow conditions. Unfortunately there was significant rainfall during the first low resolution river survey conducted on 2 February 2015. The continuous flow gauging stations at the Larsons Road Bridge and the Pahiatua Town Bridge indicate that the samples collected in the upper reaches of the Mangatainoka River may have been impacted by higher flow conditions (Fig 5.5), especially as low flow at the Larsons Road gauging station recorded flows of less than 0.2 $m^3 s^{-1}$ during February 2015. Likewise the samples collected on 3 February 2015, in the 6 km section between the Tutaekara Road Bridge and the Scarborough/Konini Road Bridge, were also impacted by higher flow conditions as the river was approximately 6 times higher than the previous day low flow conditions. Therefore, these two sections of the river were resampled when low flow conditions had returned. The upper reaches were resampled on 15 February 2015, with a flow of 0.4 $m^3 s^{-1}$, a third lower than the survey carried out on 2 February 2015, as measured at the Larsons Road gauging station. The middle reaches were resampled on 20 February 2015, with a flow of 0.9 $m^3 s^{-1}$, as measured at the Pahiatua Town Bridge gauging station, 0.2 $m^3 s^{-1}$ lower than what was measured during the 2 February 2015 survey. The initial samples taken which were affected by higher flows were not used in the analysis of the low flow radon results.

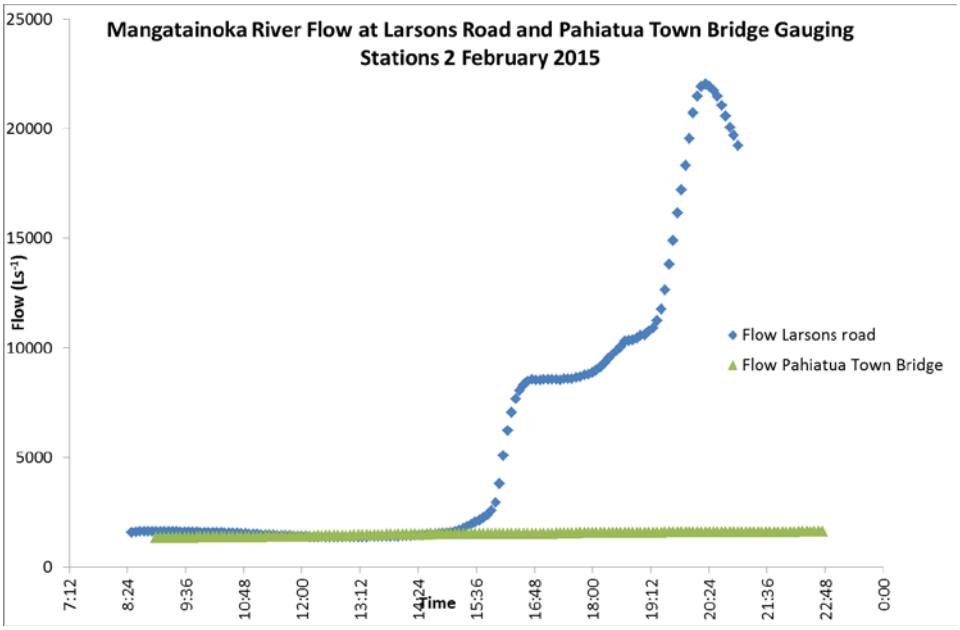

Figure 5.5: Flow of the Mangatainoka River at two gauging stations on 2 February 2015; blue-Larsons Road gauging station (upper reaches), green-Pahiatua Town Bridge gauging station (mid-lower reaches).

On 7 and 8 February 2015 two sections of the Mangatainoka River, one in the upper reaches and one in the middle reaches, were chosen for high resolution radon sampling. These two sites were chosen as a consequence of the results shown by the low resolution survey conducted on 2 February 2015. Both of these sites showed large possible areas of groundwater discharge. Higher resolution sampling would help identify these discharge patterns in greater detail. These two sites were also selected based on their ease of accessibility. The Mangatainoka River is surrounded by private farmland and high resolution sites needed to be relatively easily accessible by vehicle, hence a 2.2 km reach upstream of Site 12 (see Fig. 5.4), and a 600 m reach either side of the Mangaroa Road Bridge, Site 2 (see Fig. 5.3), were chosen for these surveys. In the middle reaches, at a low flow of 1.8 $m^3 s^{-1}$, as measured by the gauging station at the Pahiatua Town Bridge, 16 radon grab samples were collected every 75-250 m from the bridge at Scarborough/Konini Road Bridge, Site 12, to 2.2 km upstream. The distances between sampling points were determined by the ability to disembark from a kayak safely to collect a sample. Radon river width profiles were also taken at three different locations within this stretch of river to investigate whether there was a trend in radon distribution across the width of the river. River width radon profiles were conducted using a tape measure. A tape measure was erected across the width of the river and 4-5 radon samples were collected at measured intervals between 2 and 5 meters, depending on the width of the river, across the width of the river. In the upper selected reach, at a low flow of 0.6 $m^3 s^{-1}$, a total of 11 samples were collected every 40-200 m approximately 600 m upstream and 600 m downstream of the Mangaroa Road Bridge, Site 2. Again, the distances between samples were selected on their ease of accessibility to the river. The GPS coordinates, a photo of the sampling site and the sampling time were captured with each radon sample.

In both the low and high resolution sampling, radon grab samples were collected in 25 mL glass vials with foil lined caps using the field collection procedure described in chapter 3, section 3.2.1. At the

end of each sampling day the grab samples were taken to the Water Dating Laboratory at GNS Science, where they were prepared and analysed for radon using a slight variation of the direct count measurement procedure described in Chapter 3, Section 3.2.3. The variation of this procedure relates to the decay counting measurement times. Due to the large number of samples being measured at once the counting times were sometimes reduced. Counting times varied for samples and ranged from 40-100 minutes. The effect of the count rate time does not significantly impact the measured result. However, shorter counting times do result in larger measurement errors, as demonstrated in Chapter 3, Figure 3.2, Section 3.1.3.

Radon concentrations were calculated using the equations described in Chapter 3, section 3.1.3 wherein the sample preparation error is 2%.

Nitrate samples were taken in the field in the same locations where radon samples were collected. Nitrate samples were collected by firstly rinsing the 30 mL container out with river water then filling the container by dipping it in the river water. The containers were then capped, stored in a chilly bin after the sampling, and taken back to the lab and kept chilled ready for analysis the next day, or frozen if analysed at a later date. The collected samples were prepared for nitrate analysis by filtration through a 45 micron filter paper. For the analysis, 3 mL of each sample was used in an auto-analyser for nitrate-nitrogen (NO_3-N) concentration measurement. A standard curve was created using seven NO_3-N standards. Two blanks and one standard were measured for every 10 samples measured to estimate the peak height and therefore NO_3-N concentration.

5.3.2 River flow gauging

Flow gauging was carried out at and between the locations where the 25 mL higher resolution radon sampling was carried out on 7 and 8 February 2015 using a Valeport Model 801 Electromagnetic Flow meter. Flow gauging was conducted at eight sites, four gauges along each section of the river where high resolution sampling was carried out. These flow gauging measurements were taken between 200 – 1000 m apart. Deeper, narrower sections of river were preferentially chosen over wide shallow sections to reduce error in the measurement. Additional gauging was carried out along these two stretches of the river to account for tributary inputs. At each flow gauging between 9 and 16 measurement points were taken with the Valeport flow meter, depending on the width and flow of the river. Where possible, the distance between two measurement points chosen to ensure that one measurement point did not account for more than 10% of the flow. The exception to this was when very small, low flowing, tributaries were measured, where taking more than 10 measurement points was difficult to achieve.

On 5 March 2015 a river gauging campaign was undertaken by Horizons Regional Council and Massey University, where 19 flow gaugings, between 1 and 10 km apart, were carried out along the Mangatainoka River as well as additional gaugings to account for tributary gains. Gaugings were carried out using a Son Tek M9 River Surveyor, where 4-10 transects per site were measured, a Pygmy Universal Current Meter Model OSS-PC1, and visual estimates of the flow based on Q=A x V, in very small tributaries. Flow measurements were carried out in accordance with annex C of the National Environmental Monitoring Standards (LAWA, 2013). Flow readings, which were taken using the M9 River Surveyor, where a transect designated as being an outlier by the River Surveyor Son Tek Software was discarded. The river flow data collected using the other flow gauging equipment was post-processed and supplied by the Horizons Regional Council.

5.3.3 Groundwater radon samples

Groundwater radon samples were collected to compare the radon concentrations measured in the river. On 5 June 2014 two groundwater samples from groundwater wells were collected by GNS Science. One sample was taken near the middle reaches near the Tutaekara Road and the other near the lower reaches of the Mangatainoka River (Fig. 5.6). These groundwater sampling sites are located on private land. The groundwater sampling sites were selected due to permission to collect the samples being granted.

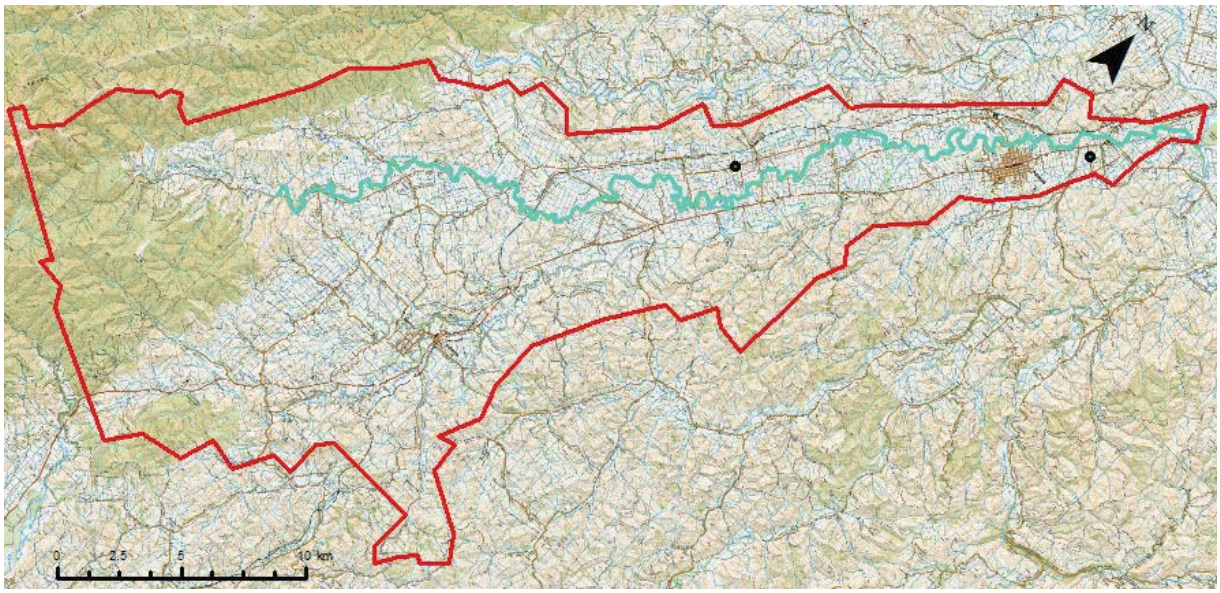

Figure 5.6: Geographical locations of two groundwater sampling sites (circular symbols) in relation to the Mangatainoka catchment (red) and Mangatainoka River (blue).

5.4 Results and discussion

5.4.1 Low resolution radon sampling

The radon concentrations for all of the low resolution surveys, not including those which were impacted by higher flows, are tabulated in appendix 2. Figures 5.7, 5.9, 5.12, 5.14-5.16 and 5.18 plots radon concentrations for the radon surveys conducted during low flows between 0.4 $m^3 s^{-1}$ and 2.0 $m^3 s^{-1}$ on 2, 7, 8, 15 and 20 February 2015 . The scaling of the radon concentrations in Figures 5.7, 5.9, 5.12, 5.14-5.16 and 5.18 was determined by plotting the frequency of radon concentration occurrence for all low resolution surveys sites, undertaken in low flow conditions, in quantile plots. The percentiles were then determined from the quantile plots and used to scale the results.

Figure 5.7 plots the results of the low resolution radon survey of the Mangatainoka River. The radon concentrations varied considerably throughout the length of the river, ranging from below the detection limit of 0.2 BqL^{-1} to 5.0 BqL^{-1}. To interpret the measured radon concentrations in the Mangatainoka River as indicating either a gaining, possibly losing or exchange with the hyporheic zone reach, the radon results from the Hutt River study in Chapter 4 is referred too. The previous radon study in the Hutt River identified that radon concentrations of approximately 0.0 BqL^{-1} - 0.4 BqL^{-1} indicate no groundwater discharge (see Section 4.4.5). Radon concentrations higher than this 0.4 BqL^{-1} threshold indicate some groundwater discharge with higher concentrations having a higher proportion of groundwater to surface water. The Hutt River study also estimated the rate of radon degassing to be 0.0002 $BqL^{-1}m^{-1}$. This degassing rate allows measured radon concentrations from groundwater discharge or residual radon concentration from an upstream discharge point to be distinguished. Furthermore, the studies in the Hutt River indicated that any measured radon concentration that increased by 0.1 BqL^{-1}, after radon loss from degassing had been taken into account, from the adjacent measured upstream site interaction with the hyporheic zone, rather than groundwater discharge at that measurement site itself. Using these radon concentration thresholds the interpreted measured radon concentrations from the Mangatainoka survey are plotted on Figure 5.9 and indicate the reaches of the river which are gaining, non-gaining and where hyporheic exchange is likely occurring. Radon concentrations are relative. These findings in radon concentrations relate to the Hutt River and are likely to be different for the Mangatainoka River. Furthermore, the Mangatainoka River has a flow approximately 75% lower than the Hutt River and the two rivers differ in morphology, which would impact the rate of radon degassing. However, the groundwater radon concentrations in the Mangatainoka at two different sampling sites were 26.7 BqL^{-1} and 27.2 BqL^{-1} which is approximately the same as the groundwater radon concentration in the Hutt River. Despite the limitations described above as to why the degassing rates between the two rivers will differ, given that the radon groundwater concentrations are similar for both areas and that both have river bed sections made up greywacke gravels, the findings in the Hutt River will be tentatively applied to the Mangatainoka River.

The spatial radon study undertaken in the Mangatainoka River (Fig. 5.7 and 5.8) has identified three major sections of the river where groundwater discharge is likely to be occurring: one in the upper reaches, one in the middle reaches and one in the lower reaches. In the headwaters of the river, low radon measurements of 0.0 BqL^{-1} to 0.6 BqL^{-1} indicate absence of any significant groundwater

inflows upstream of the Larsons Road Bridge, Site 1, with the exception of one site. Approximately 3000 m upstream of Site 1, a radon concentration of 1.3 BqL^{-1} was measured. While, this indicates groundwater discharge, it can be assumed that this is a small, isolated area of discharge, as the adjacent sampling points upstream and downstream of this site have low concentrations of radon of 0.4 BqL^{-1}. It would be expected that residual radon concentrations further downstream would be observed if this discharge site was large. The measured radon concentrations further indicate a major groundwater discharge in the Mangatainoka River between approximately 1000 m upstream and 2000 m downstream of Site 2, the Mangaroa Road Bridge. Further major groundwater discharges are indicated to occur between Site 4, Bells Road, and Site 5, Nireaha Hukanui Road and between Site 10, the Tutaikara Road Bridge, and Site 11, the Bridge Road. The final major groundwater discharge is suggested in the lower reaches of the Mangatainoka, as indicated by relatively higher radon concentrations, between Site 12, the Scarborough/Konini Road Bridge, and Site 14, the Halls Road. The Makakahi and Mangatainoka confluence occurs between these sites approximately 1.5 km downstream of Site 12. Shorter, isolated groundwater discharges were also indicated by radon at Sites 3 and downstream of Site 9.

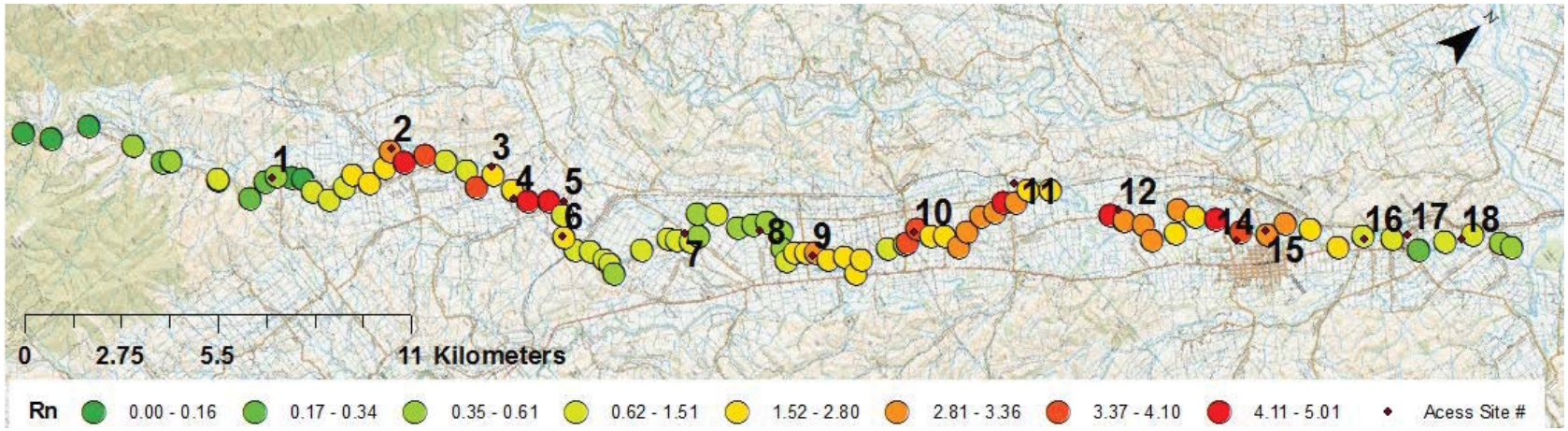

Figure 5.7: Measured radon concentrations in the Mangatainoka River at low flow between 0.4 $m^3 s^{-1}$ and 2.0 $m^3 s^{-1}$ in February 2015: The colour denotes radon concentrations in BqL^{-1} and the bold black numbers denote the site numbers as described in section 5.2.

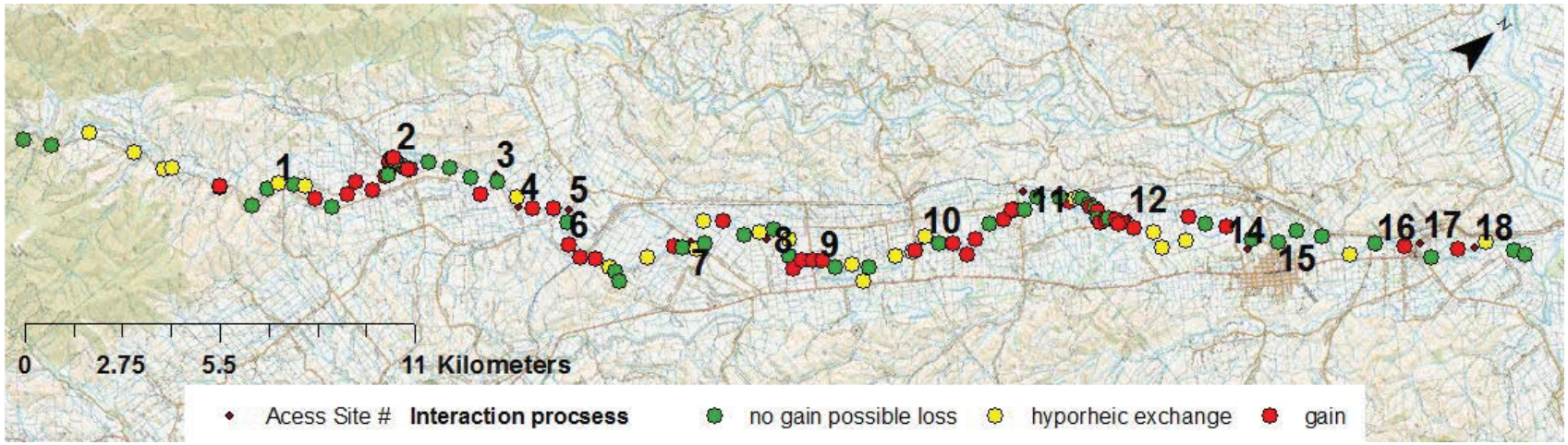

Figure 5.8: Map of groundwater-surface water interactions occurring in the Mangatainoka River as indicated by radon data.

The measured radon concentrations indicate three sections where either no groundwater discharge into the Mangatainoka River occurs or where possible recharge areas to the groundwater system occurs (Fig 5.7). In these three sections radon concentrations of 0.6 BqL^{-1} and lower are measured. The first possible losing, or non-gaining section, of the river occurs in the upper reaches approximately 1500 m upstream and downstream of Site 1, the Larsons Road Bridge. The second possible losing section of the Mangatainoka River occurs in the middle reaches between upstream of Site 7, the Hamua Hukanui Road, through Site 8, the Browns Road, and continues to upstream of Site 9, the Pukewhai Road. The third non-gaining, possible losing section of the river, as indicated by relatively low radon concentrations, occurs between downstream of Site 17, at the Mangatainoka Bridge, to the confluence at the Tiraumea. The interpreted radon concentrations (Fig 5.8) indicate that this third non-gaining section of the river starts as far upstream as Site 15, with the higher measured radon concentrations possibly caused by residual radon from an upstream discharge point.

The low resolution radon surveys (Fig. 5.7) provided approximate locations of areas of groundwater discharge and possible recharge in the Mangatainoka River system. To capture more detailed information on the groundwater-surface water dynamics, higher resolution radon surveys were undertaken along two selected reaches of the river.

The two high resolution sampling reaches were chosen prior to and at where low resolution sampling identified groundwater discharge, at Site 12 and Site 2. The high resolution sampling was first conducted at the reach of river upstream of Site 12. The high resolution sampling upstream, and at, Site 12, (Fig. 5.9) showed that the radon concentrations for the first 10 grab samples, when going from the most upstream point downstream, were relatively consistent, ranging from 1.0 BqL^{-1} to 1.5 BqL^{-1}. The 6 most downstream samples collected showed an increase in radon concentrations from 1.5 BqL^{-1} to 2.9 BqL^{-1} with the last three sites sampled increasing in radon concentration the further downstream they are. This suggests that there is continuous groundwater discharge throughout this reach, with an increasing proportion of groundwater discharge occurring closer to Site 12. These findings are also supported by the interpreted radon data, showing where discharge is occurring as opposed to measuring residual radon from upstream (Fig. 5.10).

Also, three river width radon profiles were taken over the high resolution sampling area near Site 12: one at Site 12, one at the most upstream sampling point of the high resolution survey, 2200 m upstream of Site 12, and one in between these two sites, 1200 m upstream of Site 12. At all three river width profiles, the radon concentrations measured were fairly consistent, lacking any significant variation across the river width (Fig. 5.11). This result was expected. The groundwater discharge patterns across the river profile in the Hutt River, Chapter 4, Section 4.4.4, were apparent due to the presence of a fault line which has caused bedrock to be present on the western side and gravels on the eastern side of the river. This half-graben geological unit is not present in the Mangatainoka River so the river does not have distinctive differing geological units on either side of the river bed. Therefore, the geological material is thought to be consistent across the width of the river at any one point. Because of the inexistence of a relationship between river width position and radon concentration, river width profiles were not collected at the second high resolution sampling survey location, Site 2.

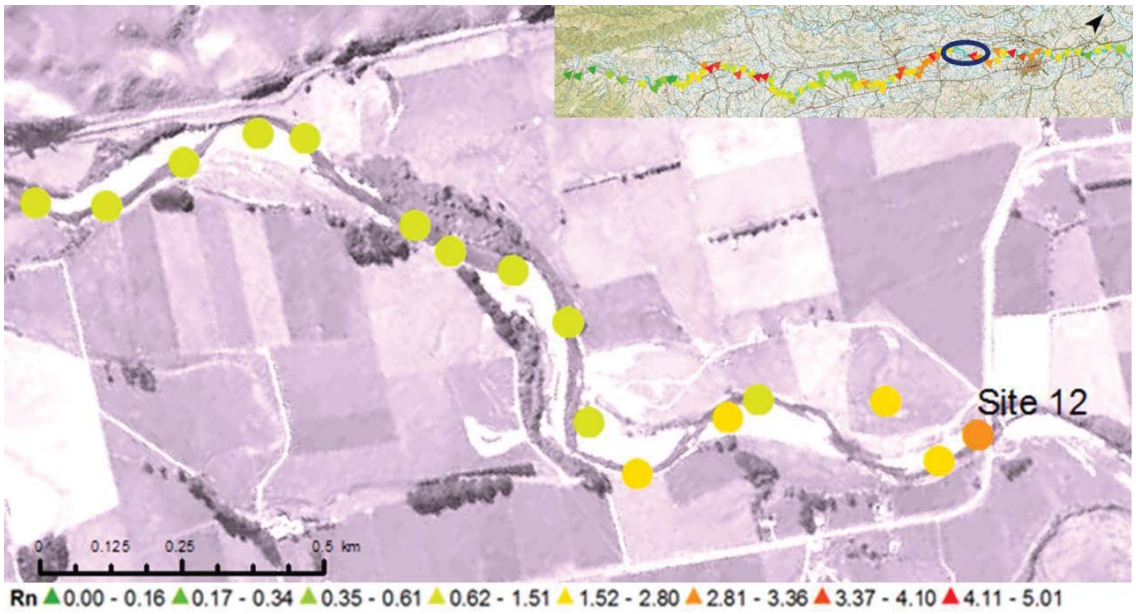

Figure 5.9: Measured radon concentrations in the Mangatainoka River at low flow upstream of site 12. The colour denotes radon concentrations in BqL^{-1}. The topographic map in the top right corner denotes the location of site 12 with a blue oval, relative to the rest of the river.

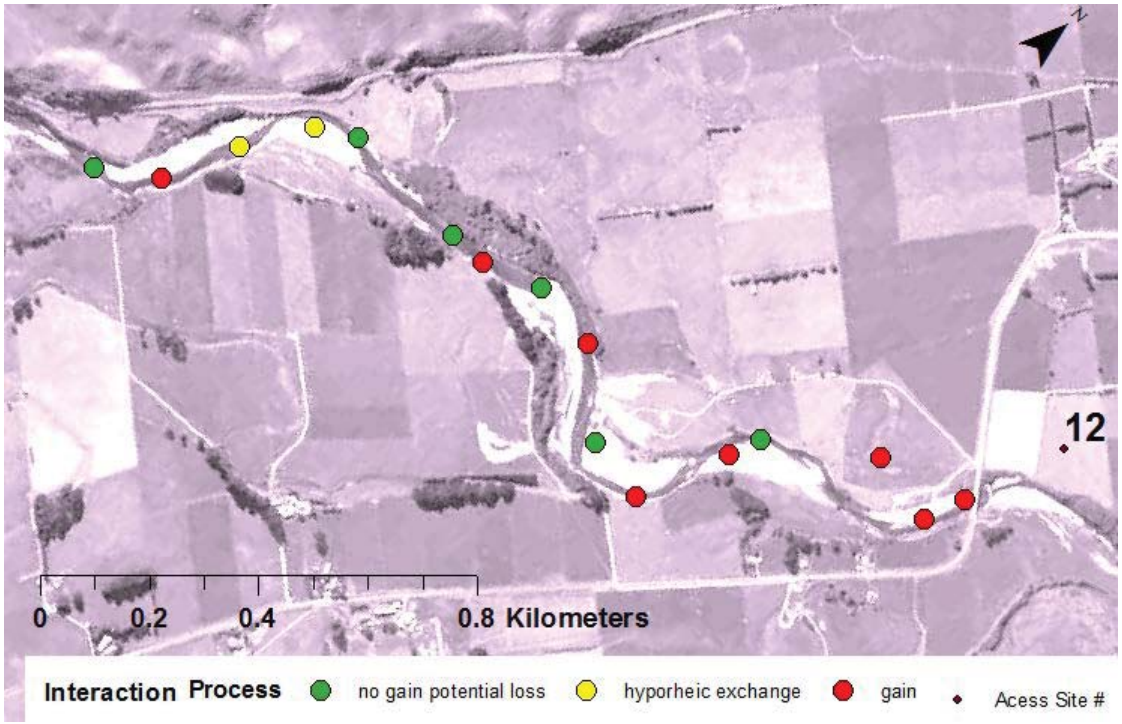

Figure 5.10: Interpreted groundwater-surface water interaction dynamics in the Mangatainoka River at low flow upstream of Site 12.

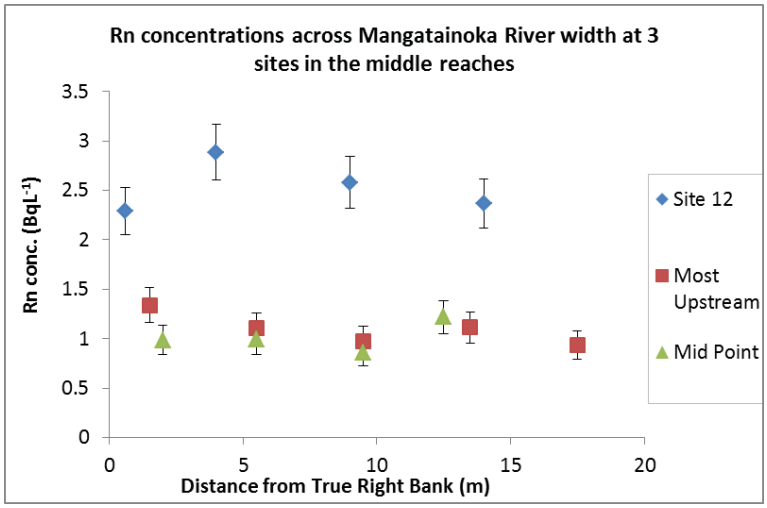

Figure 5.11: Radon concentrations across the width of the Mangatainoka River at three locations in the middle reaches: one width profile at site 12, one 2.2 km upstream of site 12 at the most upstream sampling point of the high resolution survey, and one in between these two sites 1200 m upstream of site 12.

The second high resolution sampling survey was undertaken between 600 m of either side of the Mangaroa Road Bridge. With the exception of the most downstream site at the high resolution survey undertaken at Site 2, all of the measured radon concentrations were between 1.5 BqL^{-1} and 3.0 BqL^{-1} (Fig. 5.12). There is no consistent increase in radon concentrations leading up to the highest measured radon concentration, of 3.6 BqL^{-1}, and thus likely area of significant groundwater discharge. The pattern of radon concentration distribution for the second high resolution survey is more clearly demonstrated by the interpreted results in Figure 5.13. The interpreted data show four discrete locations of groundwater discharge, one of which being the highest measured radon concentration at the most downstream site. In between these discrete discharge sites, the consistent radon concentrations measured were likely due to residual radon carried downstream or radon gained through hyporheic exchange processes. The increased radon concentration measured upstream of the Mangaroa Bridge is likely due to a small seep that was found in the gravels adjacent to the river. The radon concentration measured in the seep was 7.6 BqL^{-1}. The radon concentrations of the Mangatainoka River before and after the water from the seep enters the river are 2.1 BqL^{-1} and 3.1 BqL^{-1} respectively. The location of the seep is indicated by the blue star on Figure 5.12.

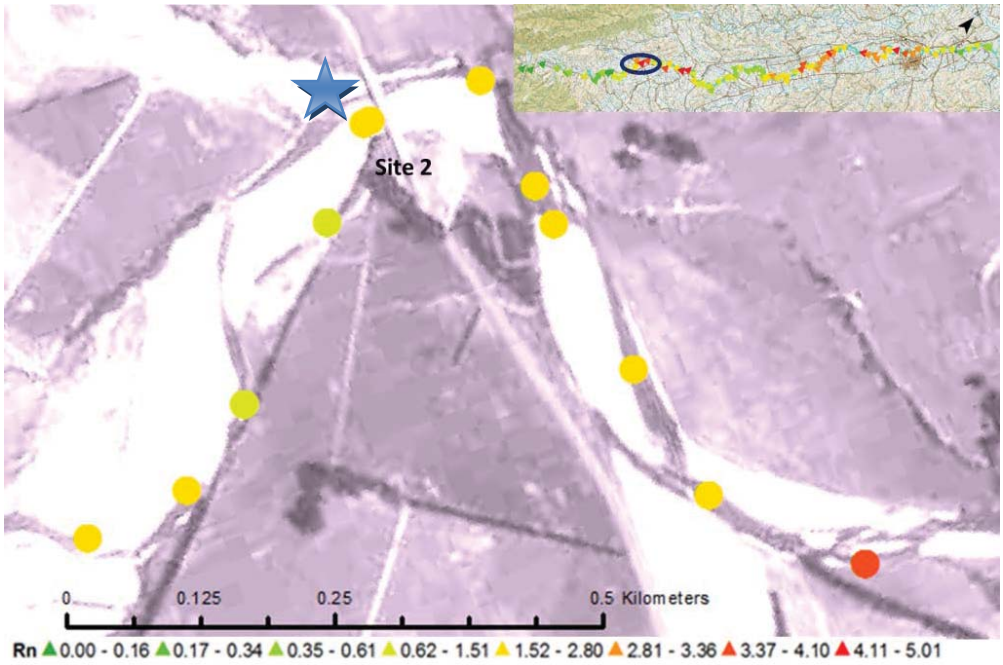

Figure 5.12: Measured radon concentrations in the Mangatainoka River, at low flow of 0.6 m^3 s^{-1}, approximately 600 m upstream and downstream of Site 2. The colour denotes radon concentrations in BqL^{-1}. The blue star on the figure denotes the position of a seep in the gravels adjacent to the river. The topographic map in the top right corner denotes the location of Site 2 with a blue oval, relative to the rest of the river.

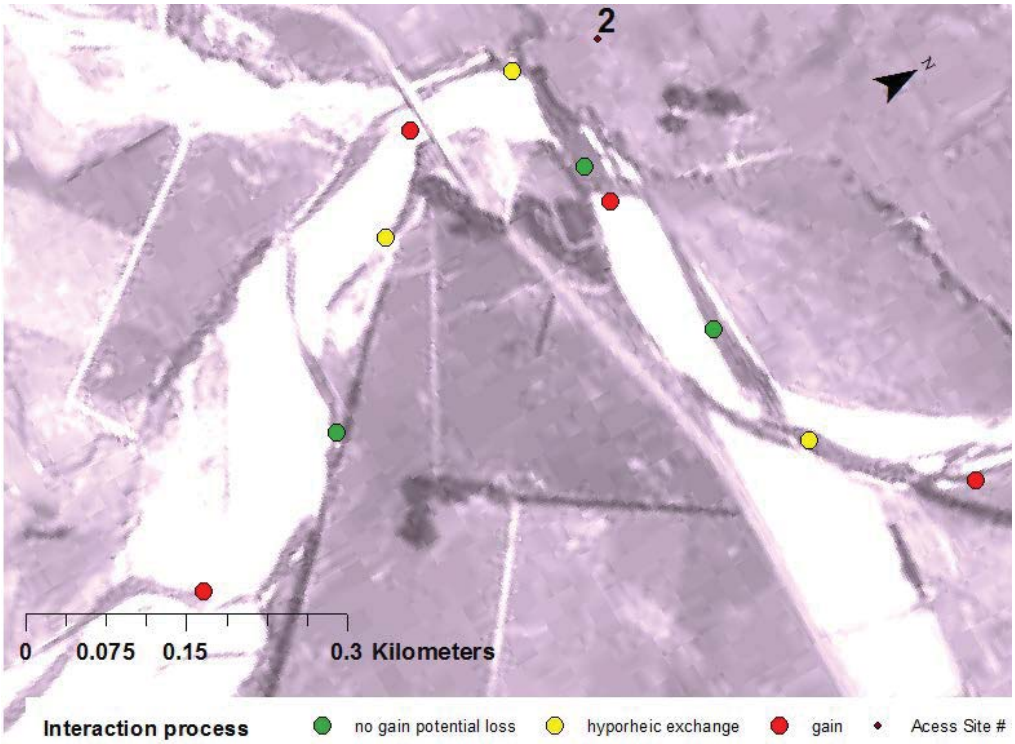

Figure 5.13: Interpreted groundwater-surface water interaction dynamics in the Mangatainoka River approximately 600 m upstream and downstream of Site 2.

Radon concentrations have shown where groundwater is discharging and possibly recharging in the Mangatainoka river system. The geological data available may provide an explanation for this spatial distribution of radon concentrations. When the radon data is plotted on Rawlinson et al. (2014) data of the modelled geology of the area (Fig 5.14), with the exception of the head waters, the Mangatainoka River flows along Quaternary deposits. Groundwater discharge in the upper to middle reaches of the river appears to occur where the Quaternary rock is thickest. Two large sections of possible groundwater recharge occur on the boundary between the Quaternary and Tertiary layers (Fig 5.14). A higher resolution geological model would be needed to determine what geological unit these sections of river actually reside on. Reducing radon concentrations are observed in an approximate 6 km section of the Mangatainoka River before the confluence with the Tiraumea. The quaternary layer in this section of the river is very shallow. This suggests that the lowered radon concentrations, caused by the radon degassing and isotopic decay, is likely caused only by this reach of river being non-gaining rather than a losing reach, as groundwater recharge/discharge can only occur in the quaternary layer (Brougham, 1987).

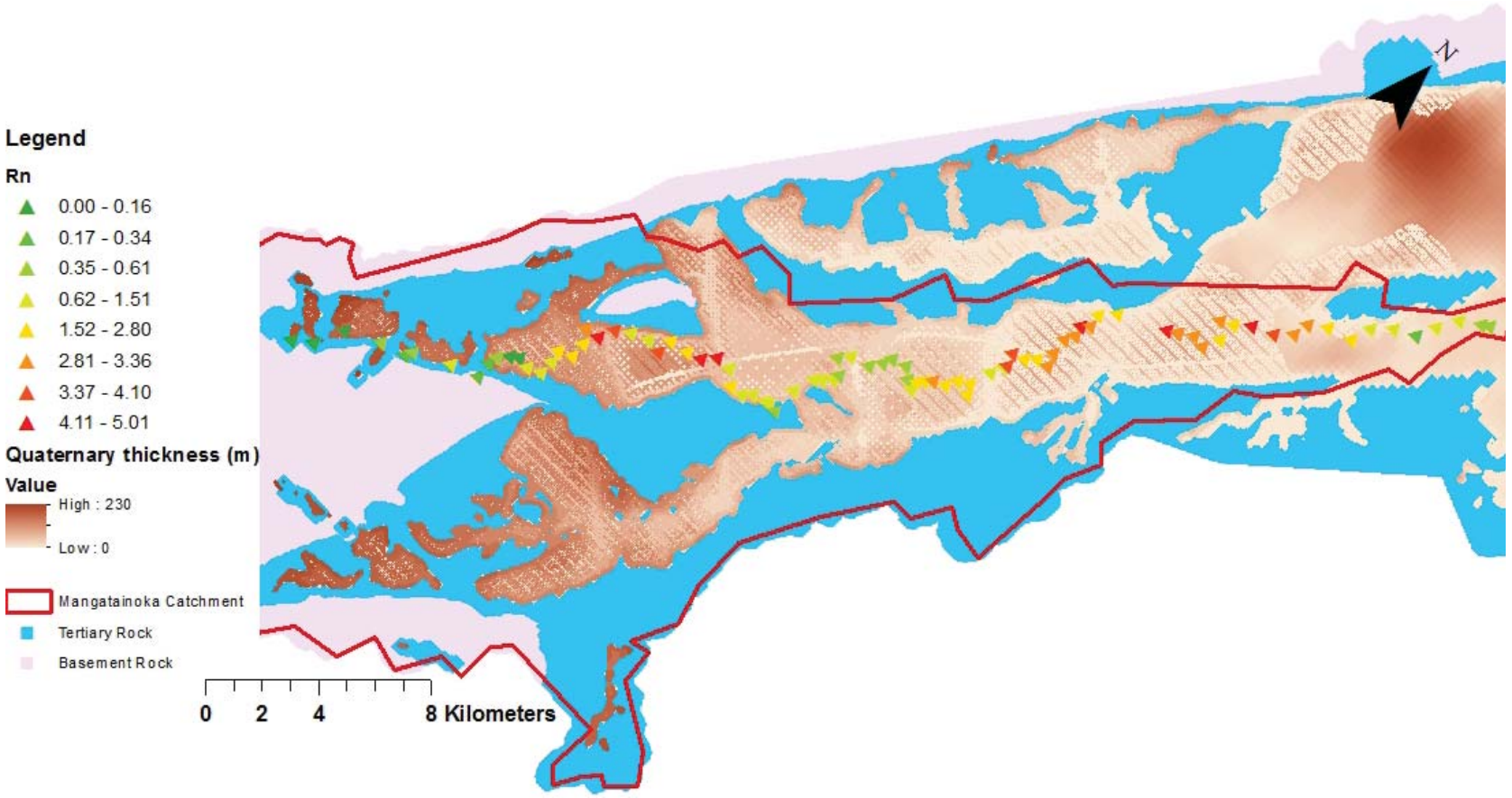

Figure 5.14: Comparison of radon concentrations in the Mangatainoka River with the depth of the quaternary layer. Geological units and their positions supplied by Rawlinson et al. (2014).

5.4.2 Comparison of river flow gauging to radon data

To assess the potential of using radon measurements in conjunction with other methods for capturing groundwater-surface water dynamics, concurrent flow gauging in the Mangatainoka River was also undertaken in February and March 2015. Although the gauging surveys were undertaken during low flow, the flow of the Mangatainoka River when measurements were taken in February was 0.6 $m^3 s^{-1}$ in the upper reaches and 2.0 $m^3 s^{-1}$ in the middle reaches, which was approximately three times that of the flow during the March gauging campaign, which had flows of 0.2 $m^3 s^{-1}$ and 0.7 $m^3 s^{-1}$ in the upper reaches and middle reaches, respectively. The flow gauging in February was undertaken at the same time as the high resolution radon sampling. The outcome of the flow gauging in February gave contradictory results when directly compared to the changes in radon concentrations. For the high resolution sampling at Site 12, going from upstream to downstream, the flow remains consistent, around 1 $m^3 s^{-1}$, as does the radon concentration (Fig. 5.15). As the radon concentration increased the flow increased slightly to 1.25 $m^3 s^{-1}$. The radon concentration increased significantly at Site 12. However, unexpectedly, the flow decreased from 1.25 $m^3 s^{-1}$ to 0.95 $m^3 s^{-1}$. A possible explanation for this decrease in flow, despite the measured radon concentrations indicating groundwater discharge, is that there is a meander prior to, and after, Site 12, causing some of the river to flow beneath the gravels. This would cause a reduced flow as measured by concurrent flow gauging even if groundwater was simultaneously being discharged.

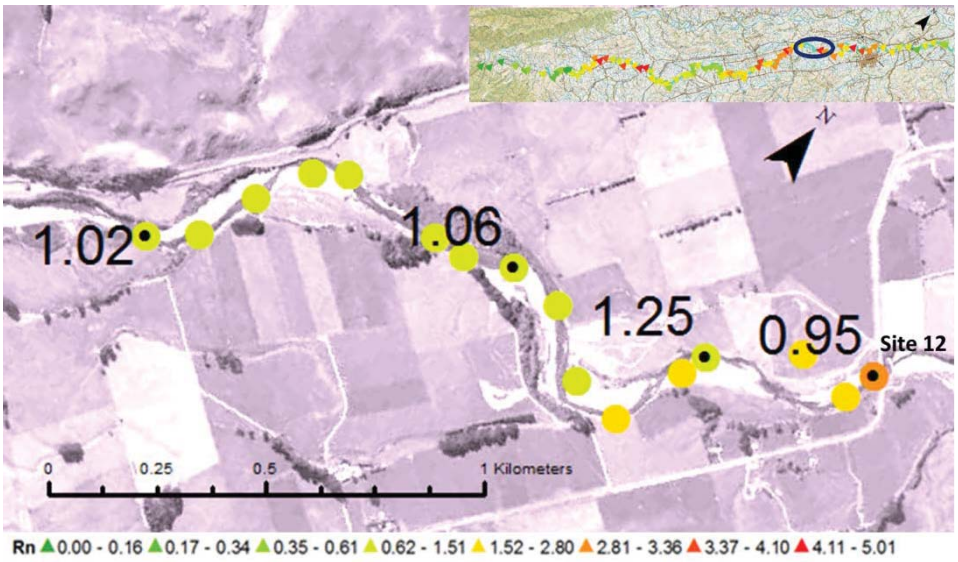

Figure 5.15: Measured flows of the Mangatainoka River between site 12 and 2.2 km upstream of site 12 (as written on figure) in $m^3 s^{-1}$ comparitive to measured radon concentrations, where the colour denotes the radon concentration.

The gauging at four locations near Site 2 also remains fairly consistent (Fig. 5.16). This flow gauging survey is consistent with the radon data as the radon data shows 3 discrete discharge points within this reach of the river that was gauged (Fig. 5.13) as well as non-gaining sections and hyporheic exchange.

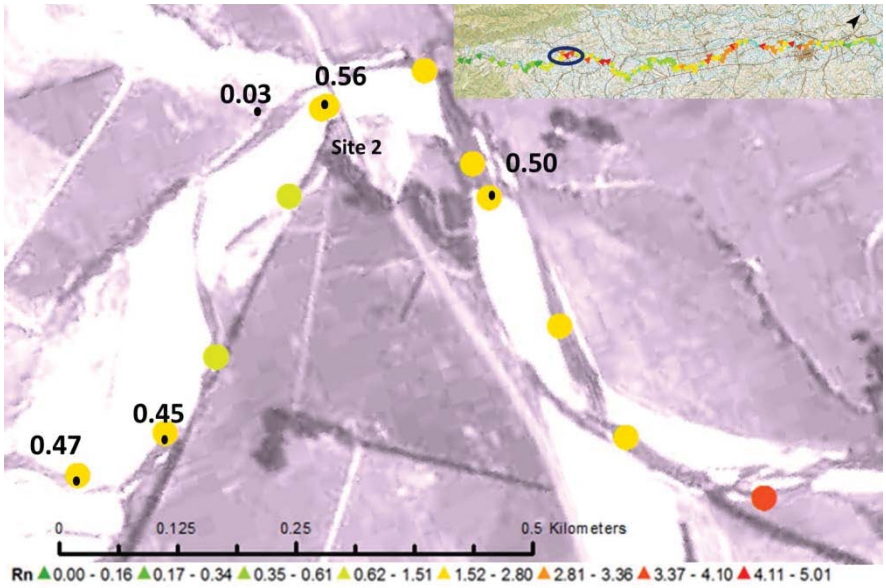

Figure 5.16: Measured flows (in $m^3 s^{-1}$) of the Mangatainoka River 600 m upstream and 600 m downstream of Site 2 (as written on figure) comparitive to the measured radon concentrations in February 2015, where the colour denotes the radon concentration in BqL^{-1}.

The flow gauging results from the March survey are compared to the measured radon concentrations from all radon surveys (Fig. 5.17), where the distance between sampling sites is estimated based on the GPS coordinates and do not reflect the true distances. Figure 5.17 shows that there are reaches of the river where the measured radon concentrations and flow show positive and negative correlations. An analysis of the measured radon concentrations and flow is described in more detail below and illustrated in Figures 5.18-5.20.

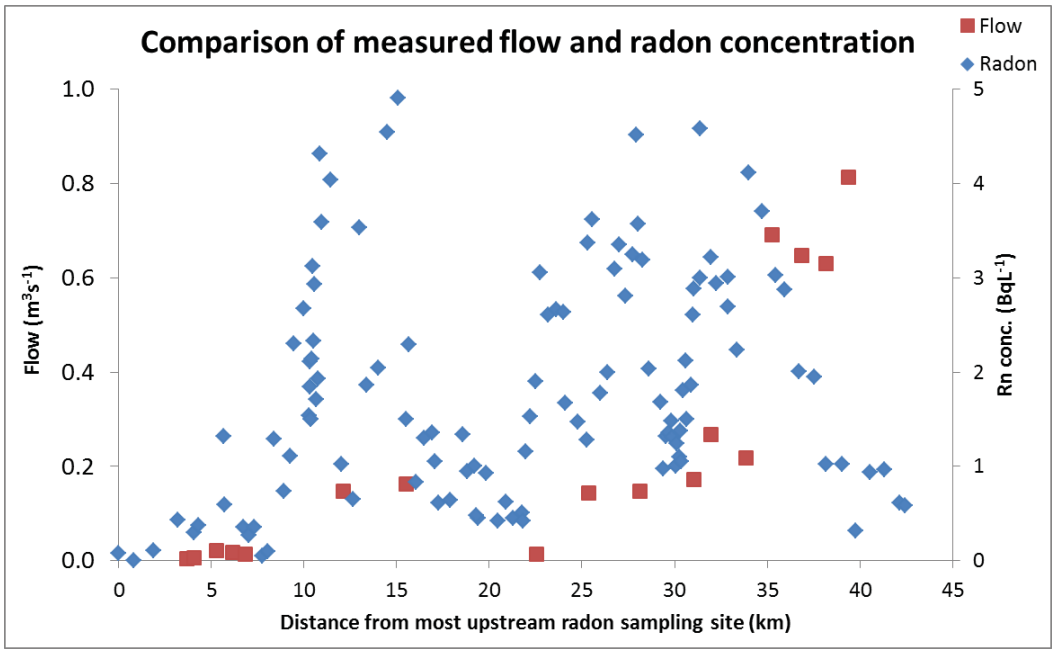

Figure 5.17: Measured flows ($m^3 s^{-1}$) on 5 March 2015 of the Mangatainoka River (red) comparitive to the measured radon concentrations sampled between 2 and 20 February (blue).

The flow gauging results from the March survey sampling sites suggest that the measured flows follow the same pattern of groundwater discharge/recharge as indicated by the radon measurements in the upper reaches of the Mangatainoka River (Fig 5.17-5.18). The flow in the upper reaches is relatively low, with small gains from tributaries. The measured radon concentrations in the upper reaches do not indicate any significant groundwater discharge, with the exception one site, 3000 m upstream of Site 1, which indicates some groundwater discharge.

In the middle to upper reaches, between Sites 3 and 5, radon concentrations are high, ranging from 1.9 BqL^{-1} - 4.9 BqL^{-1}. This strongly indicates a reach of the river where groundwater discharge is occurring. However, the flow between Sites 3 and 5 only increased by 0.015 $m^3 s^{-1}$ (Fig. 5.18). This measured increase in flow is smaller than the uncertainty of the two flow gauging measurements. Hence the groundwater discharge pattern indicated by flow gauging is ambiguous, whereas the radon measurements definitively indicate groundwater discharge.

Between Site 5 and 600 m downstream of Site 6 the measured flow increased from 0.163 $m^3 s^{-1}$ to 0.253 $m^3 s^{-1}$ (Fig. 5.18). At Site 6 the radon concentration was measured to be 2.3 BqL^{-1}. This indicates groundwater discharge and thus this radon data corresponds to the measured change in flow. Between Site 6 and upstream of Site 9 low radon concentrations of less than 0.6 BqL^{-1} were measured. These low radon concentrations indicate no groundwater discharge or possible recharge. This recharge process indicated by radon measurements is supported by the flow gauging results with a decrease in the measured flow from 0.253 $m^3 s^{-1}$ at Site 6 to 0.013 $m^3 s^{-1}$ at Site 9 (Fig. 5.18). Interestingly, approximately 1000 m upstream of Site 9 the radon concentrations become elevated again with concentrations between 1.1 BqL^{-1} and 1.9 BqL^{-1}. However, the flow gauging site at Site 9 was downstream of these increased radon measurements. This possible discrepancy between the flow gauging data and radon measurements highlights a significant limitation of using concurrent flow gauging for measuring groundwater-surface water interaction. Flow gauging only gives the net

change in flow between two gauging sites. It is possible that the river has lost more water just after the Site 6, around Sites 7 and 8, and then started gaining water as it approaches to Site 9 but not enough of a gain to result in a net positive gain in the river reach from Site 6 to Site 9.

Between Sites 9 and 10 the measured radon concentrations were relatively higher with concentrations increasing up to 3.7 BqL^{-1}, strongly indicating groundwater discharge. This is also supported by the flow gauging results as the measured flow increased from 0.013 $m^3 s^{-1}$ to 0.143 $m^3 s^{-1}$ between Sites 9 and 10 (Fig. 5.19). Between Sites 10 and 11 radon is consistently high, with concentrations measured ranging from 1.3 BqL^{-1} to 3.4 BqL^{-1}. This leads to the assumption of groundwater discharge. However, the flow gauging results are conflicting as the measured flow between the two sites remains relatively constant (Fig. 5.19). The radon concentrations between these two sites fluctuated between 1.8 BqL^{-1} and 4.5 BqL^{-1}. The interpreted radon concentration discharge patterns (Fig. 5.8) indicate that the measured radon concentrations are due to groundwater discharge rather than residual radon concentrations from an upstream discharge site. Therefore, a possible explanation for the discrepancy between the measured radon data and the flow gauging measurements is that there is underflow of the river beneath the gravels which is not captured by the flow gauging.

Between the middle and lower reaches the Makakahi River, the major tributary of the Mangatainoka River, flows into the Mangatainoka River, just upstream of Site 12. This confluence and groundwater discharge, indicated by high radon concentrations, give an increased flow from 0.172 $m^3 s^{-1}$ to 0.267 $m^3 s^{-1}$ (Fig. 5.19). As we go downstream from this site, radon concentrations remain relatively high, indicating further groundwater discharge. However, despite the high radon concentrations measured, the flow decreased to 0.218 $m^3 s^{-1}$ (Fig. 5.18). The flow then increased significantly from 0.218 $m^3 s^{-1}$ to 0.692 $m^3 s^{-1}$ at the Pahiatua Town Bridge (Fig. 5.18). This is consistent with the high radon concentrations, from 3.8 BL^{-1} to 4.1 BqL^{-1}, measured between these two sites. The measured flow then remained relatively unchanged but then again increases at Site 17, near the Tui Brewery, to 0.813 $m^3 s^{-1}$ (Fig. 5.18). Relative to the flow of the river, this is quite a large increase in measured flow. The radon measurements indicate some groundwater discharge over a short, approximate 1000 m reach (Fig. 5.8), with a measured radon concentration of 1.0 BqL^{-1}. With such a relatively large increase in flow it is surprising that there are no other measured significant radon discharges before this final flow gauging site. However, the radon sampling undertaken was done at a low resolution. The two radon sampling points between these two flow gauging sites are approximately 1000 m apart. It is possible that a major groundwater discharge was missed and the 1.0 BqL^{-1} radon measurement, taken just upstream of site 17, is the residual radon from an upstream discharge point.

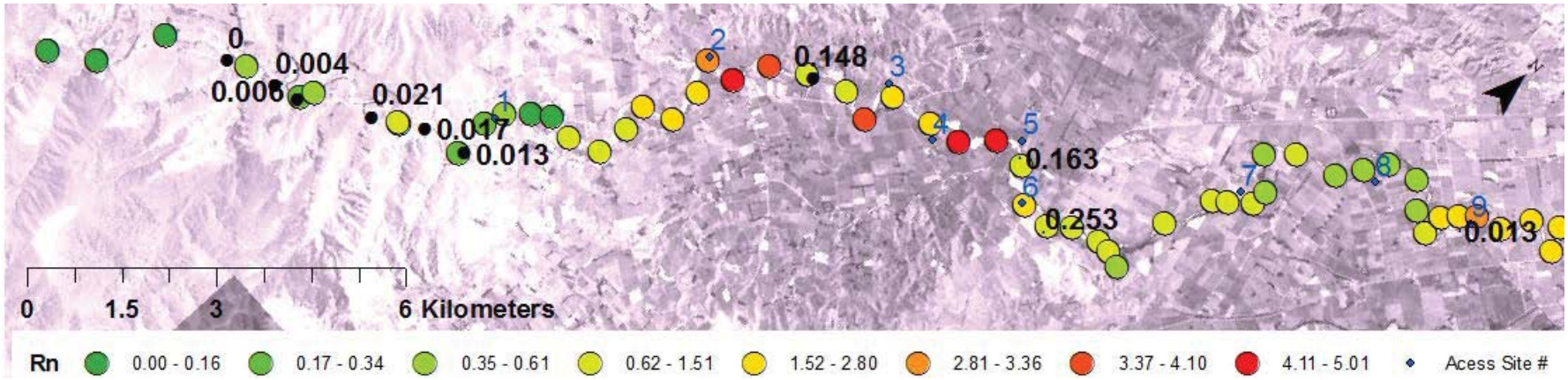

Figure 5.18: Measured flows ($m^3 s^{-1}$) on 5 March 2015 of the upper and middle reaches of the Mangatainoka River (as written on figure in black) comparitive to the measured radon concentrations sampled between 2 and 20 February, where the colour denotes the radon concentration in BqL^{-1}. The site names, as designated by Fish and Game are written in blue.

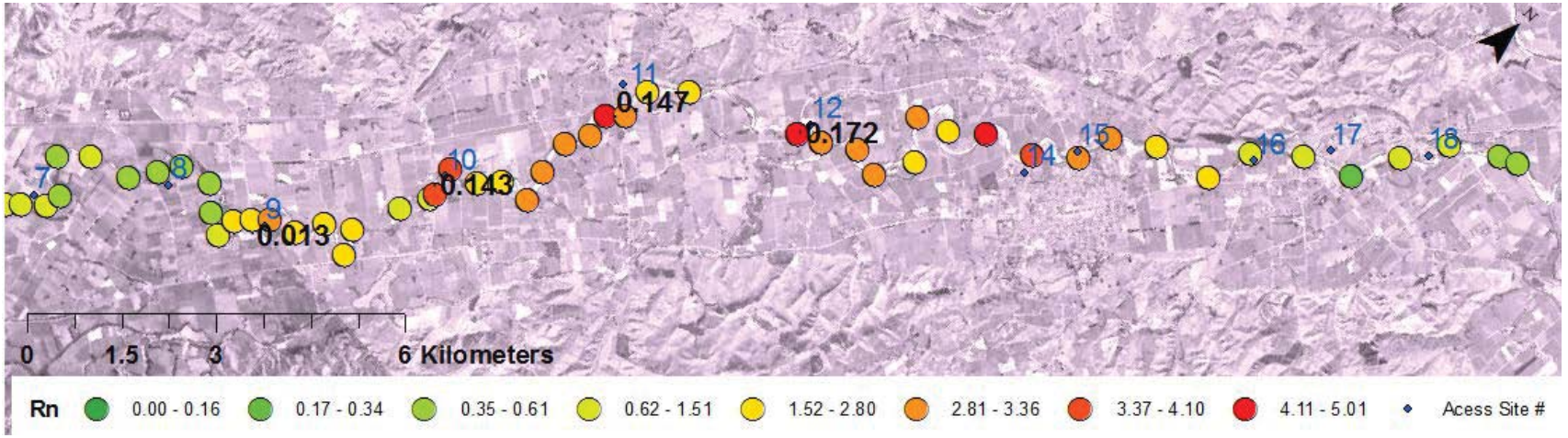

Figure 5.19: Measured flows ($m^3 s^{-1}$) on 5 March 2015 of the midddle and lower reaches of the Mangatainoka River (as written on figure in black) comparitive to the measured radon concentrations sampled between 2 and 20 February, where the colour denotes the radon concentration in BqL^{-1}. The site names, as designated by Fish and Game are written in blue.

The correlation between measured radon concentrations and flow rates in the Mangatainoka is variable. Higher radon concentrations do not always correspond to an increase in measured flow and likewise decreases in measured flow are not always associated with lower radon concentrations. There are a number of possible reasons for the discrepancy between the two hydrological measurement methods. Firstly, concurrent flow gauging only captures the net exchange in flow over large distances (Kalbus et al., 2006; McCallum et al., 2012). The exchange processes occurring between the gauging sites are not captured through flow gauging but are obtained from the radon concentrations taken at a much higher spatial resolution. Similarly, radon measurements were taken at a low resolution. The measured radon data is simply a snapshot from one site. It is unclear from the data whether the radon concentrations measured are due to groundwater discharge at the site measured, or from radon carried downstream from an upstream discharge point not sampled. However, further investigation was undertaken with flow gauging measured with the higher resolution radon sampling. These flow gaugings were taken a few hundred meters apart so would capture the exchange processes occurring that gauging at a larger spatial distribution would miss. However, these flow gauging measurements also varied in their consistency in correlating with the radon data. This is most likely caused by underflow of the river occuring through the gravels as the Mangatainoka is largely a gravel bed river. The Mangatainoka River also meanders considerably along its reach which would increase the likelihood of underflow through the meanders. Consequently it could be argued that the elevated radon concentrations measured could be due to radon being picked up by the river water when this underflow or hyporheic exchange process occurs. The high senstivity radon sampling undertaken in the Hutt River, chapter 4, section 4.4.4, demonstrated that hyporheic exchange only elevates the radon concentration by approximately 0.1 BqL^{-1}. However, the hyporheic system is likely to vary between the two rivers and within each river system themselves. It therefore cannot be ruled out that the differences in groundwater discharge patterns shown between flow gauging and the measured radon concentrations is caused by exchange within the hyporheic zone.

5.4.3 The effect of increased flow on radon concentration

In section 5.3.1 above, it was mentioned that the low resolution radon survey had to be repeated over two sections of the river due to higher flows impacting the results. Figure 5.20 compares the results of the data collected at low flow and elevated flows in the two reaches of the Mangatainoka River. The results from the different flow conditions cannot be directly compared as the radon samples were not sampled from the exact same location. However, the measured radon concentrations do show that while the radon signal in samples taken in higher flows is significantly dampened, it still shows the same general trends of radon discharge distribution observed during lower flows. Thus provided only samples taken under the same flow conditions are compared, radon concentrations taken in higher flows can still shed light on the groundwater-surface water interactions taking place. However, it should be noted that relative to the measured flows taken over a year in the Mangatainoka River, the higher flows under which the radon measurements with a dampened signal were taken are not too high (Fig. 5.21). The findings from the high resolution radon surveys in the Hutt River study, Chapter 4, Section 4.4.4, demonstrate that the higher the river flow the lower the radon signal (Fig. 4.18). Radon surveys carried out during higher flows run the risk of the radon signal being diluted beyond detection. Low flow conditions are recommended as the

areas of groundwater discharge and recharge are more easily identifiable as the changes in radon concentrations in low flow are greater.

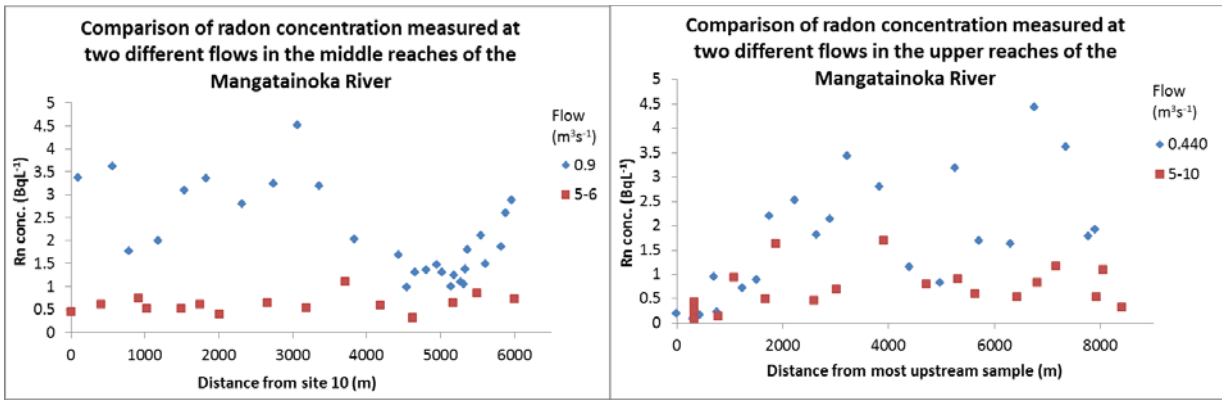

Figure 5.20: Comparison of radon concentrations collected downstream of Site 10 in the middle reaches (left) and downstream of the Larsons Road Bridge, Site 1, in the upper reaches (right) of the Mangatainoka River during two different flow conditions in February 2015.

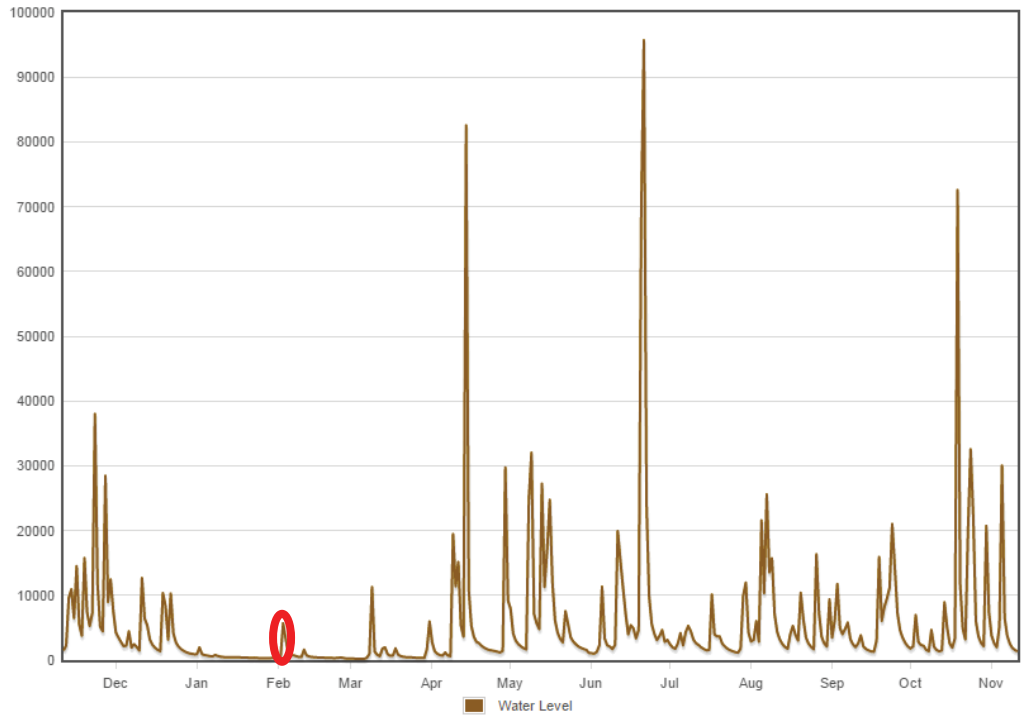

Figure 5.21: Measured flows (L s^{-1}) at the Larsons Road gauging station, where the red circle indicates the radon survey undertaken during higher flows on 2 February 2015. Image retrieved from (Horizons Regional Council, 2015).

5.4.4 River water quality parameters and their relationship with radon levels

During the low resolution radon surveys undertaken in February 2015, nitrate-nitrogen and electrical conductivity was measured concurrently. Electrical conductivities are also generally higher in groundwaters than surface waters, as the concentrations of dissolved ions are higher. Thus electrical

conductivity was measured in the Mangatainoka as river water which increases in electrical conductivity can indicate groundwater discharge. In the Mangatainoka River, non-point source contributions are thought to account for 98% of nitrate loadings in the Mangatainoka River (Horizons Regional Council, 2011). This indicates that the high nitrogen concentrations in the river are being introduced through groundwater discharges. Due to the high levels of nitrate in the groundwater it would be expected that where high concentrations of radon are measured in the river, higher concentrations of nitrate will also be measured.

An overlay of the NO_3-N and radon concentrations profiles against measurement location shows that the concentration profile patterns between the two analytes do not match (Fig. 5.22a). It would be expected that where radon concentrations are high, or increasing, that the nitrate concentration increases, yet the results shown on Figure 5.22a are variable. However, the two sites where the highest radon concentration was measured also had the two highest measured NO_3-N concentrations. There are several possible reasons for the lack of any strong relationship between the NO_3-N and radon concentrations long the river length. Firstly, while radon decays and degasses, nitrate does not. This may account for nitrate increasing or remaining relatively stable while the radon concentration fluctuates considerably. The inconsistency between high NO_3-N and radon concentrations could also indicate different sources of groundwater. One flow path of groundwater discharging into the river could have different concentrations of nitrate to another flow path or be associated with shallow or deeper groundwater discharge. This hypothesis is further supported in a study by Singh et al., (2014), where it is demonstrated that low levels of SIN leached from the root zone is attenuated before entering the river system. This is the most likely reason why there is no correlation between nitrate and radon data, especially when concentrations in the groundwater are observed in the Mangatainoka river system. Five different groundwater sites in close proximity to the Mangatainoka River have been measured by the Horizons Regional Council, the locations of which are shown in Figure 5.23 (Morgenstern et al., 2015). The NO_3-N concentrations at these sites ranged from 0 mg L^{-1} to 5.276 mg L^{-1}, with no pattern of the distribution of the nitrate concentrations being observed (Fig 5.23). Despite the findings of the concentration profiles of radon and NO_3-N not matching there is still potential for using the two hydrochemical analytes for future studies. It would be interesting to sample NO_3-N at a higher resolution where the radon concentration is now known to increase. At this high resolution the effect of groundwater discharge on the concentration distribution of NO_3-N is more likely to be observed. This is because higher resolution sampling is more likely to identify small changes in NO_3-N concentrations whereas the sampling resolution undertaken in this study only shows the cumulative effects of NO_3-N from upstream. The electrical conductivity measured in the Mangatainoka River increases as you go downstream of the Mangatainoka River (Fig. 5.22b). There appears to be no correlation between electrical conductivity and radon concentration. The likely reason for this is due to radon decaying and degassing whereas the electrical conductivity, which is related to total dissolved solids, has a cumulative effect as you go downstream.

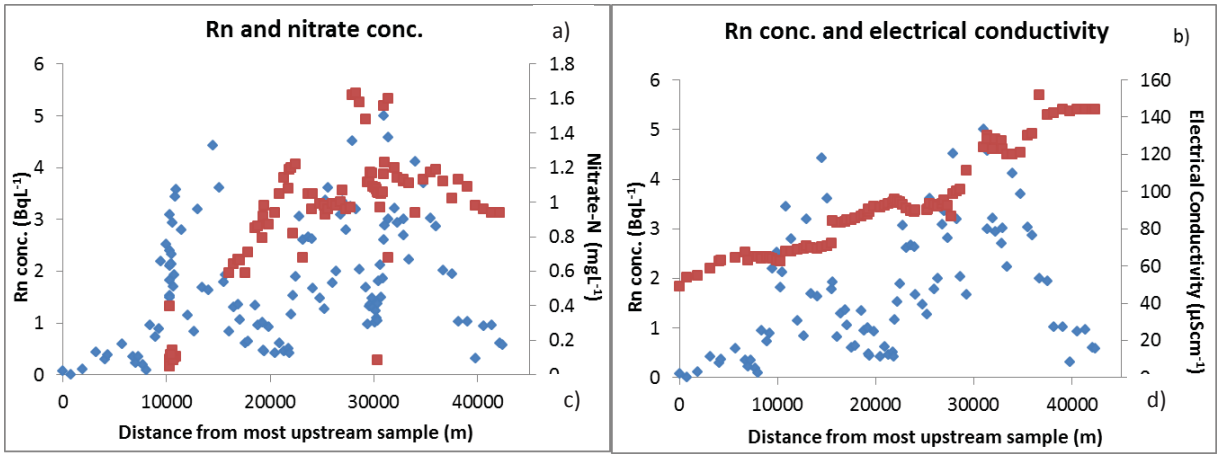

Figure 5.22: Measured radon concentrations (blue) and NO_3-N (red) (a) and electrical conductivity (red) (b), in the Mangatainoka River at low flow in February 2015.

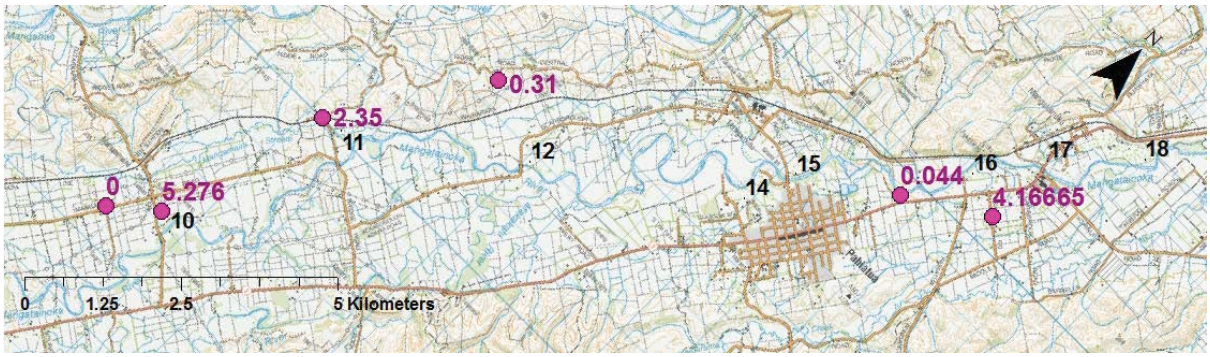

Figure 5.23: Locations of groundwater wells sampled for NO_3-N (purple symbol) with the NO_3-N concentrations designated by the purple numbers in mgL^{-1}. The blank numbers on the diagram represent the site numbers as designated by Fish and Game.

5.4.5 Comparison of findings with previous work

The gaining and losing stretches of the Mangatainoka River, indicated by radon measurements (Fig. 5.8), are similar to the conclusions drawn by Broughnam (1987), summarised in Fig 5.25. However, the radon measurements provide much higher spatial resolution of the groundwater-surface water interaction processes occurring in the river system. Broughnam (1987) concludes that gains are seen at the Scarborough/Konini Road Bridge. However, the radon measurements indicate that groundwater discharge begins to occur as far upstream as approximately 1 km downstream of the Browns Road. Relatively higher radon concentrations at the Bridge Road Bridge, Site 11, and upstream of the Pahiatua Town Bridge also indicate areas of significant groundwater discharge that were not mentioned by Broughnam (1987). Furthermore, Broughnam (1987) suggests that groundwater discharge in the lower reaches of the Mangatainoka River continues approximately 2 km further downstream, to near the Tui Brewery, than what the radon measurement suggests.

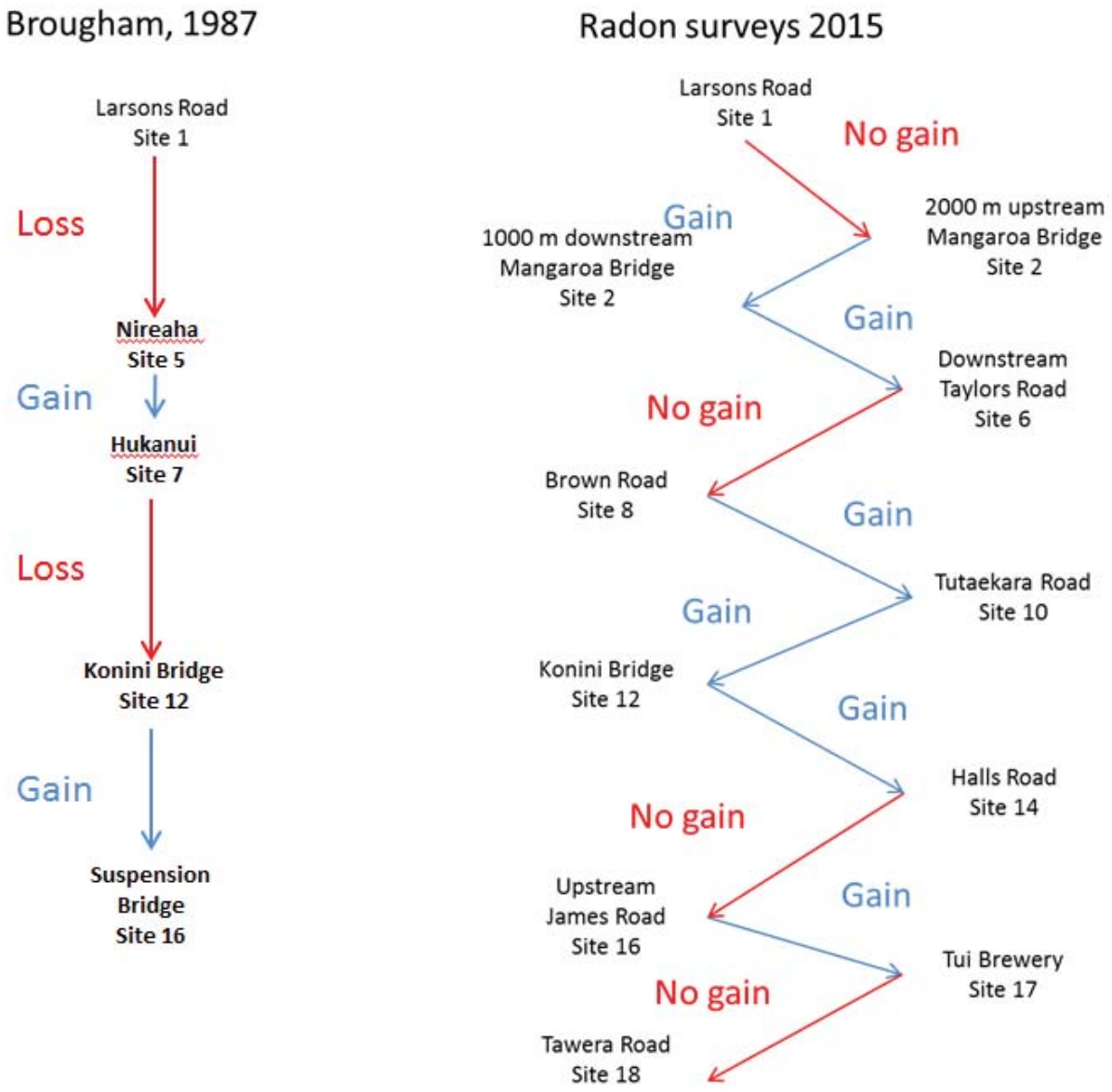

Figure 5.24: Flow diagrams of groundwater gains and loss/no gains as concluded from flow gauging data by Brougham (1987) and the radon surveys in the Mangatainoka River.

5.4.6 Further work

The cliché that research can lead to more questions than answers can be applied to the study undertaken in the Mangatainoka. Three aspects of the study which need some or further attention are temporal variations in radon measurements, the rate of degassing of radon in the Mangatainoka River and the variation in radon concentrations within the hyporheic zone.

Section 5.4.3 highlights that the radon concentrations measured, regardless of flow, show the same general pattern of discharge. However, this is a large assumption to make with only two sets of data. Will groundwater continue to discharge at the same locations regardless of flow, or will changes in the hydraulic head with varying flow force changeable discharge patterns? Further investigation into the change in radon concentrations with changing flow is needed.

In order to establish with more certainty where the gaining and losing sections of the Mangatainoka River are, the rate at which the radon gas degasses also needs to be known. This will determine with more clarity than applying the Hutt River findings to the Mangatainoka River as to whether the radon concentration of a measured sample is indeed due to groundwater discharge, or whether it is radon from an upstream discharge source.

5.5 Chapter summary

The radon study in the Mangatainoka River was undertaken to identify groundwater-surface water discharge patterns along the entire reach of the river. Spatial low and high resolution radon studies help to identify the areas of groundwater discharge and recharge in the Mangatainoka River system. Geological data of the Mangatainoka River is limited. However, a large variation in groundwater-surface water interaction appears to occur predominantly where the quaternary deposits are deepest. The largest possible losing and gaining reaches identified by radon both occur in the middle reaches. The non-gaining/losing reach occurs in the upper middle reaches. The river water lost then re-emerges further downstream in the middle reaches.

The potential of using concurrent NO_3-N and electrical conductivity measurements with radon measurements were also assessed. No pattern between the measured radon concentration profiles and the concentration profiles of these hydrological tools was observed in the Mangatainoka River. This is likely due to a large variation in the concentrations of NO_3-N within the groundwater system so a spatial pattern in this analytes distribution in conjunction with radon is unlikely. Furthermore, radon decays whereas NO_3-N and electrical conductivity do not. However, despite this further work using a combination of these three hydrological tools could be useful. Such work could include the study of differential increases in electrical conductivity and/or NO_3-N as where known increases in radon concentrations were measured an exaggerated change in electrical conductivity and NO_3-N may be observed.

The potential of using radon data in combination with concurrent stream gauging was assessed in the Mangatainoka River. This investigation highlighted the limitations of using flow gauging data alone to assess river gains and losses. Flow gauging shows only the net gain or loss between gauging sites and does not capture any groundwater-surface water interactions that occur between the two gauging sites. The radon data enables a much more detailed understanding of the exchange processes occurring within the Mangatainoka River to be captured than the flow gauging data alone. Higher resolution flow gauging may reduce the differences observed in discharge patterns between the two techniques. However, radon sampling is much quicker to achieve at a higher spatial resolution than flow gauging. Furthermore, underflow beneath the gravels and other parafluvial exchange processes have been identified as likely occurring in the Mangatainoka and can give ambiguous flow gauging results. However, until the degassing rate of radon under different flow conditions, and the radon concentration variation within the hyporheic zone is either established, or confirmed as being equal to those estimated from the Hutt River, some ambiguity remains as to whether the measured radon concentrations indicates groundwater discharge or residual radon from an upstream discharge point. Despite this limitation, the flow gauging data combined with radon concentrations gives a much clearer understanding of the groundwater and river water interaction processes that are occurring.

Chapter 6 - Conclusions and further work

6.1 Summary and conclusions

Understanding how surface waters and groundwaters interact is an integral component of managing New Zealand's natural waterways. This is very important to better understand how eutrophic causing nutrients, such as nitrogen and phosphorus, are transported in our waterways. However, the interactions between groundwater and surface water are highly variable and complex, making the measurement and mapping of such interactions difficult. A tool used for measuring this interaction is radon-222. The use of radon-222 as a tool for measuring the interaction between groundwater and surface water has been used in numerous studies abroad (Burnett et al., 2001; Burnett et al., 2013; Burnett et al., 2010; Close, 2014; Cook et al., 2003; Dimova et al., 2013; Dulaiova et al., 2010; Hammond et al., 1977; Hoehn & Von Gunten, 1989; Kies et al., 2005; Rajashekara et al., 2007; Santos & Eyre, 2011; Stellato et al., 2013), as described in chapter 2. However, the radon technique has not yet been exploited in New Zealand. Thus the purpose of the research undertaken in this study was to assess the potential of using radon for measuring groundwater-surface water interaction dynamics in the New Zealand environment.

The radon analysis method chosen for this study was liquid scintillation (LSC). LSC enables large numbers of samples to be collected over a short time as the sampling procedure is efficient and large numbers of samples could be measured at one time (Belloni et al., 1995). The disadvantage of the direct count LSC method however, is that the lower limit of detection is quite high, at 0.2 BqL^{-1}. This relatively high lower limit of detection of the direct count LSC method limits its application for measuring low radon levels in surface water of relatively fast flowing gravel-bed rivers in the New Zealand environment.

To enable the investigation of the interaction processes occurring in river waters with very low concentrations of radon in more detail, a time effective, cost effective and easily reproducible high sensitivity radon method was developed. This involved the enriching of scintillation cocktail in a larger sample volume, 240 mL, than the direct count method, in a specially shaped flask with an elongated neck. The enriched cocktail was then extracted using a syringe and measured in scintillation vials. The new procedure enabled radon samples to be enriched by a factor of 14.9 ± 0.3. Furthermore, the transfer efficiency of this method was approximately 60% with a lower limit of detection of 0.006 BqL^{-1}. This is an improvement to the lower limit of detection on the previously published method of Freyer et al. (1997), which only achieved 0.05 BqL^{-1}, but not that of Leaney and Herczeg (2006) who achieved a lower limit of detection of 0.003 BqL^{-1}. While the lower limit of detections of the different methods cannot be directly compared as they were calculated differently, comparable advantage of the newly developed method is that it only uses 240 mL of sample water. This is more than 1 L less sample water than the method of Leaney and Herczeg (2006). Furthermore, the proposed method also requires no handling of scintillation cocktail in the field and there is no loss of radon during storage due to diffusion through the sample bottle.

The potential of radon measurements to investigate groundwater-surface water interactions was further evaluated by conducted spatial and temporal radon surveys in the Hutt and Mangatainoka Rivers, in the Lower North Island. In both rivers spatial radon studies were able to capture where groundwater is discharging into a river and locations where no, or very little, groundwater is being discharged. Potentially the areas identified as not discharging could be reaches of groundwater

recharge. However, further research would need to be conducted to investigate this. Furthermore, the high sensitivity method, developed in Chapter 3, was applied in the Hutt River and evaluated in conjunction with the spatial radon studies to help infer further knowledge on the groundwater-surface water interaction dynamics. Using this high sensitivity method, the rate of radon degassing could be estimated in a section of the Hutt River where no groundwater discharge occurs. This estimation on the radon degassing was then used to account for degassing effects on measured spatial radon concentrations allowing to identify the gaining sections, possible losing sections and areas where the dominant process occurring was hyporheic exchange, of the Hutt and Mangatainoka Rivers

Measured radon concentrations were not only able to identify the approximate locations of groundwater discharge, but also that these groundwater discharge locations did not change between two river surveys carried out a year apart. Therefore, the data in the Hutt River showed that the areas of groundwater discharge and recharge remain consistent with time. Furthermore, in the Lower Hutt section of the Hutt River, sampling during higher flows was able to identify more accurately the areas of groundwater discharge. Thus, it can be concluded that applying high resolution spatial radon studies to both the Mangatainoka and Hutt Rivers enabled groundwater-surface water dynamic processes to be captured. Given the success of these findings it can be assumed that the use of radon for measuring groundwater-surface water interactions could be easily applied in other gravel rivers within New Zealand. This assumption is supported by the findings of Close (2014) and Close et al. (2014) who also successfully used radon to measure groundwater surface-water interaction dynamics in Canterbury and Marlborough, in the South Island of New Zealand. However, to validate this finding, further radon surveys should be carried out in different riverine environments throughout the country, particularly in non-gravel bed river environments.

In the Hutt River an attempt was made to complement radon concentration measurements with other hydrochemical parameters. This was carried out using HCA analysis. In this instance the HCA analysis did not show possible complementary tracer(s) to be used with radon. This conclusion seems somewhat unlikely to be the case, which may be due to the limited dataset used and warrants further investigation.

Furthermore, extensive concurrent flow gauging surveys were carried out in both of the study rivers, the results of which were compared to the radon measurements taken. The flow gauging and radon data showed numerous instances in both rivers where the datasets of the two techniques did not correlate with each other. Concurrent flow gauging does not give an accurate picture on where the exchange processes are occurring; only the net result between the gauging sites. As highlighted in both Chapters 4 and 5, this is likely due to underflow occurring beneath the gravel-bed rivers and that the concurrent flow gauging undertaken on a much lower resolution, measures only net changes in river flow across large distances, whereas radon enables the river water and groundwater exchange processes to be observed on a higher resolution. However, in both case study rivers, this divergence between the radon and concurrent flow gauging datasets was also observed when flow gauging was undertaken at a higher resolution. The comparison of radon measurements to the other hydrological tools used in the study exemplifies the complex nature of groundwater flow paths and the interaction with surface water.

Both the study rivers were gravel bed-rivers, and thus a comparison between these two study areas is interesting. In the Hutt River case study, observed radon concentrations could be explained by the geology. The Mangatainoka catchment geology is not as well known, so whether a relationship between groundwater discharge and geology exists cannot yet be determined. In further comparisons, the Mangatainoka River was found to have a higher frequency of higher concentrations of radon than the Hutt River. There are several possible reasons as to why this may be the case. It could simply be due to approximately 70 km of the Mangatainoka River being surveyed as opposed to 16 km in the Hutt River. The Mangatainoka River could have a higher proportion of gaining sections, with a higher proportion of groundwater discharge and thus more radon, than the Hutt River. Another reason for the differences between the two rivers could be due to the rate of radon degassing. In low flow the Hutt River has a flow in places of more than ten times the flow of the Mangatainoka River. With less flow, there will be less turbulence, which could reduce the rate of degassing in the Mangatainoka River and thus allow radon to remain in the surface water for longer. Lastly, despite both rivers being gravel-bed rivers, the geology of the Hutt and Mangatainoka River catchments differ. Differing geology can impact emanation rates and therefore cause comparatively different concentrations of radon for the same rate of groundwater discharge. However, the measured groundwater radon samples from both study areas were similar indicating that emanation rates between the two study sites were also similar. Clearly all of these possibilities need to be investigated to provide more clarity to the radon results collected to date.

The study undertaken exemplifies that radon is an effective tool for measuring groundwater-surface water interaction and has the ability to be applied in hydrological studies in New Zealand gravel-bed river systems.

6.2 Further work

The radon studies carried out in the Hutt and Mangatainoka Rivers provided insightful information into the groundwater-surface water interaction processes occurring. However, further investigation to delve deeper into the findings of the study is still needed. If future research into radon in gravel-bed rivers continues, the following is suggested:

- In both the Mangatainoka and Hutt Rivers the measured river flows and radon concentrations in some river reaches gave conflicting results. In this study it was concluded that this was likely due to underflow of the river beneath the gravels, which is not captured by concurrent flow gauging. To assess whether this hypothesis is correct salt or dye tracer injections, should be carried out where the radon and flow measurements were conflicting.

- In Chapter 5, the Mangatainoka case study, the radon concentration thresholds for determining groundwater discharge/recharge were taken from the findings of the high sensitivity study completed in the Hutt River. To reduce ambiguity of what concentration of radon indicates groundwater discharge, recharge or hyporheic exchange, high sensitivity radon studies should be conducted in the Mangatainoka River. Furthermore, if the same radon concentration thresholds exist in the Mangatainoka River as in the Hutt River, then these thresholds could be applied with confidence to other gravel bed rivers in New Zealand.

- The findings of the high sensitivity study completed in one small reach of the Hutt River were applied throughout the entire reach of both rivers surveyed. However, the rates of radon degassing could change significantly throughout the course of a river, due to river channel shape, size and bedform. Further investigation as to how the rate of radon degassing changes along the entire reach of a river is needed.

- The high sensitivity radon study in Chapter 4 also allowed for the concentrations of radon picked up due to hyporheic exchange to be estimated. However, the size, residence time, bank and bed material, and depth of the hyporheic zone are likely to change significantly throughout the course of the river. Thus further investigation looking into the radon concentrations in the hyporheic zone is needed.

- Locating areas in rivers where groundwater is being discharged into the river and surface water is being recharged back into the aquifer system is useful. The next step for this research would be to quantify what these radon concentrations mean in terms of the volume of water being discharged/recharged. Several studies which quantify radon data have been made, all of which require multiple tracers and models (Burnett et al., 2013; Cook et al., 2003; Dimova et al., 2013; McCallum et al., 2012; Stellato et al., 2013). However, given the number of variables that affect the measured radon concentration, such as emanation, wind, water turbidity, temperature, water currents and degassing rates, it is almost impossible to achieve with radon data alone. Further work on the HCA analysis study is needed to improve the ability to find other hydrological parameters that will complement radon measurements. This may aid in the development of a simplified method for quantifying radon concentrations in river water in terms of groundwater discharge flow rates.

References

Alley, W. M., Reilly, T. E., & Franke, O. L. (1999). *Sustainability of Ground-Water Resources*. Denver: U.S. Geological Survey.

Anderson, M. P. (2003). What Is 'Ground Water'? *Ground Water, 41*(6), 721-721. doi: 10.1111/j.1745-6584.2003.tb02410.x

Anderson, M. P. (2005). Heat as a Ground Water Tracer. *Ground Water, 43*(6), 951-968. doi: 10.1111/j.1745-6584.2005.00052.x

Angermann, L., Tacklenburg, C., & Blume, T. (2013). *Spatial variability in river-catchment interaction: Combining radon measurements and salt tracer experiments*. Paper presented at the EGU General Assembly 2013.

Anibas, C., Buis, K., Verhoeven, R., Meire, P., & Batelaan, O. (2011). A simple thermal mapping method for seasonal spatial patterns of groundwater–surface water interaction. *Journal of Hydrology, 397*(1–2), 93-104. doi: http://dx.doi.org/10.1016/j.jhydrol.2010.11.036

Asikainen, M. (1981). State of disequilibrium between 238U, 234U, 226Ra and 222Rn in groundwater from bedrock. *Geochimica et Cosmochimica Acta, 45*(2), 201-206. doi: http://dx.doi.org/10.1016/0016-7037(81)90163-0

Baskaran, S., Ransley, T., Brodie, R., & Baker, P. (2009). Investigating groundwater–river interactions using environmental tracers. *Australian Journal of Earth Sciences, 56*(1), 13-19.

Becker, M. W., Georgian, T., Ambrose, H., Siniscalchi, J., & Fredrick, K. (2004). Estimating flow and flux of ground water discharge using water temperature and velocity. *Journal of Hydrology, 296*(1–4), 221-233. doi: http://dx.doi.org/10.1016/j.jhydrol.2004.03.025

Bekesi, G. (2005). Groundwater Allocation of the Alexandra Basin Dunedin: Otago Regional Council.

Belloni, P., Cavaioli, M., Ingrao, G., Mancini, C., Notaro, M., Santaroni, P., . . . Vasselli, R. (1995). Optimization and comparison of three different methods for the determination of Rn-222 in water. *Science of The Total Environment, 173–174*(0), 61-67. doi: http://dx.doi.org/10.1016/0048-9697(95)04754-9

Boon, D., Perrin, N., & Dellow, G. (2011). *NZS1170. 5: 2004 site subsoil classification of Lower Hutt*.

Boon, D., Perrin, N., Dellow, G., & Lukovic, B. (2010). It's our fault - Geological and Geotechnical Characterisation and Site Subsoil Class Revision of the Lower Hutt Valley. Wellington.

Boulton, A. J., Findlay, S., Marmonier, P., Stanley, E. H., & Valett, H. M. (1998). The Functional Significance of the Hyporheic Zone in Streams and Rivers. *Annual Review of Ecology and Systematics, 29*(ArticleType: research-article / Full publication date: 1998 / Copyright © 1998 Annual Reviews), 59-81. doi: 10.2307/221702

Brougham, G., C. (1987). Mangatainoka Water Resource Assessment *Board, M. C. B. A. R. W.* Palmerston North: Manawatu Catchment Board and Regional Water Board.

Bruckner, M. (n.d, 29 May 2015). A Primer on Stable Isotopes and Some Common Uses in Hydrology Retrieved 1 June, 2015, from http://serc.carleton.edu/microbelife/research_methods/environ_sampling/stableisotopes.html

Bureau of Reclamation. (2012). Reclamation. *Yuma Area Water Management System (YAWMS) - Groundwater Basics* Retrieved 8 September 2014, 2014, from http://www.usbr.gov/lc/yuma/programs/YAWMS/GROUNDWATER.html

Burnett, W. C., Kim, G., & Lane-Smith, D. (2001). A continuous monitor for assessment of 222Rn in the coastal ocean. *Journal of Radioanalytical and Nuclear Chemistry, 249*(1), 167-172. doi: 10.1023/a:1013217821419

Burnett, W. C., Peterson, R. N., Chanyotha, S., Wattayakorn, G., & Ryan, B. (2013). Using high-resolution in situ radon measurements to determine groundwater discharge at a remote location: Tonle Sap Lake, Cambodia. *Journal of Radioanalytical and Nuclear Chemistry, 296*(1), 97-103. doi: 10.1007/s10967-012-1914-8

Burnett, W. C., Peterson, R. N., Santos, I. R., & Hicks, R. W. (2010). Use of automated radon measurements for rapid assessment of groundwater flow into Florida streams. *Journal of Hydrology, 380*(3–4), 298-304. doi: http://dx.doi.org/10.1016/j.jhydrol.2009.11.005

Burnett, W. C., & Tai, W. C. (1992). Determination of radium in natural waters by .alpha. liquid scintillation. *Analytical Chemistry, 64*(15), 1691-1697. doi: 10.1021/ac00039a012

Busenberg, E., & Plummer, L. N. (1992). Use of chlorofluorocarbons (CCl3F and CCl2F2) as hydrologic tracers and age-dating tools: The alluvium and terrace system of central Oklahoma. *Water Resources Research, 28*(9), 2257-2283. doi: 10.1029/92wr01263

Cantaloub, M., Higginbotham, J., Istok, J., & Semprini, L. (1998). *Interaction of sample, cocktail, and headspace volume when measuring aqueous Rn in small volume samples.* Paper presented at the BIOASSAY ANALYTICAL AND ENVIRONMENTAL RADIOCHEMISTRY CONFERENCE.

Cecil, D., & Green, J. (2000). Radon-222. In P. G. Cook & A. L. Herczeg (Eds.), *Environmental Tracers In Subsurface Hydrology* (pp. 175-194). Massachusetts: Kluwer Academic Publishers.

Cey, E. E., Rudolph, D. L., Parkin, G. W., & Aravena, R. (1998). Quantifying groundwater discharge to a small perennial stream in southern Ontario, Canada. *Journal of Hydrology, 210*(1–4), 21-37. doi: http://dx.doi.org/10.1016/S0022-1694(98)00172-3

Close, M. (2014). Analysis of radon data from the Wairau River and adjoining Wairau Plains aquifer February 2014 Christchurch: ESR.

Close, M., Matthews, M., Burbery, L., Abraham, P., & Scott, D. (2014). Use of radon to characterise surface water recharge to groundwater. *Journal of Hydrology, 53*(2), 113.

Constantz, J. (1998). Interaction between stream temperature, streamflow, and groundwater exchanges in alpine streams. *Water Resources Research, 34*(7), 1609-1615. doi: 10.1029/98wr00998

Cook, P., Favreau, G., Dighton, J. C., & Tickell, S. (2003). Determining natural groundwater influx to a tropical river using radon, chlorofluorocarbons and ionic environmental tracers. *Journal of Hydrology, 277*(1–2), 74-88. doi: http://dx.doi.org/10.1016/S0022-1694(03)00087-8

Cook, P., & Herczeg, A. (2000). *Environmental Tracers in Subsurface Hydrology*: Springer US.

Cook, P., Wood, C., White, T., Simmons, C., Fass, T., & Brunner, P. (2008). Groundwater inflow to a shallow, poorly-mixed wetland estimated from a mass balance of radon. *Journal of Hydrology, 354*(1–4), 213-226. doi: http://dx.doi.org/10.1016/j.jhydrol.2008.03.016

Daughney, C. J. (2010). Spreadsheet for automatic processing of water quality data: 2010 Update - Calculation of percentiles and tests for seasonality. Lower Hutt: GNS Science.

Daughney, C. J., Jones, A., Baker, T., Hanson, C., Davidson, P., Zemansky, G. M., . . . Thompson, M. (2006). A national protocol for state of the environment groundwater sampling in New Zealand. Wellington: Ministry for the Environment.

Daughney, C. J., Meilhac, C., & Zarour, H. (2009). Spatial and temporal variation and trends in groundwater quality in the Manawatu-Wanganui Region. Lower Hutt: GNS Science.

Daughney, C. J., & Reeves, R. R. (2005). Definition of hydrochemical facies in the New Zealand national groundwater monitoring programme. *Journal of Hydrology (New Zealand), 44*(2), 105.

Davidson, P., & Wilson, S. (2011). *Groundwaters of Marlborough*. Christchurch: The Caxton Press.

Davis, S. N., Thompson, G. M., Bentley, H. W., & Stiles, G. (1980). Ground-Water Tracers—A Short Review. *Groundwater, 18*(1), 14-23.

Dimova, N. T., Burnett, W. C., Chanton, J. P., & Corbett, J. E. (2013). Application of radon-222 to investigate groundwater discharge into small shallow lakes. *Journal of Hydrology, 486*(0), 112-122. doi: http://dx.doi.org/10.1016/j.jhydrol.2013.01.043

Dulaiova, H., & Burnett, W. (2006). Radon loss across the water-air interface (Gulf of Thailand) estimated experimentally from 222Rn-224Ra. *Geophysical Research Letters, 33*(5).

Dulaiova, H., Camilli, R., Henderson, P. B., & Charette, M. A. (2010). Coupled radon, methane and nitrate sensors for large-scale assessment of groundwater discharge and non-point source pollution to coastal waters. *Journal of Environmental Radioactivity, 101*(7), 553-563. doi: http://dx.doi.org/10.1016/j.jenvrad.2009.12.004

Eappen, K. (2010). Radon measurement techniques in environmental and geophysical studies. *Radon Contamination in Groundwater and Application of Isotopes in Groundwater Studies*, 5.

Ellins, K. K., Roman-Mas, A., & Lee, R. (1990). Using 222Rn to examine groundwater/surface discharge interaction in the Rio Grande de Manati, Puerto Rico. *Journal of Hydrology, 115*(1–4), 319-341. doi: http://dx.doi.org/10.1016/0022-1694(90)90212-G

Flury, M., & Wai, N. N. (2003). Dyes as tracers for vadose zone hydrology. *Reviews of Geophysics, 41*(1).

Folger, P., Poeter, E., Wanty, R., Frishman, D., & Day, W. (1996). Controls on 222Rn variations in a fractured crystalline rock aquifer evaluated using aquifer tests and geophysical logging. *Groundwater, 34*(2), 250-261.

Freeze, R. A., & Cherry, J. A. (1979). *Groundwater*: Prentice-Hall.

Freyer, K., Treutler, H. C., Dehnert, J., & Nestler, W. (1997). Sampling and measurement of radon-222 in water. *Journal of Environmental Radioactivity, 37*(3), 327-337. doi: http://dx.doi.org/10.1016/S0265-931X(96)00102-6

Garcia-Vindas, J., & Monnin, M. (2005). Radon concentration measurements in the presence of water and its consequences for Earth sciences studies. *Radiation Measurements, 39*(3), 319-322.

Gesell, T., F., & Lowder, W., M. . (1978). *Natural Radiation Environment III* Paper presented at the International Symposium on the Natural Radiation Environment, Houston, Texas.

Gómez Escobar, V., Vera Tomé, F., Lozano, J. C., & Sánchez, A. M. (1996). Determination of 222Rn and 226Ra in aqueous samples using a low-level liquid scintillation counter. *Applied Radiation and Isotopes, 47*(9–10), 861-867. doi: http://dx.doi.org/10.1016/S0969-8043(96)00076-0

Gooddy, D. C., Darling, W. G., Abesser, C., & Lapworth, D. J. (2006). Using chlorofluorocarbons (CFCs) and sulphur hexafluoride (SF 6) to characterise groundwater movement and residence time in a lowland Chalk catchment. *Journal of Hydrology, 330*(1), 44-52.

Greater Wellington Regional Council. (2004). Flooding Hazard - Hutt Valley. In G. W. R. Council (Ed.), (Vol. GWRP-G-04/02). Wellington: Greater Wellington Regional Council.

Greater Wellington Regional Council. (2012a, 27/07/2012). Groundwater. *Environmental monitoring and research* Retrieved 18 July, 2015, from http://graphs.gw.govt.nz/R27-7004/

Greater Wellington Regional Council. (2012b, 10/05/2013). Rainfall. *Environmental monitoring and research* Retrieved 18 July, 2015, from http://graphs.gw.govt.nz/rainfall-2/

Greater Wellington Regional Council. (2013). Toxic algae in Wellington's rivers Retrieved 4 November, 2015, from http://www.gw.govt.nz/assets/Our-Environment/Environmental-monitoring/Toxic-algae-brochure-2013web.pdf

Greater Wellington Regional Council. (2015). Toxic algae in Hutt River at Boulcott Retrieved 4 November, 2015, from http://www.gw.govt.nz/toxic-algae-in-hutt-river-at-boulcott/

Guggenmos, M., Daughney, C., Jackson, B., & Morgenstern, U. (2011). Regional-scale identification of groundwater-surface water interaction using hydrochemistry and multivariate statistical methods, Wairarapa Valley, New Zealand. *Hydrology and Earth System Sciences Discussions, 8*(4), 6443-6487.

Güler, C., Thyne, G. D., McCray, J. E., & Turner, K. A. (2002). Evaluation of graphical and multivariate statistical methods for classification of water chemistry data. *Hydrogeology Journal, 10*(4), 455-474.

Gyopari, M. (2014). Lower Hutt Aquifer Model Revision (HAM3): Sustainable Management of the Waiwhetu Aquifer. Wellington.

Hahn, P. B., & Pia, S. H. (1991). *Determination of Radon in Drinking Water by Liquid Scintillation Counting Method 913*. Las Vegas, Nevada, U.S.A.: U.S. Environmental Protection Agency.

Hammond, D. E., Simpson, H. J., & Mathieu, G. (1977). Radon 222 distribution and transport across the sediment-water interface in the Hudson River estuary. *Journal of Geophysical Research, 82*(27), 3913-3920. doi: 10.1029/JC082i027p03913

Hatch, C. E., Fisher, A. T., Revenaugh, J. S., Constantz, J., & Ruehl, C. (2006). Quantifying surface water–groundwater interactions using time series analysis of streambed thermal records: Method development. *Water Resources Research, 42*(10).

Herczeg, A. L., & Edmunds, M. (2000). Inorganic Ions as Tracers. In P. G. Cook & A. L. Herczeg (Eds.), *Environmental Tracers In Subsurface Hydrology* (pp. 31-78). Massachusetts: Kluwer Academic Publishers.

Hoehn, E., & Von Gunten, H. R. (1989). Radon in groundwater: A tool to assess infiltration from surface waters to aquifers. *Water Resources Research, 25*(8), 1795-1803. doi: 10.1029/WR025i008p01795

Horiuchi, K., & Murakami, Y. (1981). A new procedure for the determination of radium in water by extraction of radon and application of integral counting with a liquid scintillation counter. *The International journal of applied radiation and isotopes, 32*(5), 291-294.

Horizons Regional Council. (2011). OURS. The Manawatu River Leaders' Accord Action Plan. *OURS. The Manawatu River Leaders' Accord*. Retrieved from http://www.horizons.govt.nz/assets/Managing-our-Enviroment/Resource-Management/Manawatu-River-Leaders-Forum-Action-Plan-electronic.pdf

Horizons Regional Council. (2015). Mangatainoka at Larsons Road Retrieved 15 November, 2015, from http://www.horizons.govt.nz/managing-environment/resource-management/water/river-heights-and-rainfall/Choose-river-rainfall-chart/detail?Collection=Flow&Site=Mangatainoka%20at%20Larsons%20Road

Hughes, B. (1996). *Resource Monitoring in the Lower Hutt Groundwater Zone: Inputs to outputs. Hydrology '96 "From Inputs to Outputs" Field Trip Notes.* Paper presented at the Joint NZ Hydrological Society Symposium and 10th Australasian Hydrographic Workshop, Wellington.

IAL. (2004, 26/06/2004). Channel Seepage Management Tool Retrieved 3 March, 2015, from http://www.channelseepage.org.au/3_3_31_pointMeasPrinc.html

Johnson, S. L. (2003). Stream temperature: scaling of observations and issues for modelling. *Hydrological Processes, 17*(2), 497-499.

Jones, A. G., & Baker, T. (2005). *Groundwater monitoring technical report*: Greater Wellington Regional Council.

Kalbus, E., Reinstorf, F., & Schirmer, M. (2006). Measuring methods for groundwater–surface water interactions: a review. *Hydrology and Earth System Sciences, 10*(6), 873-887.

Katz, B. G., Coplen, T. B., Bullen, T. D., & Davis, J. H. (1997). Use of Chemical and Isotopic Tracers to Characterize the Interactions Between Ground Water and Surface Water in Mantled Karst. *Ground Water, 35*(6), 1014-1028. doi: 10.1111/j.1745-6584.1997.tb00174.x

Kaye-Blake, B., Schilling, C., Nixon, C., & Destremau, K. (2014). Water management in New Zealand. A road map for understanding water value. Wellington: NZ Institute of Economic Research.

Kies, A., Hofmann, H., Tosheva, Z., Hoffmann, L., & Pfister, L. (2005). Using 222 Rn for hydrograph separationin a micro basin (Luxembourg). [radon;hydrology;tracer;hydrograph separation]. *Annals of Geophysics, 48*(1).

Kiliari, T., & Pashalidis, I. (2008). Determination of aquatic radon by liquid scintillation counting and airborne radon monitoring system. *Radiation Measurements, 43*(8), 1463-1466. doi: http://dx.doi.org/10.1016/j.radmeas.2008.03.006

Kronenberg, S., Brucker, G. J., & Horne, S. A. (2002). Alpha, beta, and gamma monitor for measuring concentrations of ionizing radiation emitters in ambient air or other media: Google Patents.

LAWA. (2013). National Environmental Monitoring Standards *Open Channel Flow Measurement*: Land Air Water Aotearoa.

Lawrence, J., Reisinger, A., Tegg, S., & Quade, D. (2011). Vulnerability and adaptation to increased flood risk with climate change—Hutt Valley summary. Wellington: The New Zealand Climate Change Research Institute.

Leaney, F. W., & Herczeg, A. L. (2006). A rapid field extraction method for determination of radon-222 in natural waters by liquid scintillation counting. *Limnology and Oceanography: Methods, 4*, 254-259.

Lee, D. (1977). A device for measuring seepage flux in lakes and esturies. *Limnology and Oceanography, 22*(1), 140-147.

Lee, J., & Kim, G. (2006). A simple and rapid method for analyzing radon in coastal and ground waters using a radon-in-air monitor. *Journal of Environmental Radioactivity, 89*(3), 219-228. doi: http://dx.doi.org/10.1016/j.jenvrad.2006.05.006

Lefebvre, K., Barbecot, F., Ghaleb, B., Larocque, M., & Gagné, K. (2013). Full range determination of 222Rn at the watershed scale by liquid scintillation counting. *Applied Radiation and Isotopes, 75*(0), 71-76. doi: http://dx.doi.org/10.1016/j.apradiso.2013.01.027

Lenzen, M., & Neugebauer, H. J. (1996). A theoretical investigation in the Lucas cell. *Nuclear Instruments and Methods in Physics Research Section A: Accelerators, Spectrometers, Detectors and Associated Equipment, 368*(2), 479-483. doi: http://dx.doi.org/10.1016/0168-9002(95)00681-8

Lowry, C. S., Walker, J. F., Hunt, R. J., & Anderson, M. P. (2007). Identifying spatial variability of groundwater discharge in a wetland stream using a distributed temperature sensor. *Water Resources Research, 43*(10), W10408. doi: 10.1029/2007wr006145

McArthur, K., & Clark, M. (2007). Nitrogen and Phosphorus Loads to Rivers in the Manawatu-Wanganui Region : An Analysis of Low Flow State. Palmerston North.

McCallum, J. L., Cook, P. G., Berhane, D., Rumpf, C., & McMahon, G. A. (2012). Quantifying groundwater flows to streams using differential flow gaugings and water chemistry. *Journal of Hydrology, 416–417*(0), 118-132. doi: http://dx.doi.org/10.1016/j.jhydrol.2011.11.040

McDonnell, J., Stewart, M., & Owens, I. (1991). Effect of catchment-scale subsurface mixing on stream isotopic response. *Water Resources Research, 27*(12), 3065-3073.

Ministry for the Environment. (2014). About fresh water in New Zealand. Wellington: Ministry for the Environment.

Ministry of Health. (2008). Drinking-water Standards for New Zealand 2005 (Revised 2008). Wellington: Ministry of Health.

Miskell, B. (2012). Hutt landscape study 2012 landscape character description. Wellington.

Moore, R. (2004). Introduction to salt dilution gauging for streamflow measurement: Part 1. *Streamline Watershed Management Bulletin, 7*(4), 20-23.

Morgenstern, U., Matthews, A., Begg, J., Roygard, J., Townsend, B., Clark, M., & Martindale, H. (2014). Groundwater lag times in the water discharges from the Whanganui, Rangitikei and Manawatu catchments (Vol. 2014/35). Lower Hutt: GNS Science.

Morgenstern, U., & Taylor, C. B. (2009). Ultra low-level tritium measurement using electrolytic enrichment and LSC. *Isotopes in Environmental and Health Studies, 45*(2), 96-117. doi: 10.1080/10256010902931194

Morgenstern, U., van der Raaij, R., & Baalousha, H. (2012). Groundwater flow pattern in the Ruataniwha Plains as derived from the isotope and chemistry signature of the water. Lower Hutt: GNS Science.

Morgenstern, U., van der Raaij, R., Martindale, H., Trompetter, V., Toews, M., Matthews, A., & Stewart, M. (2015). Groundwater dynamics and hydrochemical evolution as inferred from Horizon's Regional Age. Lower Hutt: GNS Science.

Murdoch, L. C., & Kelly, S. E. (2003). Factors affecting the performance of conventional seepage meters. *Water Resources Research, 39*(6), 1163. doi: 10.1029/2002wr001347

Mwashote, B., Burnett, W., Chanton, J., Santos, I. R., Dimova, N., & Swarzenski, P. (2010). Calibration and use of continuous heat-type automated seepage meters for submarine groundwater discharge measurements. *Estuarine, Coastal and Shelf Science, 87*(1), 1-10.

Nazaroff, W. W. (1992). Radon transport from soil to air. *Reviews of Geophysics, 30*(2), 137-160.

Noguchi, M. (1964). New method of radon activity measurement with liquid scintillator. *Radioisotopes, 13*, 362-368.

Noguchi, M., & Wakita, H. (1973). Measurements of low-level radon for the determination of radium in marine carbonates. *Geochem. J., 7*(2), 81-88. doi: 10.2343/geochemj.7.81

Norman, R. (n.d). Fonterra needs to lead in cleaning up the Mangatainoka River Retrieved 12 November, 2015, from https://home.greens.org.nz/misc-documents/fonterra-needs-lead-cleaning-mangatainoka-river

Phreatos. (2001). Waiwhetu Artesian Aquifer Saltwater Intrusion Risk Management Review. Wellington: Phreatos Limited.

Phreatos. (2003). Revision of the numerical model for the Lower Hutt groundwater zone (R. I. D. WELLINGTON REGIONAL COUNCIL, TECHNICAL REPORT, Trans.). Wellington: Greater Wellington Regional Council.

Plummer, L. N., & Busenberg, E. (2000). Chlorofluorocarbons. In P. G. Cook & A. L. Herczeg (Eds.), *Environmental Tracers In Subsurface Hydrology* (pp. 441-478). Massachusetts: Kluwer Academic Publishers.

Rajashekara, K. M., Narayana, Y., & Siddappa, K. (2007). 222Rn concentration in ground water and river water of coastal Karnataka. *Radiation Measurements, 42*(3), 472-478. doi: http://dx.doi.org/10.1016/j.radmeas.2006.12.010

Rawlinson, Z. J., & Begg, J. (2014). Hydrogeology of the Upper Manawatu and Mangatainoka catchments, Tararua (pp. 48). Wellington: GNS Science.

Rosenberry, D. O. (2008). A seepage meter designed for use in flowing water. *Journal of Hydrology, 359*(1–2), 118-130. doi: http://dx.doi.org/10.1016/j.jhydrol.2008.06.029

Saito, M., & Takata, S. (1992). Improvements for measurement of 222Rn in water. *Radioisotopes, 41*, 391-396.

Sakoda, A., Ishimori, Y., & Yamaoka, K. (2011). A comprehensive review of radon emanation measurements for mineral, rock, soil, mill tailing and fly ash. *Applied Radiation and Isotopes, 69*(10), 1422-1435. doi: http://dx.doi.org/10.1016/j.apradiso.2011.06.009

Santos, I. R., & Eyre, B. D. (2011). Radon tracing of groundwater discharge into an Australian estuary surrounded by coastal acid sulphate soils. *Journal of Hydrology, 396*(3–4), 246-257. doi: http://dx.doi.org/10.1016/j.jhydrol.2010.11.013

Santos, I. R., Eyre, B. D., & Huettel, M. (2012). The driving forces of porewater and groundwater flow in permeable coastal sediments: A review. *Estuarine, Coastal and Shelf Science, 98*(0), 1-15. doi: http://dx.doi.org/10.1016/j.ecss.2011.10.024

Scanlon, B. R., Healy, R. W., & Cook, P. G. (2002). Choosing appropriate techniques for quantifying groundwater recharge. *Hydrogeology Journal, 10*(1), 18-39.

Scarsbrook, M., & Halliday, J. (1996). The hyporheic zone: the hidden dimension of stream ecosystems. *Water & Atmosphere, 4*(4). Retrieved from

Selker, J. S., Thevenaz, L., Huwald, H., Mallet, A., Luxemburg, W., Van De Giesen, N., . . . Parlange, M. B. (2006). Distributed fiber-optic temperature sensing for hydrologic systems. *Water Resources Research, 42*(12).

Shaw, G. D., White, E. S., & Gammons, C. H. (2013). Characterizing groundwater–lake interactions and its impact on lake water quality. *Journal of Hydrology, 492*(0), 69-78. doi: http://dx.doi.org/10.1016/j.jhydrol.2013.04.018

Singh, R., Rivas, A., Espanto, P., Elwan, A., Horne, D., Roygard, J., . . . Clothier, B. (2014). Assessment of transport and transformation of nitrogen in the subsurface environment of Manawatu River catchment – work in progress. In R. D. Currie & C. L. Christensen (Eds.), *Nutrient management for the farm, catchment and community* (pp. 11). Palmerston North: Fertilizer and Lime Research Centre.

Skeppström, K., & Olofsson, B. (2007). Uranium and radon in groundwater. *European Water, 17*(18), 51-62.

Smart, P., & Laidlaw, I. (1977). An evaluation of some fluorescent dyes for water tracing. *Water Resources Research, 13*(1), 15-33.

Smerdon, B., & Redding, T. (2007). Ground wa ter: More than water below the ground. *Stream line 10 (2): 1, 6*.

Sophocleous, M. (2002). Interactions between groundwater and surface water: the state of the science. *Hydrogeology Journal, 10*(1), 52-67.

Stellato, L., Petrella, E., Terrasi, F., Belloni, P., Belli, M., Sansone, U., & Celico, F. (2008). Some limitations in using 222Rn to assess river–groundwater interactions: the case of Castel di Sangro alluvial plain (central Italy). *Hydrogeology Journal, 16*(4), 701-712. doi: 10.1007/s10040-007-0263-0

Stellato, L., Terrasi, F., Marzaioli, F., Belli, M., Sansone, U., & Celico, F. (2013). Is 222Rn a suitable tracer of stream–groundwater interactions? A case study in central Italy. *Applied Geochemistry, 32*(0), 108-117. doi: http://dx.doi.org/10.1016/j.apgeochem.2012.08.022

Stewart, M., & Morgenstern, U. (2001). Age and source of groundwater from isotope tracers. *Groundwaters of New Zealand (Eds. Rosen MR. and White PW.), The Caxton Press, Christchurch*, 161-184.

Taylor, P., Ryan, D., Hughes, J., Chakraborty, M., Clark, M., Brown, L., & Roygard, J. (2015). Environmental farm plans - our experience in the Mangatainoka Catchment. In R. D. Currie & L. L. Burkitt (Eds.), *Moving Farm Systems to Improved Attenuation* (Vol. 2015). Palmerston North: Horizons Regional Council.

Theodorsson, P., & Gudjonsson, G. I. (2003). Increased radon detection sensitivity: Extraction from 200 mL of water and liquid scintillatin counting. *Health Physics, 85*(5), 610-612.

University of Wisconsin - Milwaukee. (n.d). Liquid scintillation counting Retrieved 28 August 2015, from http://www.bio.huji.ac.il/upload/beta_counter_protocol.pdf

Vinson, D. S., Vengosh, A., Hirschfeld, D., & Dwyer, G. S. (2009). Relationships between radium and radon occurrence and hydrochemistry in fresh groundwater from fractured crystalline rocks, North Carolina (USA). *Chemical Geology, 260*(3), 159-171.

Wellington Regional Council. (1995). Hydrology of the Hutt Catchment (R. I. DEPARTMENT, Trans.) (Vol. 2: Groundwater). Wellington.

West, A. G., February, E. C., & Bowen, G. J. (2014). Spatial analysis of hydrogen and oxygen stable isotopes ("isoscapes") in ground water and tap water across South Africa. *Journal of Geochemical Exploration, 145*(0), 213-222. doi: http://dx.doi.org/10.1016/j.gexplo.2014.06.009

White, D. S. (1993). Perspectives on Defining and Delineating Hyporheic Zones. *Journal of the North American Benthological Society, 12*(1), 61-69. doi: 10.2307/1467686

Winter, T. C. (1999a). *Ground water and surface water: a single resource* (Vol. 1139): DIANE Publishing.

Winter, T. C. (1999b). Relation of streams, lakes, and wetlands to groundwater flow systems. *Hydrogeology Journal, 7*(1), 28-45.

Woessner, W. W. (2000). Stream and fluvial plain ground water interactions: rescaling hydrogeologic thought. *Groundwater, 38*(3), 423-429.

Woessner, W. W., & Anderson, M. P. (2002). The Hydro-Malaprop and the Ground Water Table. *Ground Water, 40*(5), 465-465. doi: 10.1111/j.1745-6584.2002.tb02529.x

Yanase, N., Payne, T. E., & Sekine, K. (1995). Groundwater geochemistry in the Koongarra ore deposit, Australia (II): activity ratios and migration mechanisms of uranium series radionuclides. *Geochem. J, 29*(1), 31-54.

Appendix 1 – Hutt River low resolution radon surveys

Sampling Date	Northing	Easting	Radon conc. (BqL^{-1})	1 sigma Rn	Sampling Date	Northing	Easting	Radon conc. (BqL^{-1})	1 sigma Rn
4/04/2014	5437531	1760941	2.4	0.2	4/04/2014	5443536	1767956	2.1	0.2
4/04/2014	5436654	1759693	1.8	0.2	30/08/2014	5437722	1761167	1.1	0.1
4/04/2014	5436695	1759750	1.8	0.2	30/08/2014	5437806	1761253	1.1	0.1
4/04/2014	5436796	1759856	2.0	0.2	30/08/2014	5437833	1761328	0.9	0.1
4/04/2014	5436861	1759947	1.7	0.2	30/08/2014	5437863	1761432	1.0	0.1
4/04/2014	5436958	1760078	2.6	0.2	30/08/2014	5437907	1761627	1.1	0.1
4/04/2014	5437108	1760193	2.2	0.2	30/08/2014	5438002	1761651	1.2	0.1
4/04/2014	5437167	1760306	2.0	0.2	30/08/2014	5438164	1762080	0.6	0.1
4/04/2014	5437236	1760418	2.7	0.2	30/08/2014	5438036	1761774	1.1	0.1
4/04/2014	5437273	1760513	2.2	0.2	30/08/2014	5438074	1761819	1.4	0.1
4/04/2014	5437406	1760708	2.9	0.2	30/08/2014	5438146	1761911	1.0	0.1
4/04/2014	5437497	1760806	1.9	0.2	30/08/2014	5437355	1760642	1.2	0.1
4/04/2014	5437554	1760919	2.2	0.2	30/08/2014	5437445	1760789	1.3	0.1
4/04/2014	5443138	1767610	2.2	0.2	30/08/2014	5437537	1760942	1.2	0.1
4/04/2014	5442951	1767305	1.5	0.1	30/08/2014	5437641	1761045	1.0	0.1
4/04/2014	5442788	1767085	0.9	0.1	10/01/2015	5446450	1772118	0.1	0.0
4/04/2014	5442660	1766930	1.0	0.1	10/01/2015	5446298	1771822	0.1	0.0
4/04/2014	5442248	1766684	0.7	0.1	10/01/2015	5446071	1771434	0.1	0.0
4/04/2014	5441951	1766496	0.7	0.1	10/01/2015	5445725	1771122	0.2	0.0
4/04/2014	5441591	1766200	0.5	0.1	10/01/2015	5445405	1770776	0.6	0.1
4/04/2014	5441393	1765772	0.6	0.1	10/01/2015	5445187	1770351	0.7	0.1
4/04/2014	5440990	1765279	0.7	0.1	10/01/2015	5444901	1769902	1.1	0.1
4/04/2014	5440955	1764958	0.6	0.1	10/01/2015	5444578	1769582	1.3	0.1
4/04/2014	5440848	1764708	0.7	0.1	10/01/2015	5444239	1769143	2.0	0.2
4/04/2014	5440564	1764477	0.6	0.1	10/01/2015	5443817	1768412	1.7	0.2
4/04/2014	5440312	1764219	0.7	0.1	10/01/2015	5443158	1767640	1.7	0.2
4/04/2014	5440143	1763967	0.7	0.1	10/01/2015	5442882	1767265	0.7	0.1
4/04/2014	5439777	1763624	0.6	0.1	10/01/2015	5442521	1766859	0.6	0.1
4/04/2014	5439517	1763386	0.5	0.1	10/01/2015	5442061	1766568	0.7	0.1
4/04/2014	5439297	1763135	0.6	0.1	10/01/2015	5441608	1766186	0.5	0.1
4/04/2014	5439044	1763002	0.5	0.1	10/01/2015	5441319	1765779	0.6	0.1
4/04/2014	5438712	1762685	0.5	0.1	10/01/2015	5441003	1765317	0.5	0.1
4/04/2014	5438402	1762343	0.5	0.1	10/01/2015	5440872	1764702	0.6	0.1
4/04/2014	5438404	1762343	0.7	0.1	10/01/2015	5440312	1764212	0.6	0.1
4/04/2014	5438074	1761824	4.8	0.3	10/01/2015	5439658	1763528	0.3	0.1
4/04/2014	5437884	1761519	2.8	0.2	10/01/2015	5439145.5	1763049	0.3	0.1
4/04/2014	5437765	1761195	2.8	0.2	10/01/2015	5438633	1762570	0.4	0.1
4/04/2014	5445429	1770668	2.2	0.2	10/01/2015	5438323	1762284	0.5	0.1
4/04/2014	5445259	1770448	1.5	0.1	10/01/2015	5438082	1761819	1.7	0.2
4/04/2014	5444945	1769911	1.6	0.1	10/01/2015	5437897	1761538	1.7	0.2
4/04/2014	5444583	1769584	2.1	0.2	10/01/2015	5437731	1761127	1.3	0.1
4/04/2014	5444305	1769296	2.5	0.2	10/01/2015	5437425	1760708	1.8	0.2
4/04/2014	5444169	1768895	2.7	0.2	10/01/2015	5437144	1760225	1.4	0.1

Appendix 2 – Mangatainoka River low resolution radon surveys

Sampling Date	Northing	Easting	Radon conc. (BqL^{-1})	1 sigma Rn
2/02/2015	1815357	5493455	0.1	0.0
2/02/2015	1815995	5493943	0.0	0.0
2/02/2015	1816424	5495008	0.1	0.1
2/02/2015	1817653	5495633	0.4	0.1
2/02/2015	1818566	5495947	0.3	0.1
2/02/2015	1818673	5496164	0.4	0.1
2/02/2015	1819938	5496838	0.6	0.1
2/02/2015	1820921	5497212	0.4	0.1
2/02/2015	1827988	5503351	0.8	0.2
2/02/2015	1828282	5503648	1.3	0.2
2/02/2015	1828736	5503801	1.4	0.2
2/02/2015	1828932	5503816	1.1	0.2
2/02/2015	1829220	5503747	0.6	0.1
2/02/2015	1829199	5504775	0.6	0.1
2/02/2015	1829452	5505555	1.3	0.2
2/02/2015	1829620	5505733	1.0	0.2
2/02/2015	1829913	5506008	1.0	0.2
2/02/2015	1829928	5506283	0.4	0.1
2/02/2015	1829453	5506664	0.5	0.1
2/02/2015	1829796	5507059	0.9	0.2
2/02/2015	1830458	5507282	0.4	0.1
2/02/2015	1830699	5507679	0.6	0.1
2/02/2015	1830888	5508020	0.5	0.1
2/02/2015	1831369	5508186	0.5	0.1
2/02/2015	1831738	5507874	0.4	0.1
2/02/2015	1832079	5507732	1.2	0.2
2/02/2015	1832071	5508065	1.5	0.2
2/02/2015	1832250	5508299	1.9	0.2
2/02/2015	1832439	5508507	3.1	0.3
2/02/2015	1832848	5508667	2.6	0.3
2/02/2015	1833066	5509107	2.7	0.3
2/02/2015	1833635	5509008	2.6	0.3
2/02/2015	1833437	5509367	1.7	0.2
2/02/2015	1833679	5510152	1.5	0.2
2/02/2015	1833887	5510612	1.3	0.2
2/02/2015	1837019	5515618	5.0	0.4
2/02/2015	1837384	5515817	4.6	0.4
2/02/2015	1837384	5515817	3.0	0.3
2/02/2015	1837852	5516171	3.2	0.3
2/02/2015	1838316	5516090	2.9	0.3
2/02/2015	1838601	5516702	2.7	0.3
2/02/2015	1838122	5517210	3.0	0.3
2/02/2015	1838593	5517424	2.2	0.2
2/02/2015	1839037	5517838	4.1	0.4
2/02/2015	1839778	5518165	3.7	0.3
2/02/2015	1840300	5518679	3.0	0.3
2/02/2015	1840398	5519270	2.9	0.3
2/02/2015	1840985	5519720	2.0	0.2
2/02/2015	1841888	5520001	1.9	0.2
2/02/2015	1842076	5520749	1.0	0.2
2/02/2015	1842670	5521342	1.0	0.2
2/02/2015	1843397	5521692	0.3	0.1
2/02/2015	1843700	5522451	0.9	0.2
2/02/2015	1844076	5523174	1.0	0.2
2/02/2015	1844746	5523641	0.6	0.1
2/02/2015	1845019	5523784	0.6	0.1
15/02/2015	1821221	5498494	0.0	0.0
15/02/2015	1821473	5498688	0.1	0.0
15/02/2015	1821907	5498671	1.3	0.1
15/02/2015	1822398	5498888	0.7	0.1
15/02/2015	1822407	5499440	1.1	0.1
15/02/2015	1822317	5499869	2.3	0.2
15/02/2015	1822787	5500088	2.7	0.2
15/02/2015	1822733	5500668	1.8	0.2
15/02/2015	1822456	5501117	3.1	0.2
15/02/2015	1822955	5501215	4.3	0.3
15/02/2015	1823182	5501791	4.0	0.2
15/02/2015	1823683	5502142	1.0	0.1
15/02/2015	1824294	5502413	0.7	0.1
15/02/2015	1824823	5502348	3.5	0.2
15/02/2015	1824848	5502918	1.9	0.2
15/02/2015	1825568	5503068	2.0	0.2
15/02/2015	1826065	5503215	4.5	0.3
15/02/2015	1826457	5503664	4.9	0.3
15/02/2015	1827015	5503692	1.5	0.2
15/02/2015	1827510	5503304	2.3	0.2
15/02/2015	1820844	5497825	0.3	0.0
15/02/2015	1820932	5498158	0.4	0.0
20/02/2015	1833905	5510710	3.4	0.2
20/02/2015	1833761	5511159	3.6	0.3
20/02/2015	1834202	5511331	1.8	0.2
20/02/2015	1834467	5511641	2.0	0.2
20/02/2015	1834929	5511736	3.1	0.2
20/02/2015	1834770	5512213	3.3	0.2
20/02/2015	1834690	5512784	2.8	0.2
20/02/2015	1834853	5513174	3.2	0.2
20/02/2015	1834777	5513543	4.5	0.3
20/02/2015	1834999	5513781	3.2	0.2
20/02/2015	1834948	5514295	2.0	0.2
20/02/2015	1835389	5514782	1.7	0.1
20/02/2015	1819924	5496828	1.3	0.1